

Jimma University
School of Graduate Studies
Jimma Institute of Technology
Faculty of Civil and Environmental Engineering
Structural Engineering Stream

**BEHAVIOR OF COMPOSITE COLUMN SECTION SUBJECTED TO
AXIAL AND TORSIONAL LOADS**

A Thesis submitted to the School of Graduate Studies of Jimma University in Partial Fulfillment of the Requirements for the Degree of Master of Science in Civil Engineering (Structural Engineering)

By: Abdulmeymin Yusuf

April, 2018
Jimma, Ethiopia

Jimma University
School of Graduate Studies
Jimma Institute of Technology
Faculty of Civil and Environmental Engineering
Construction Engineering and Management Stream

**BEHAVIOR OF COMPOSITE COLUMN SECTION SUBJECTED TO
AXIAL AND TORSIONAL LOADS**

A Thesis submitted to the School of Graduate Studies of Jimma University in Partial fulfillment of the requirements for the Degree of Master of Science in Civil Engineering (Structural Engineering)

By: Abdulmeymin Yusuf

Advisor: Prof. Emer T. Quezon

Co-Advisor: Engr. Elmer C. Agon

April, 2018

Jimma, Ethiopia

DECLARATION

I, the undersigned, declare that this research report entitled “Behavior of Composite Column Sections Subjected to Axial and Torsional Loads” is original work of my own, has not been presented for a degree of any other university and that all sources of material used for the thesis have been duly acknowledged.

Abdulmeymin Yusuf



Signature

Date

This thesis has been submitted for the examination with my approval as a university supervisor.

Name

1. Prof. Emer T. Quezon



Advisor

Signature

Date

2. Eng. Elmer C. Agon, Associate Professor

Co-Advisor

Signature

Date

ACKNOWLEDGMENT

I would like to thank first of all almighty Allah who granted me the strength, patience, power and knowledge to fulfill the requirements for the Master's degree. My deepest gratitude goes to my advisor Prof. Emer T. Quezon and my co-advisor Eng. Elmer C. Agon for all their interest in my work and appreciation of my efforts and for providing me useful reference material needed to achieve my goal.

Secondly, my deepest appreciation goes to Jimma University, School of Graduate Studies, Jimma Institute of Technology, Civil Engineering Department, Structural Engineering Stream for their assistance and guidance in getting my graduate career, financial support and helping me through all the period of working on my thesis.

Lastly, my I wish to thank my parents, my friends for their love and encouragement often provided the most needed motivation to go through the hard times.

Abstract

This paper presents the behavior and performance of composite column subjected to axial load with torsion. Torsion failure is an undesirable brittle form of failure which should be avoided specially in the earthquake prone areas. Torsion in buildings during earthquake shaking may be caused from non-symmetrical distribution of mass and stiffness. So for un-symmetrical building it is necessary to design the beam and column for torsional moment.

In order to achieve the goal of study, a parametric investigation procedure is undertaken, on a series of sample column with different section of steel tube as circular, rectangular, square and encased I-section steel with and without providing longitudinal reinforcement. The material quality used for all composite column are of the same grade. Each composite column is made to be subjected to 0.4, 0.5 and 0.6 of its ultimate axial capacity with a constant Torsion of about 60 KN-m. In this work, four specimens of composite column (rectangular, square, circular composite column) is taken for analysis with making bottom end restrained against all degrees of freedom and the top end is restrained in two direction and free in direction of load.

In this study behavior of composite column conceived as dependant variable and type and magnitude of load as independent variable. The analysis is performed by finite element method using the software package Abaqus. A three dimensional model is defined using solid elements for both materials and paying special attention to the steel to concrete contact. Nonlinear behavior of steel and concrete is taken into account steel rigid plate is placed at the top and bottom of each composite column. Concentrated load and Torsion is applied on steel rigid plate placed at the top along y-direction.

The FEM output was then examined to determine the effect of different levels of axial loads on behavior of columns under torsion loading. Assessing and identifying the high stress and strain zones as the axial load is applied with and without torsion and evaluating the effects of the level of axial load on deflection/compression, rotation and twisting of the column by keeping torsion constant while axial load applied is increasing.

The finite element analysis results demonstrate that the encased composite columns reached the highest rotation/Twisting among column specimens due to the encased steel while concrete filled circular composite column shows lower rotation and twisting under torsion. Moreover, the elastic flexural stiffness as well as ductility decreases significantly with an increase in the axial loads level under constant torsion.

Keywords: Torsional Capacity, Axial Capacity, Axial load, Finite Element Method, Twisting of Column, Compression of Column, Torsion, Rotation.

Table of Contents

Contents

DECLARATION	i
ACKNOWLEDGMENT.....	ii
Abstract.....	iii
Table of Contents.....	v
LIST OF TABLES.....	vii
LIST OF FIGURES	viii
List of Symbols.....	xi
CHAPTER ONE.....	1
1.1. Background	1
1.2. Statement of the problem	3
1.3. Research questions	3
1.4. Objectives.....	3
1.4.1. General Objective	3
1.4.2. Specific Objectives	4
1.5. Significance of the study	4
CHAPTER TWO	5
REVIEW OF RELATED LITERATURES	5
2.1. Theoretical Review	5
2.2. Types of Composite Columns	8
2.2.1. Concrete Encased Composite Column	9
2.2.2. Concrete-filled composite column.....	9
2.3. Composite Column Design via the Eurocode 4	10
2.3.1. Composite Section Design.....	10
2.3.2. Eurocode 4 Beam-Column Design	17
CHAPTER THREE	25
RESEARCH METHODOLOGY AND FINITE ELEMENT MODELLING.....	25
3.1 Research Methodology.....	25
3.2. Finite Element Modelling	27
3.2.1. Introduction	27

3.2.2 Geometry	28
3.2.3 Material Definition	32
3.2.4 Interaction between concrete and steel	33
3.2.5 Loading and boundary conditions	34
3.2.6 Meshing	35
3.3 Verification of FEM of the Composite Columns	37
CHAPTER 4	39
RESULTS AND DISCUSSIONS	39
4.1 General	39
4.2 Effect of combined action of Axial and Torsion loads	39
4.2.1 Behavior of Composite Column	39
4.2.1.1 Behavior of Composite Column Under Axial Load Only	39
4.2.1.2 Behavior of Composite Column Under Axial Load and Torsion	60
4.2.1.3 Behavior of CFST section without longitudinal reinforcement under Torsion ...	77
CHAPTER 5	85
5 CONCLUSIONS AND RECCOMENDATION	85
5.1 Conclusion	85
5.2 Reccomendation	86
REFERENCES	87
Appendix A: Design of Composite Columns	89

LIST OF TABLES

Table 2.1: Buckling Curves and Member Imperfections for Composite Columns (Source: Eurocode 4, 2004)	15
Table 2.2: Buckling Reduction Factor, χ (Source: Eurocode 4, 2004)	16
The following table (Table 2.3) demonstrates the previous procedure which leads to a better understanding.....	21
Table 2.3: Stress Distributions at each Point of Interaction Curve (Major Axis Bending (Source: Kim, 2005)).....	21
Table 2.4: Stress Distributions at each Point of Interaction Curve (Minor Axis Bending) (Source: Kim, 2005).....	24
Table 3.1 Detailed cross-section and material properties	27
Table 3.2 summary of the mechanical properties of materials.	33
Table 4.1 Summary of the applied axial load.....	40
Table 4.2 Summary of the applied axial load and Torsion	60

LIST OF FIGURES

Fig. 2.1: Typical Cross-Section of Composite Columns with Fully or Partially Concrete-Encased H-sections (Source: Buick Davison, 2012)	8
Fig. 2.2: Typical Cross-Section of Composite Columns with fully or partially Concrete filled Hollow sections. (Source: Buick Davison, 2012).....	8
Fig. 2.3: European Buckling Curves.....	17
Fig. 2.4 Simplified Interaction Curve and Corresponding Stress Distributions	18
Fig.3.1 Cross-section taken for the analysis without longitudinal reinforcement.	26
Fig.3.2 Cross-section taken for the analysis with longitudinal reinforcement	26
Fig 3.3 Three dimensional steel tube (a) and concrete core (b).....	29
Fig.3.5 Three dimension square steel tube (a) and concrete core (b)	30
Fig.3.6 Three dimensional Encased I-section (a) and concrete core (b).....	31
Fig.3.7 Modelling parts that used for composite column analysis	32
Fig.3.8 Meshing of steel tube.....	35
Fig.3.9 Meshing of concrete core	36
Fig 3.10 Complete mesh of composite column	37
Fig 4.1 Axial load vs Compression at 40% of Axial Capacity of composite column	40
Fig 4.2 Axial load vs Compression at 50% of Axial Capacity of composite column	41
Fig 4.3 Axial load vs Compression at 60% of Axial Capacity of composite column	42
Fig 4.4 Compression at the center of composite column-40%P.....	43
Fig 4.5 Compression at the centre of composite column-50%P.....	44
Fig 4.6 Compression at the center of composite column-60%P.....	45
Fig 4.7 Stress – strain diagram – 40%P	46
Fig.4.8 Stress – strain diagram – 50%P	47
Fig. 4.9 Stress – strain diagram – 60%P	47
Fig.4.10 Stress of steel and concrete of RCC @ 40%P (a & b),@50%P (c & d) and @ 60%P (e & f) respectively	49
Fig 4.11 Displacement/Compression of RCC @ 40% (a), 50% (b) and 60% (c) of axial capacity	50
Fig.4.12 Stress of steel and concrete of SCC @ 40%P (a & b),@50%P (c & d) and @ 60%P (e & f) respectively.	52

Fig 4.13 Displacement/Compression of SCC @ 40% (a), 50% (b) and 60% (c) of axial capacity 53

Fig.4.14 Stress of steel and concrete of CCC @ 40%P (a & b),@50%P (c & d) and @ 60%P (e & f) respectively 55

Fig 4.15 Displacement/Compression of CCC @ 40% (a), 50% (b) and 60% (c) of axial capacity 56

Fig.4.16 Stress of steel and concrete of Encased I-section @ 40%P (a & b),@50%P (c & d) and @ 60%P (e & f) respectively 58

Fig 4.17 Displacement/Compression of CCC @ 40% (a), 50% (b) and 60% (c) of axial capacity 59

Fig 4.18 Axial load vs displacement @ 40% P 61

Fig 4.19 Axial load vs displacement @ 50% P 62

Fig 4.20 Axial load vs displacement @ 60% P 63

Fig 4.21 Torsion vs rotation of composite column as Axial Load is 40%P(a), 50%P(b), 60%(c)..... 64

Fig.4.22 Stress of steel and concrete of RCC @ 40%P (a & b),@50%P (c & d) and @ 60%P (e & f) respectively with constant Torsion. 66

Fig 4.23 Displacement/Compression of RCC @ 40% (a), 50% (b) and @ 60% (c) 67

Fig.4.24 Stress of steel and concrete of SCC @ 40%P (a & b),@50%P (c & d) and @ 60%P (e & f) respectively with constant Torsion. 69

Fig 4.25 Displacement/Compression of SCC @ 40% (a), 50% (b) and @ 60% (c) 70

Fig.4.26 Stress of steel and concrete of CCC @ 40%P (a & b),@50%P (c & d) and @ 60%P (e & f) respectively with constant Torsion. 72

Fig 4.27 Displacement/Compression of SCC @ 40% (a), 50% (b) and @ 60% (c) 73

Fig.4.28 Stress of steel and concrete of Encased I-section @ 40%P (a & b),@50%P (c & d) and @ 60%P (e & f) respectively with constant Torsion. 75

Fig 4.29 Displacement/Compression of SCC @ 40% (a), 50% (b) and @ 60% (c) 76

Fig 4.30 Axial Load vs displacement @ 40%P(a), @50%P(b) & @60%P(c) and constant T 77

Fig 4.31 Torsion vs Rotation @ 40%P (a), @50%P (b) and 60%P (c) Axial load with constant T..... 78

Fig.4.32 Stress of steel and concrete of RCC without longitudinal reinforcement @ 40%P (a & b),@50%P (c & d) and @ 60%P (e & f) respectively with constant Torsion. 80

Fig.4.33 Stress of steel and concrete of SCC without longitudinal reinforcement @ 40%P (a & b),@50%P (c & d) and @ 60%P (e & f) respectively with constant Torsion. 82

Fig.4.34 Stress of steel and concrete of CCC without longitudinal reinforcement @ 40%P (a & b),@50%P (c & d) and @ 60%P (e & f) respectively with constant Torsion. 84

List of Symbols

A	Cross-sectional area
Aa	Cross-sectional area of the structural steel section
Ac	Cross-sectional area of concrete
ACI	American Institute of Construction
A _{eff}	Effective area of a cross-section
AISC	American Institute of Steel Construction
A _r	Area of reinforcing steel
b,d	Dimension of the section
CCC	Circular Composite Column
CCFST	Circular Concrete Filled Steel Tube
CFST	Concrete Filled Steel Tubes
D,d	external and internal Dimension of the circular section
E _a	Modulus of elasticity of structural steel
E _c	Tangent modulus of elasticity of the concrete
E _{cm}	Secant modulus of elasticity of concrete
(EI) _{eff}	Effective flexural stiffness for calculation of relative slenderness
E _s	Design value of modulus of elasticity of reinforcing steel
FEA	Finite Element Analysis
FEM	Finite Element Method
f _c	The longitudinal compressive concrete stress
f _{cd}	Design value of the cylinder compressive strength of concrete
f _{ck}	Characteristic compressive cylinder strength of concrete at 28 days
f _{rd}	Design value of the cylinder compressive strength of reinforcement
f _{sd}	Design value of the yield strength of reinforcing steel in composite columns
f _y	Nominal value of the yield strength of structural steel in composite columns,

f_{yd}	Design value of the yield strength of structural steel in composite columns
I_a	Second moments of area of the structural steel section
I_c	Second moments of area of the concrete section
I_s	Second moment of area of the steel reinforcement
K_e	Correction factor, confinement effectiveness coefficient
L	Buckling length of the column (effective length)
LRFD	Load and Resistance Factor Design
M_{ED}	Design bending moment
$M_{pl,Rd}$	Design value of the elastic resistance moment of the steel section with full shear connection
M_{max}	The maximum internal moment
N_{cr}	Elastic critical normal force in composite columns
N_{pm}	Axial force resistance of concrete portion of cross-section
$N_{pl,Rd}$	Design value of plastic resistance of the composite section to compressive normal force
$N_{pl,Rk}$	Is the characteristic value of the plastic resistance of the composite section to compressive normal strength
RCC	Rectangular Composite Column
RCFST	Rectangular Concrete Filled Steel Tube
SCFST	Square Concrete Filled Steel Tube
SCC	Square Composite Column
SRC	Steel Reinforced Concrete
t	Is the wall thickness of the steel tube
t_f	Thickness of a flange of structural steel section

t_w	Thickness of a web of the structural steel section
W_{pc}	Plastic modulus of overall concrete cross-section
W_{pa}	Plastic modulus of steel section
W_{pr}	Plastic modulus of reinforcement
η_a	Factor for increasing concrete compressive strength due to confinement
η_c	Reduction factor for steel yield stress due to confinement
η_{ao}, η_{co}	Intermediate values for confinement calculations
α	Imperfection factor
λ	Slenderness ratio
δ	Steel contribution ratio
χ	Reduction factor for the relevant buckling mode

CHAPTER ONE

1.1. Background

Numerous different structural systems are used today to meet performance or functional requirements in structures. Composite construction uses the structural and constructional advantages of both concrete and steel to achieve long spans, longer story heights, and provide additional lateral stiffness. Concrete has low material costs, good fire resistance, and is easy to place. Steel has high ductility and high strength-to-weight and stiffness-to-weight ratios. When properly combined, steel and concrete can produce synergetic high load carrying capacity, admirable structural integrity, and excellent structural and dimensional stability (Kwan & Chung, 1996).

Most of composite structures consist of structural steel frame with steel-concrete composite columns to satisfy the requirements of strength and serviceability under all probable condition of loading. Composite frames have been shown to be an effective option for use as the primary lateral force resistance system of building structures; and in many cases offer significant advantages over other lateral force resistance systems (Hajjar 2002).

Buildings with non-uniform mass, stiffness and/or strength over their plan are often described as being torsionally irregular. Even for structures designed to be perfectly regular, the movement of live loads around the structure can cause torsional irregularity which in turn changes the member demands. There is currently an understanding of how different parameters may influence torsion (Au, 2007), however, the degree to which these factors influence torsion is relatively unknown.

When a member is subject to torsion it will twist about a longitudinal axis which passes through the shear center of the cross section. However, torsion will not occur if the section is loaded in such a manner that the resultant force passes through the shear center. In the majority of design situations, the loads are applied so that the resultant force passes through the centroid. If the section is doubly symmetric, this automatically eliminates torsion because the centroid and the shear center coincide.

Composite columns provide the required stiffness to limit the total drift of the building to acceptable levels of the lateral displacement, resist the lateral seismic and wind loads very

effectively and speed up the construction process by advancing the erection of the structural steel formwork to support several floors at time before casting the concrete column encasement which produce an economic structure. There are two basic kinds of composite columns: steel sections encased in concrete (steel-reinforced concrete sections or SRC) and steel sections filled with concrete (concrete filled tubes or CFT). The latter can be either circular (CCFT) or square/rectangular (RCFT) in cross-section.

Steel structural hollow sections are the most efficient of all the structural sections in resisting compression load and filling these sections with plain concrete significantly increases load-bearing capacity. CFST columns have a number of advantages as follows: a) it combines tension properties of steel and compression properties of concrete and provides the hollow steel sections with greater strength and stiffness, b) the confinement of concrete by steel enhances failure strength of concrete, c) column size may be reduced more than necessary for pure steel or RC column and provide greater floor area for use, d) the steel tube provides the permanent formwork for concrete, e) steel tube column can be erected rapidly for a number of story heights, allowing to add floors before filling tubes with concrete, f) good seismic resistance because of good ductility and high energy absorbing properties (Kvedaras et al. 2006). In encased sections, the concrete delays failure by local buckling and acts as fireproofing while the steel provides substantial residual gravity load-carrying capacity after the concrete fails.

The use of composite structures has become widespread in the Middle East, with Dubai today housing some of the highest buildings in the world, in Japan and China. Also, there are extensive interests of using composite systems for the seismic resistance design.

The current design provisions for composite columns come primarily from the Manual of Steel Construction - Load and Resistance Factor Design (LRFD) [AISC 1999]. These provisions are based in rules developed in the 1960s and 1970s (SSRC TG20, 1979) and utilize an approach in which the composite column is turned into an equivalent steel one. This approach has been shown to yield very low reliability indices (Leon and Aho, 2000), and a complete reassessment of the design for composite columns has been made in 2005 AISC Specification. BS EN 1994-1-1 Eurocode 4 presents the latest design recommendations for all types of composite columns (Buick Davison and Graham W. Owen, 2012).

1.2. Statement of the problem

The main aim of composite column construction is to achieve a higher level of performance than would have been the case had the two materials functioned separately. The flexural capacity and ductility of composite columns decreased when a constant torsion was simultaneously applied (Hsu et al. 2003).

Torsional behaviour of asymmetric building is one of the most frequent causes of structural damage and failure during strong ground motions. The torsional moment may reduce the shear capacity of the columns.

An un-symmetrical building structures are almost unavoidable in modern construction due to various type of functional and architectural requirements. Torsion in buildings during earthquake shaking may be caused from non-symmetrical distribution of mass and stiffness. So for un-symmetrical building it is necessary to design the beam and column for torsional moment. In this study the researcher investigated different section of composite column under axial and torsional loads to determine suitable section of composite columns.

1.3. Research questions

The research questions that this study go to explain; are as follows:

1. What are the possible effects of composite column sections subjected to axial and torsional loads?
2. Which type of steel section and composite column are preferable under axial and torsional loads?
3. Which high stress and strain zones can be formed on composite column section when it is subjected to axial and torsional loads?

1.4. Objectives

1.4.1. General Objective

The main objective of the study were to investigate behavior or response of composite column sections under axial and torsional loads.

1.4.2. Specific Objectives

1. To evaluate and analyze the effect of combined action of axial and torsional loads on composite column
2. To identify possible steel section type and column section suitable for composite column subjected to axial and torsional loads.
3. To Identify the high stress and strain zones of composite column subjected to axial and torsional loads.

1.5. Significance of the study

- The study evaluates the torsional strength of different composite column section.
- This study compares the torsional strength of reinforced concrete column section to that of composite column.
- The study provides/determine appropriate sections of composite column to be used in seismic areas and when beam-column jointing is eccentric.
- The findings help to reduce/eliminate the cracks that will appear on the column faces at seismic areas by recommending suitable section.

CHAPTER TWO

REVIEW OF RELATED LITERATURES

2.1. Theoretical Review

Composite columns are structural members, which are subjected mainly to axial compressive forces and end moments. The general term 'composite column' refers to any compression member in which the steel element acts compositely with the concrete. So that both elements contribute to the strength. These columns have been used widespread as they speed up construction by eliminating formwork and the need for tying of longitudinal reinforcement. Composite columns have recently undergone increased usage throughout the world, which has been influenced by the development of high strength concrete permitting these columns to be considerably economized. Columns designed to resist the majority of axial force by concrete alone can be further economized by the use of thin-walled steel columns. New developments, including the use of high strength concrete and the credit of the enhanced local buckling capacity of the steel has allowed much more economical designs to evolve. Concrete filled steel tubes (CFST) are widely used in recent decades.

CFSTs have shown better structural performance such as strength, stiffness, and ductility than that of bare steel or reinforced concrete members. Conventionally, CFSTs are designated by the shape of the steel tube which includes rectangular, square, circular and elliptical hollow sections. For CFST columns of circular section (CCFST) in particular, the steel tube provides significant confinement to the concrete core, which leads to an increase in both strength and ductility of the concrete, while the steel tube also acts as permanent formwork as well as reinforcement for the concrete. The concrete core, in turn, restricts inward local buckling of the steel tube. Comprehensive experimental and analytical researches on concrete filled tubular steel columns have been ongoing throughout the world for many years and were reported in the literatures (Yin and Lu 2010). The majority of these experiments however have been on moderate scale specimens (CCFST for example, less than 200 mm in diameter) using normal and high-strength concrete. Experimental study also showed (Han and Yao 2003) that the concrete compaction would affect the interaction between the steel tube and the concrete core, and thus the behaviour of the composite columns.

Codes and design specifications have been evaluated and developed, more or less in an enormous dissimilarity in the analytical models for evaluating the strength of a CFST composite column and the effect of confinement. Specifically, the ACI provisions (ACI Committee 318 2011) assume that the capacity of a CFST column can be predicted by treating the column as an ordinary reinforced concrete column, while in AISC provisions (American Institute of Steel Construction 2010), the design philosophy is to create modified cross sectional properties from the composite column and then design the composite column as an equivalent steel column using the modified properties in place of the steel properties. For calculating the axial capacity, codes such as ACI and Japanese Standards (Architectural Institute of Japan 1997) do not take into consideration of the concrete confinement, while some such as Eurocode 4 (European Committee for Standardization. 2004) take the strength contribution from the concrete confinement.

Most researches carried out to date on concrete filled steel tubes are based on the assumption that there is inherent perfect interaction between the concrete and the steel tube (Liang and Fragomeni 2010, Uwe et al. 2010, Xu et al. 2010, Bahrami et al. 2011). In construction practice, however, defects like concrete inanity or debonding of the concrete from steel tube have been found at the steel-concrete interface of the concrete-filled steel tubes. Debonding separation at the steel concrete interface of a CFST composite member could be induced by plastic shrinkage, and long term effect of concrete like temperature, shrinkage and creep as well as improper concrete casting. These concrete defects would penalize the structural performance of the composite columns. Besides, some defects of inanity between the steel plate and the concrete are identified being inherent shortcomings of concrete casting owing to substantial plastic shrinkage in concrete.

The negative influences of the debonding on the axial loading capacity of the CFST columns were investigated experimentally by Liu et al. (2011). The defects of inanity between the steel tube, steel plate and the concrete were found to affect the structural behaviour and performance of the concrete filled steel tubes. The ultimate load capacity and the ductility of the CFSTs were also found significantly decreased with an increase of the debonding separation gap. In the CFST column construction practice, using low shrinkage concrete or even self compact concrete is one way to improve the construction quality, but more or less, the defects of inanity

still occur between the steel and concrete in the concrete-filled steel tubes. As far as the defects are inspected, the essential retrofit and repair are required which are normally expensive and time consuming.

A lot of experiments have been carried out to investigate the parameters that affect the axial capacity of composite columns. It was found that there are various parameters, including shape of steel section, longitudinal steel reinforcement, material properties of the concrete, the confinement effect of the concrete, slenderness ratio of the column, and concrete and steel strength. (Ellobody & Young, 2011).

Ellobody et al.(2010) studied the responses of concrete encased steel composite columns to eccentrically load acting along the major axis. Many variables that influence this response such as the concrete strength, the steel section yield stress, eccentricities, column dimensions, and structural steel sizes were investigated. A three-dimensional finite element analysis using ABAQUS has been developed and it has been validated against experimental result. Eccentric Load–concrete strength curves, axial load-moment curves, and ultimate capacity were obtained. The results showed that the increase in steel section yield stress has significant effect on the strength of eccentrically load composite column with small eccentricity with concrete lower than 70 MPa compressive strength. A conclusion was drawn after compared the results with Eurocode 4 (Eurocode 4, 2004) that the eccentric load were predicted correctly but the moment values were overestimated.

Han LH (2002), has done a research on the behavior of composite CFT columns under pure torsion. Han in this research examined the performance of square steel tubular columns filled with concrete under pure torsion using the ABAQUS software. The finite element method (FEA) was used to assess the impact of important parameters that determine the ultimate tensional strength of composite sections. Han found that steel pipe plays an important role in the tensional resistance of composite columns which are square or circular, and the composite columns show a good Stability and plastic behaviour under torsion.

El-Boghdadi MH,(2009). performed a Research on composite columns under earthquake loads. He found that CFT columns under seismic loads, show very high levels of ductility and

energy dissipation. It was also observed that the test samples maintained the flexural capacity until the test to be concluded.

2.2. Types of Composite Columns

There are two basic types of composite columns mostly used in buildings: those with steel sections encased in concrete (steel-reinforced concrete sections or SRC) and those with the steel sections filled with concrete (concrete filled tubes or CFT). The latter can be either circular (CCFT) or square/rectangular (RCFT) in cross-section, examples of which are shown in Figures 2.1 and 2.2 respectively.

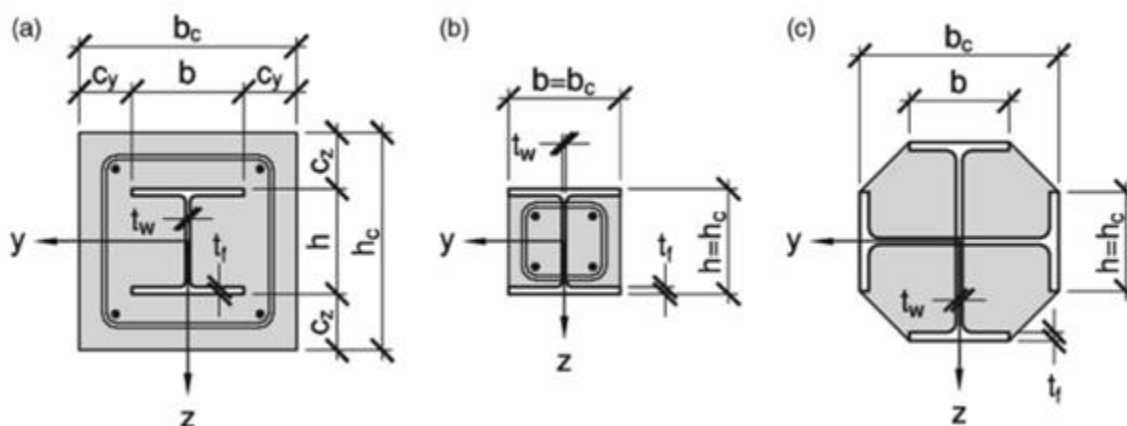


Fig. 2.1: Typical Cross-Section of Composite Columns with Fully or Partially Concrete-Encased H-sections (Source: Buick Davison, 2012)

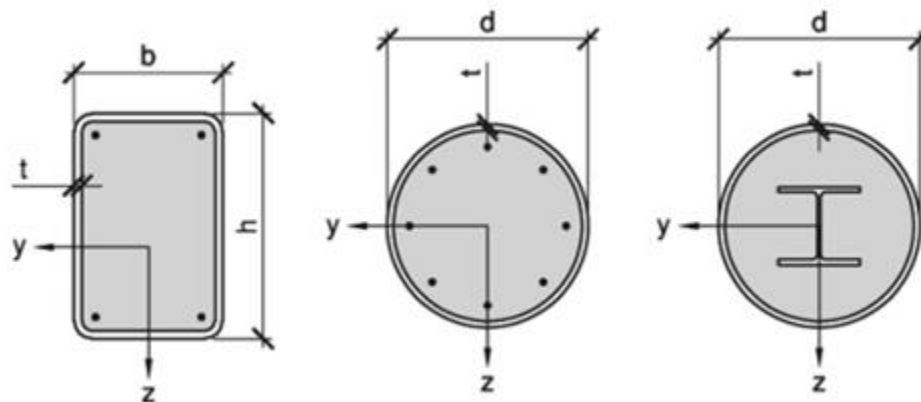


Fig. 2.2: Typical Cross-Section of Composite Columns with fully or partially Concrete filled Hollow sections. (Source: Buick Davison, 2012)

2.2.1. Concrete Encased Composite Column

One of the common and popular columns is the encased steel profile (Figure.2.1) where a steel H-section is encased in concrete. Sometimes, structural pipe, tube, or built up section is placed instead of the H-section. In addition to upholding a proportion of the load acting on the column, the concrete encasement enhances the behavior of the structural steel core by horizontal bar reinforcement, and so making it more effective against both local and overall buckling. In encased sections, the concrete delays failure by local buckling and acts as fireproofing while the steel provides substantial residual gravity load-carrying capacity after the concrete fails. The cross sections, which normally are square or rectangular, must have one or extra longitudinal bars placed in every single corner and these have to be tied by lateral ties at regular vertical intervals in the manner of a reinforced concrete column. Ties are effective in rising column strength, confinement and ductility. Furthermore, they stop the longitudinal bars from being displaced during construction and they resist the tendency of these same bars to buckle outward under load, which would cause spalling of the outer concrete cover even at low load levels, remarkably in the case of eccentrically loaded columns. It will be noted that these ties will be open and U-shaped. Otherwise, they might not be installed, because the steel column shapes will have always been erected at an earlier time.

2.2.2. Concrete-filled composite column

In this type of composite columns, a steel pipe, steel tubing, or built up section is filled with concrete (Figure.2.2). The most common steel sections used are the hollow rectangular and circular tubes. Filled composite columns may be the most efficient application of materials for column cross sections. It provides forms for the inexpensive concrete core and increases the strength and stiffness of the column. In addition, because of its relatively high stiffness and tensile resistance, the steel shell provides transverse confinement to the concrete, making the filled composite column very ductile with remarkable toughness to survive local overloads. In concrete-filled tubes, the steel increases the strength of the concrete because of its confining effect, the concrete inhibits local buckling of the steel, and the concrete formwork can be omitted.

2.3. Composite Column Design via the Eurocode 4

For satisfaction of the main aim of this study; investigate the behavior of composite columns subjected to Axial and Torsional loads by comparing the capacity of different section of steel of composite column and reinforced concrete column section, it is first necessary to review the design procedures that will be used for composite and reinforced concrete columns to be able to use them in preliminary design.

In fact, Eurocode presents the most recent rules and comprehensive review among other design codes and specifications. As a result, Eurocode 2 and 4 were chosen for design of reinforced concrete and composite columns respectively. This section will be elucidated on the design procedure of composite columns according to Eurocode 4 (EN 1994) to resist axial loads and torsion moments. Whereas the design procedures of reinforced concrete columns, which will be used for the comparison purposes, will be summarized in appendix.

To begin with, there are two design methods mentioned in Eurocode 4 for composite columns design; the general method which appropriate for non-symmetrical or nonuniform columns and the simple method for members of doubly symmetrical and uniform over the member length.

For the composite columns design, Eurocode has mentioned some limitations which shall satisfy; Slenderness parameter of the column should be less than 2%, the longitudinal reinforcement which can be used should be no more than 6% and not less than 0.3% of the concrete area, 0.2 and 0.5 are given as limits for the depth to width ratio of the composite cross-section.

2.3.1. Composite Section Design

The plastic resistance to compression $N_{pl,Rd}$ of a composite cross-section should be calculated by adding the plastic resistances of its components; the structural steel, the concrete and the reinforcement, should be added. The plastic resistance equation for encased-composite column is:

$$N_{pl,Rd} = A_a f_{yd} + 0.85 A_c f_{cd} + A_s f_{sd} \quad (2.1)$$

where

- A_a the cross-sectional area of the structural steel
 A_c the cross-sectional area of the concrete
 A_s the cross-sectional area of the reinforcement
 f_{cd} Design value of the cylinder compressive strength of concrete
 f_{sd} Design value of the yield strength of reinforcing steel
 f_{yd} Design value of the yield strength of structural steel

For filled-composite column, the coefficient 0.85 may be replaced by 1.0.

The plastic resistance of circular cross-section equation is:

$$N_{pl,Rd} = \eta_a A_a f_{yd} + A_c f_{cd} \left[1 + \eta_c \frac{t}{d} \frac{f_y}{f_{ck}} \right] + A_s f_{sd} \quad (2.2)$$

where

- f_y Nominal value of the yield strength of structural steel
 f_{ck} Characteristic compressive cylinder strength of concrete at 28 days
 d Is the outside diameter of the steel tube
 t Is the wall thickness of the steel tube
 η_a, η_c Factors related to the confinement of concrete

When the eccentricity of loading, e, equal to 0, the values of η_a = η_{a0} and η_c = η_{c0} are given by the following expressions:

$$\eta_{a0} = 0.25(3 + 2\lambda) \quad \text{but } \leq 1 \quad (2.3)$$

$$\eta_{c0} = 4.9 - 18.5\lambda + 17\lambda^2 \quad \text{but } \geq 0 \quad (2.4)$$

where

- η_{a0}, η_{c0} Factors related to the confinement of concrete

λ General slenderness parameter

When eccentricity to outside diameter ratio, e/d , falls between 0 and 0.1, the values η_a and η_c should be determined from (Equation 2.5) and (Equation 2.6), where η_{a0} and η_{c0} are given by (2.3) and (2.4):

$$\eta_a = \eta_{a0} + (1 - \eta_{a0})(10e/d) \quad (2.5)$$

$$\eta_c = \eta_{c0}(1 - 10e/d) \quad (2.6)$$

For $e/d > 0.1$, $\eta_a = 1.0$ and $\eta_c = 0$.

The eccentricity of loading, e , is defined as

$$e = \frac{M_{ED}}{N_{ED}} \quad (2.7)$$

where

M_{Ed} Design bending moment

N_{Ed} Design value of the compressive normal force

The steel contribution ratio δ is defined as:

$$\delta = \frac{A_a f_{yd}}{N_{pl,rd}} \quad (2.8)$$

where:

$N_{pl,Rd}$ is the plastic resistance to compression

The relative slenderness, λ , is defined by:

$$\lambda = \sqrt{\frac{N_{pl,Rk}}{N_{cr}}} \quad (2.9)$$

Where

$N_{pl,Rk}$ the characteristic value of the plastic resistance to compression given by (Equation 2.1)

N_{cr} the elastic critical normal force for the relevant buckling mode, calculated with the effective flexural stiffness $(EI)_{eff}$

$$N_{cr} = \frac{(EI)_{eff} \pi^2}{(KL)^2} \quad (2.10)$$

where

L buckling length of the column (effective length)

$(EI)_{eff}$ Effective flexural stiffness given by (Equation 2.11)

$$(EI)_{eff} = E_a I_a + E_s I_s + K_e E_{cm} I_c \quad (2.11)$$

where

K_e correction factor that should be taken as 0.6

I_a the second moment of area of the structural steel section

I_c the second moment of area of the un-cracked concrete section

I_s the second moment of area of the reinforcing steel

E_a Modulus of elasticity of structural steel

E_{cm} The secant modulus of concrete, (Equation 2.12)

E_s Design value of modulus of elasticity of reinforcing steel

$$E_{cm} = 22 \left[\frac{f_{cm}}{10} \right]^{0.3} \quad (2.12)$$

$$f_{cm} = f_{ck} + 8 \quad (2.13)$$

For simplification for members in axial compression, the design value of the normal force N_{ed} ought to satisfy:

$$\frac{N_{Ed}}{\chi N_{pl,Rd}} \leq 1.0 \quad (2.14)$$

where

$N_{pl,Rd}$ The plastic resistance of the composite section but with f_{yd} determined using the partial factor γ_{M1} which is equal 1 for buildings

χ The reduction factor for column slenderness

$$\chi = \frac{1}{\phi + \sqrt{\phi^2 - \lambda^2}} \leq 1.0 \quad (2.15)$$

Where

$$\phi = 0.5[1 + \alpha(\lambda - 0.2) + \lambda^2] \quad (2.16)$$

α imperfection factor which can consider as 0.21 for concrete-filled circular and rectangular hollow sections, 0.34 for completely or partly concrete encased I-section with bending about the major axis of the profile, and 0.49 for completely or partly concrete-encased I-section with bending about the minor axis of the profile

The relevant buckling curves for cross-sections of composite columns are given in Table 2.1, where ρ_s is the reinforcement ratio, A_s / A_c . In order to find the value of the reduction factor, χ the relative slenderness, λ should be calculated first according to (Equation 2.9) then Figure 2.1, or Table 2.2 can be used.

Table 2.1: Buckling Curves and Member Imperfections for Composite Columns (Source: Eurocode 4, 2004)

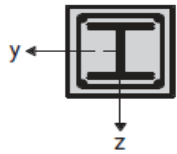
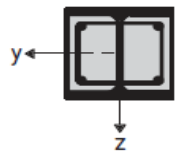
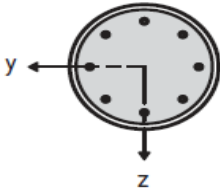
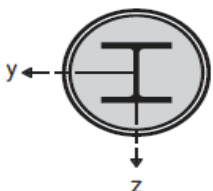
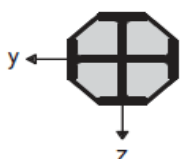
Cross-section	Limits	Axis of buckling	Buckling curve	Member imperfection
concrete encased section 		y-y	b	$L/200$
		z-z	c	$L/150$
partially concrete encased section 		y-y	b	$L/200$
		z-z	c	$L/150$
circular and rectangular hollow steel section 	$\rho_s \leq 3\%$	any	a	$L/300$
	$3\% < \rho_s \leq 6\%$	any	b	$L/200$
circular hollow steel sections with additional I-section 		y-y	b	$L/200$
		z-z	b	$L/200$
partially concrete encased section with crossed I-sections 		any	b	$L/200$

Table 2.2: Buckling Reduction Factor, χ (Source: Eurocode 4, 2004)

λ	Buckling curve			
	a	b	c	d
0.00	1.00	1.00	1.00	1.00
0.10	1.00	1.00	1.00	1.00
0.20	1.00	1.00	1.00	1.00
0.30	0.98	0.96	0.95	0.92
0.40	0.95	0.93	0.90	0.85
0.50	0.92	0.88	0.84	0.78
0.60	0.89	0.84	0.79	0.71
0.70	0.85	0.78	0.72	0.64
0.80	0.80	0.72	0.66	0.58
0.90	0.73	0.66	0.60	0.52
1.00	0.67	0.60	0.54	0.47
1.10	0.60	0.54	0.48	0.42
1.20	0.53	0.48	0.43	0.38
1.30	0.47	0.43	0.39	0.34
1.40	0.42	0.38	0.35	0.31
1.50	0.37	0.34	0.31	0.28
1.60	0.33	0.31	0.28	0.25
1.70	0.30	0.28	0.26	0.23
1.80	0.27	0.25	0.23	0.21
1.90	0.24	0.23	0.21	0.19
2.00	0.22	0.21	0.20	0.18
2.10	0.20	0.19	0.18	0.16
2.20	0.19	0.18	0.17	0.15
2.30	0.17	0.16	0.15	0.14
2.40	0.16	0.15	0.14	0.13
2.50	0.15	0.14	0.13	0.12
2.60	0.14	0.13	0.12	0.11
2.70	0.13	0.12	0.12	0.11
2.80	0.12	0.11	0.11	0.10
2.90	0.11	0.11	0.10	0.09

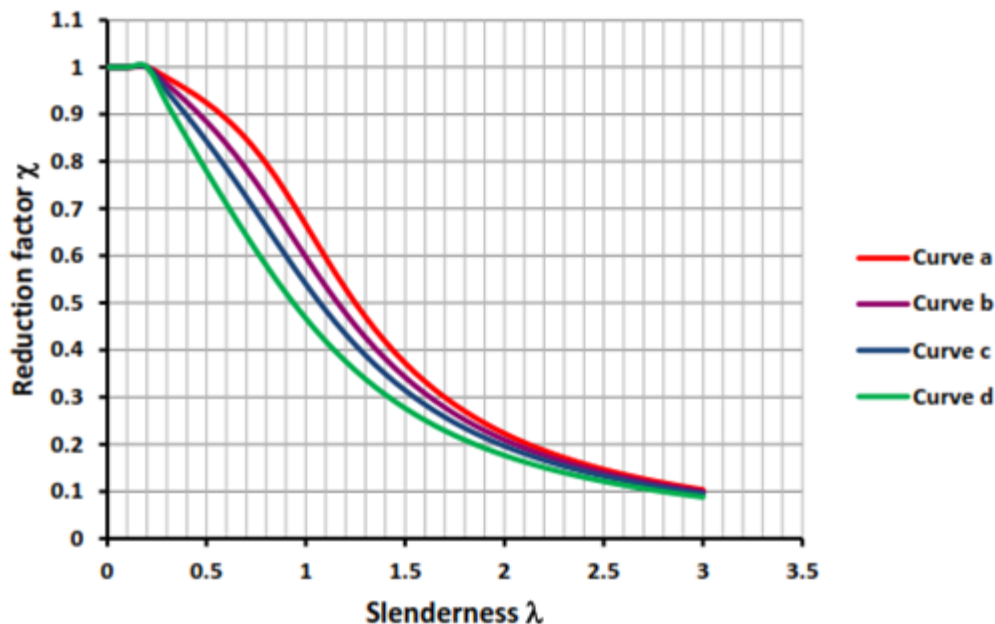


Fig. 2.3: European Buckling Curves (Source: Eurocode 3, 2005)

2.3.2. Eurocode 4 Beam-Column Design

The behavior of column subjected to axial load and bending moment can be given by interaction curve showing the reduction of ultimate load with increasing moment. An approximation to this curve can be obtained by considering fully plastic sections for different arbitrary positions of the neutral axis. The values of the moment and axial compression calculated from the stress block will give the points to construct the curve. Generally, the numbers of points required for drawing the interaction curve depend on moment application about which axis; if the end moment about major axis, four key points from A-D are required (see Figure 2.2). Otherwise, one additional key point is required at end of structural steel section if the end moment about minor axis; five key points from A-E.

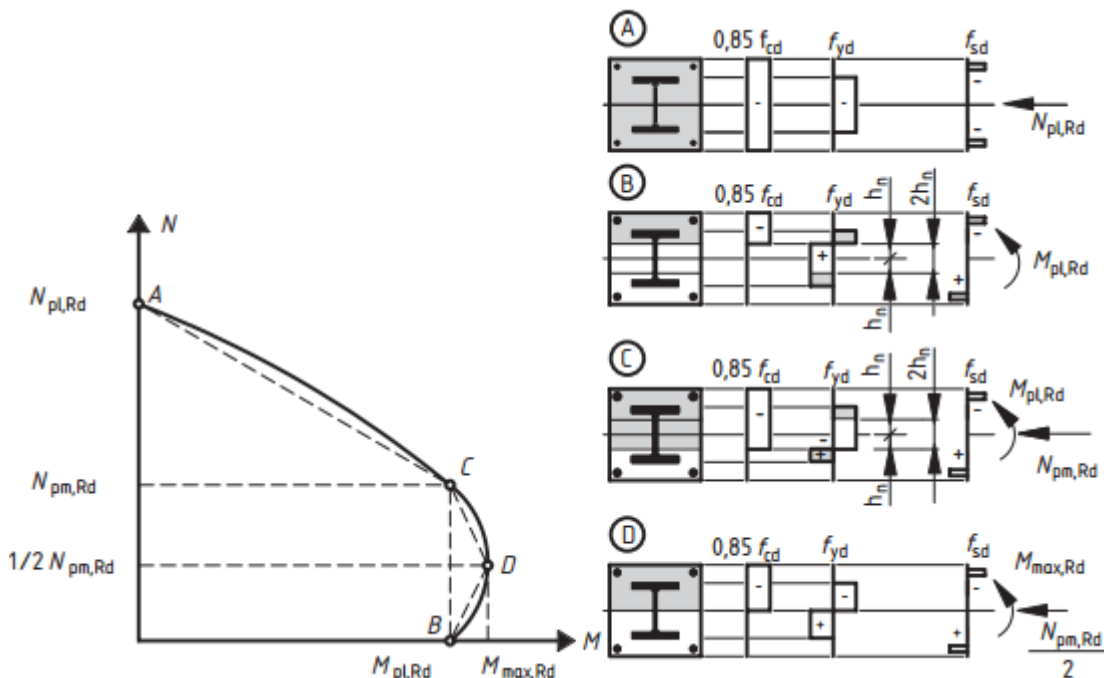


Fig. 2.4 Simplified Interaction Curve and Corresponding Stress Distributions

(Source : Eurocode 4, 2004)

The maximum internal moment at point D is:

$$M_{\max} = Z_s f_{yd} + \frac{1}{2} Z_c f_{cd} + Z_r f_{sd} \quad (2.17)$$

where

Z_s plastic modulus of steel cross-section

Z_c plastic modulus of overall concrete cross-section.

Z_r plastic modulus of reinforcement

The plastic modulus of the reinforcement can be calculated as:

$$Z_r = \sum_{i=1}^n A_{ri} e_i \quad (2.18)$$

where

A_{ri} area of one reinforcing bar

e_i distance to the bending axis considered

For the region equal twice the distance between centroid axis and neutral axis, $2h_n$, the plastic moment can be calculated as:

$$M_{pn} = Z_{sn} f_{yd} + \frac{1}{2} Z_{cn} f_{cd} + Z_{rn} f_{sd} \quad (2.19)$$

where

Z_{sn} Plastic section modulus of steel section within $2h_n$ region

Z_{rn} Plastic section modulus of reinforcing steel within $2h_n$ region

Z_{cn} Plastic section modulus of concrete within $2h_n$ region

For concrete incased I- steel section, the plastic modulus about major axis can be taken from the design tables (Table 2.3), or the following equation can be used:

$$Z_s = \frac{(d - 2t_f)t_w^2}{4} + b_f t_f (d - t_f) \quad (2.20)$$

where

d Overall depth of the structural steel section

b_f Width of the flange of a steel section

t_f Thickness of a flange of the structural steel section

t_w Thickness of a web of the structural steel section

The plastic modulus of the concrete is:

$$Z_c = \frac{h_1 h_2}{4} - Z_s - Z_r \quad (2.21)$$

where

h_1, h_2 Dimension of the section

There are three possible zones to look into position of the neutral axis; neutral axis in the web ($h_n \leq d/2 - t_f$), neutral axis in the flange ($d/2 - t_f \leq h_n \leq d/2$), and Neutral Axis outside the steel section ($d/2 \leq h_n \leq h/2$). For finding the location of the neutral axis, assume h_n is located on a certain region, then use (Equations 2.22 to 2.26) to find new value for h_n . If the value of h_n is inside the supposed region, the assumption was correct. Otherwise, select another region and repeat the procedure.

The distance h_n and plastic modulus can be calculated according to possible position as follow:

Neutral Axis in the web ($h_n \leq d/2 - t_f$)

$$h_n = \frac{N_{pm} - A_{rn}(2f_{sd} - f_{cd})}{2h_1f_{cd} + 2t_w(2f_{yd} - f_{cd})} \quad (2.22)$$

Where

A_{rn} Is the sum of reinforcement inside within the $2h_n$ region

N_{pm} Axial force resistance of concrete portion of cross-section

$$Z_{sn} = t_w h_n^2 \quad (2.23)$$

Neutral Axis in flange ($d/2 - t_f \leq h_n \leq d/2$)

$$h_n = \frac{N_{pm} - A_{rn}(2f_{sd} - f_{cd}) + (b_f - t_w)(d - 2t_f)(2f_{yd} - f_{cd})}{2h_1f_{cd} + 2b_f(2f_{yd} - f_{cd})} \quad (2.24)$$

$$Z_{sn} = b_f h_n^2 - \frac{(b_f - t_w)(d - 2t_f)^2}{4} \quad (2.25)$$

Neutral Axis outside the steel section ($d/2 \leq h_n \leq h/2$)

$$h_n = \frac{N_{pm} - A_{rn}(2f_{sd} - f_{cd}) - A_s(2f_{yd} - f_{cd})}{2h_1f_{cd}} \quad (2.26)$$

$$Z_{sn} = Z_s \quad (2.27)$$

The plastic modulus of the concrete in the region of $2h_n$ is given as

$$Z_{cn} = h_1 h_n^2 - Z_{sn} - Z_{rn} \quad (2.28)$$

The following table (Table 2.3) demonstrates the previous procedure which leads to a better understanding.

Table 2.3: Stress Distributions at each Point of Interaction Curve (Major Axis Bending)
(Source: Kim, 2005)

	Section	Stress Distribution	Equation
A			$N = P_{pl} = A_c \cdot f_{cd} + A_s \cdot f_{yd} + A_r \cdot f_{rd}$ $f_{cd} = 0.85 \cdot f'_c / \gamma_c, f_{yd} = F_y / \gamma_s, f_{rd} = F_{yr} / \gamma_r$ $\gamma_c, \gamma_s, \gamma_r : \text{partial safety factors}$ $A_c = h_1 \cdot h_2 - A_s - A_r$ $M = 0$
B			$N = 0$ $h_n \rightarrow h_1 \cdot a \cdot f_{cd} = (h_2 - 2a) \cdot t_w \cdot f_{yd}$ $M = M_{pn} = Z_{sn} \cdot f_{yd} + \frac{1}{2} \cdot Z_{cn} \cdot f_{cd} + Z_{rn} \cdot f_{rd}$ $Z_{sn} = t_w \cdot h_n^2 ; Z_{cn} = h_1 \cdot h_n^2 - Z_{sn} - Z_{rn}$
C			$N = N_{pm} = A_c \cdot f_{cd}$ $h_n \rightarrow h_1 \cdot a \cdot f_{cd} = (h_2 - 2a) \cdot t_w \cdot f_{yd}$ $M = M_{pn} = Z_{sn} \cdot f_{yd} + \frac{1}{2} \cdot Z_{cn} \cdot f_{cd} + Z_r \cdot f_{rd}$
D			$N = \frac{1}{2} \cdot N_{pm} = \frac{1}{2} \cdot A_c \cdot f_{cd}$ $M = M_{max} = Z_s \cdot f_{yd} + \frac{1}{2} \cdot Z_c \cdot f_{cd} + Z_r \cdot f_{rd}$ $Z_s = \frac{(d - 2 \cdot t_f) \cdot t_w^2}{4} + b_f \cdot t_f \cdot (d - t_f)$ $Z_c = \frac{h_1 \cdot h_2^2}{4} - Z_s - Z_r$

In case the end moment about minor axis, the plastic modulus can be taken from Table 2.4, or it calculates as:

$$Z_s = \frac{(d - 2t_f)t_w^2}{4} + \frac{2t_f b_f^2}{4} \quad (2.29)$$

For the concrete, the plastic modulus is obtained from:

$$Z_c = \frac{h_1 h_2}{4} - Z_s - Z_r \quad (2.30)$$

Here, for the location of the neutral axis, two regions need to be considered; neural axis in the flanges ($tw/2 \leq hn \leq bf/2$), and neural axis in the flanges ($bf/2 \leq hn \leq h2/2$). The same iterative procedure should be used. The following equations explain the way for finding the distance hn and plastic modulus.

Neutral Axis in the web ($tw/2 \leq hn \leq bf/2$)

$$h_n = \frac{N_{pm} - A_{rn}(2f_{sd} - f_{cd}) - t_w(2t_f - d)(2f_{yd} - f_{cd})}{2h_1 f_{cd} + 4t_f(2f_{yd} - f_{cd})} \quad (2.31)$$

$$Z_{sn} = 2t_f h_n^2 + \frac{(d - 2t_f)t_w^2}{4} \quad (2.32)$$

Neutral Axis in the flanges ($bf/2 \leq hn \leq h2/2$)

$$h_n = \frac{N_{pm} - A_{rn}(2f_{sd} - f_{cd}) - A_s(2f_{yd} - f_{cd})}{2h_1 f_{cd}} \quad (2.33)$$

$$Z_{sn} = Z_s \quad (2.34)$$

The plastic modulus of the concrete in the region of $2hn$ is given as

$$Z_{cn} = h_1 h_n^2 - Z_{sn} - Z_{sn} \quad (2.35)$$

The axial force at point E is given as

$$N_E = h_2(h_E - h_n)f_{cd} + 2t_f(h_E - h_n)(2f_{yd} - f_{cd}) + A_{rE}(2f_{sd} - f_{cd}) + N_{pm} \quad (2.36)$$

$$M_E = M_{\max} - \Delta M_E \quad (2.37)$$

Where

$$\Delta M_E = Z_{sE} f_{yd} + \frac{1}{2} Z_{cE} f_{cd} + Z_{rE} F_{sd} \quad (2.38)$$

- M_{\max} The maximum internal moment
- Z_{cE} Plastic section modulus of concrete within $2h_E$ region
- Z_{rE} Plastic section modulus of reinforcing steel within $2h_E$ region
- Z_{sE} Plastic section modulus of steel section within $2h_E$ region

Which the terms Z_{sE} , Z_{cE} , and Z_{rE} can be calculated from the appropriate equations above by substituting h_E instead of h_n .

Table 2.4: Stress Distributions at each Point of Interaction Curve (Minor Axis Bending) (Source: Kim, 2005)

	Section	Stress Distribution	Equation
A			$N = P_{pl} = A_c \cdot f_{cd} + A_s \cdot f_{yd} + A_r \cdot f_{rd}$ $A_c = h_1 \cdot h_2 - A_s - A_r$ $f_{cd} = 0.85 \cdot f'_c / \gamma_c, f_{yd} = F_y / \gamma_s, f_{rd} = F_{yr} / \gamma_r$ $M = 0$
B			$N = 0$ $h_n \rightarrow h_1 \cdot a \cdot f_{cd} = 2 \cdot (h_2 - 2a) \cdot t_f \cdot f_{yd} + (d - 2 \cdot t_f) \cdot t_w \cdot f_{yd}$ $M = M_{pn} = Z_{sn} \cdot f_{yd} + \frac{1}{2} \cdot Z_{cn} \cdot f_{cd} + Z_r \cdot f_{rd}$ $Z_{sn} = 2 \cdot t_f \cdot h_n^2 + \frac{(d - 2 \cdot t_f) \cdot t_w^2}{4}$ $Z_{cn} = h_1 \cdot h_n^2 - Z_{sn} - Z_r$
C			$N = N_{pm} = A_c \cdot f_{cd}$ $M = M_{pn} = Z_{sn} \cdot f_{yd} + \frac{1}{2} \cdot Z_{cn} \cdot f_{cd} + Z_r \cdot f_{rd}$
D			$N = \frac{1}{2} \cdot N_{pm} = \frac{1}{2} \cdot A_c \cdot f_{cd}$ $M = M_{max} = Z_s \cdot f_{yd} + \frac{1}{2} \cdot Z_c \cdot f_{cd} + Z_r \cdot f_{rd}$ $Z_s = \frac{(d - 2 \cdot t_f) \cdot t_w^2}{4} + \frac{1}{2} \cdot t_f \cdot b_f^2$ $Z_c = \frac{h_1 \cdot h_2^2}{4} - Z_s - Z_r$
E			$N = \frac{1}{2} \cdot (P_{pl} + N_{pm})$ $M = M_{max} - \Delta M_E, \Delta M_E = Z_{sE} \cdot f_{yd} + \frac{1}{2} \cdot Z_{cE} \cdot f_{cd} + Z_{rE} \cdot f_{rd}$ $Z_{sE} = 2 \cdot t_f \cdot h_E^2 + \frac{(d - 2 \cdot t_f) \cdot t_w^2}{4}$ $Z_{cE} = h_1 \cdot h_E^2 - Z_{sE} - Z_{rE}$

CHAPTER THREE

RESEARCH METHODOLOGY AND FINITE ELEMENT MODELLING

3.1 Research Methodology

The main purpose of this study was to determine the effects of torsion on different levels of axial loads on the capacity of different section of composite column. To achieve this, a finite element analysis was conducted with all appropriate parameters considered. The finite element method is a numerical analysis technique for obtaining approximate solutions to a wide variety of engineering problems.

Examining the behavior of Rectangular composite column (RCC), Square Composite Column (SCC), Circular Composite Column (CCC), Encased I-section composite column with and without providing longitudinal reinforcement under different levels of axial loads and constant Torsion will be carried out by taking different cross section of composite column with approximately equal areas of concrete and steel section and calculating its axial load capacity then comparing their behaviors.

In these study behavior of four specimens rectangular composite column, square composite column, circular composite column and Encased I-section are subjected to 40%, 50% and 60% of their respective axial capacity without applying torsion moment and analyzed under axial load only using abaqus software. from result output the compression/deflection in the direction of load, stress distribution for all four column is evaluated for each case of loading.

In the second case keeping all condition of composite column and axial loading same to previous one but applying a constant Torsion with increasing axial load, the results again evaluated in terms of compression/deflection, rotation, stress distribution and compared with the first case.

On the third case, analysis is done by providing longitudinal reinforcement in the composite column. The result also compared to other specimen which are analyzed without providing longitudinal reinforcement in terms of rotation, compression and stress distribution. The cross section of each composite column used for analysis is taken by considering approximately

equal section area of concrete and steel with the same grade/quality of both material for all specimens of composite column.

The cross section of composite column taken are as follow.

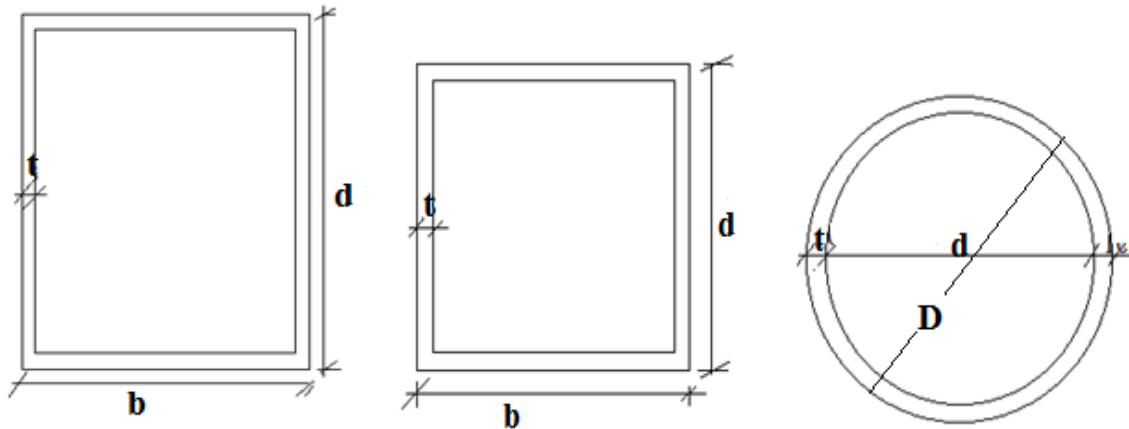


Fig.3.1 Cross-section taken for the analysis without longitudinal reinforcement.

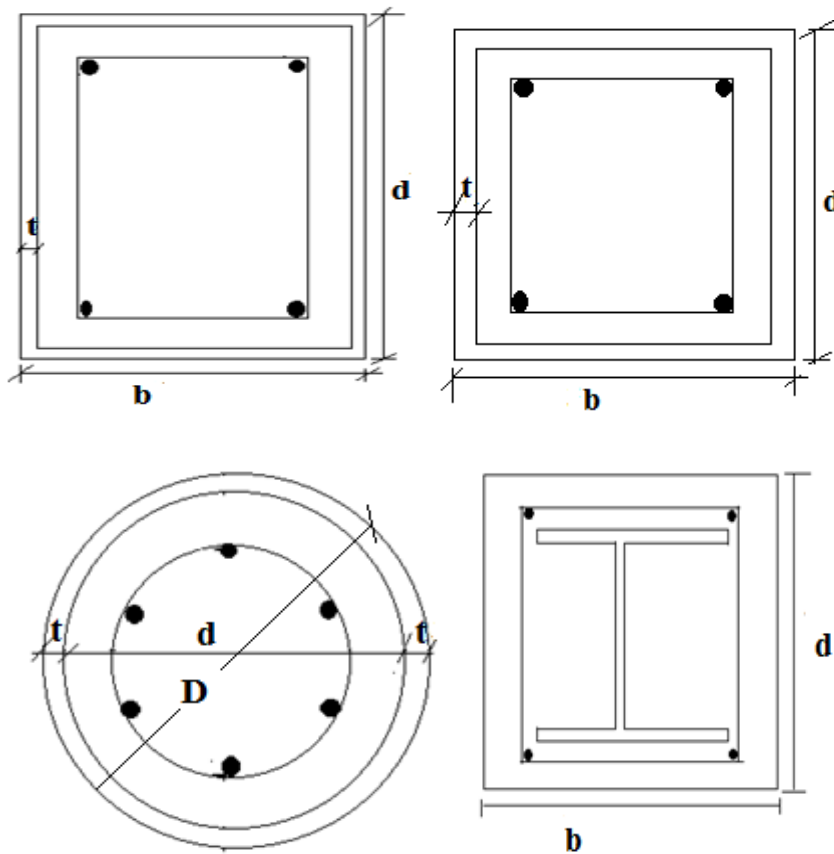


Fig.3.2 Cross-section taken for the analysis with longitudinal reinforcement

Table 3.1 Detailed cross-section and material properties

column	dimension		Steel section	reinforcement	stirups	Material properties		
	b(D)(mm)	d(mm)				fc	fs	fr
Rectangular composite column(RCC)	300	400	t=8	4 ϕ 14	Φ 8	25	355	400
Square composite column(SCC)	350	350	t=8	4 ϕ 14	Φ 8	25	355	400
Circular composite column(CCC)	390	370	t=10	4 ϕ 14	Φ 8	25	355	400
Encased I-section	350	350	HE280	4 ϕ 14	Φ 8	25	355	400

Where f_y , f_{y_r} , f_c is yield strength of structural steel, reinforcement bar and characteristic strength of concrete respectively

3.2. Finite Element Modelling

3.2.1. Introduction

In the study done by Ellobody et al. (2006) in the analysis of the axially loaded circular CFT columns, the finite element method was developed by the program Abaqus using the three dimensional eight – node elements for the concrete core and the steel tube. According to the authors of that study, the 3D solid elements were found more appropriate for the study because of the previous decision to model only the compact steel tubes, and because of the clearly defined boundaries of their elements. The efficiency of these elements was first verified by modeling the empty circular compact steel tubes and comparing the FE results with the results of the tests conducted by Giakoumelis and Lam (2004) and Sakino et al. (2004). In another study done by Hu et al. (2005), both the concrete core and the steel tube were modeled by 27-node solid elements with a reduced integration rule.

In this study, the Abaqus /CAE was used to prepare the simulations while the Abaqus/Explicit was used to run the nonlinear analysis of the models. To make a valid simulation of the

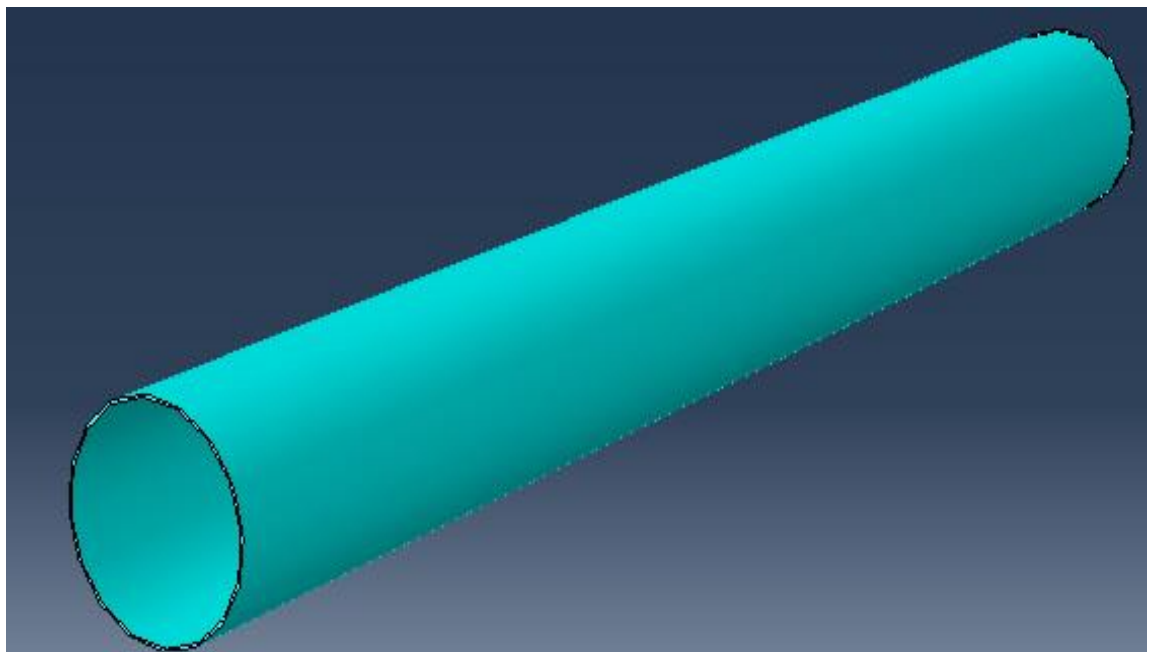
behaviour of the Composite columns, the modeling has to be done properly. The main elements which have to be modeled are the steel tube, the concrete which has to be confined, and the interaction between the steel and the concrete. Apart from these parameters, it is also important to choose the appropriate type of the finite elements and the size of the mesh in order to obtain as accurate results as possible with reasonable computing time.

In the analysis presented in this document the finite element (FE) model developed in the context of ABAQUS software is intend to simulate CFST columns with circular, square, rectangular and Encased I-section cross-section under axial compression and then under combined axial compression and constant Torsion.

3.2.2 Geometry

The analysis is conducted on the three-dimensional numerical model. The frist model consists of five independent components which are later related to each other by interaction model and constraints. The geometry of each composite column is

1. The circular steel tube, with the outer diameter D , the inner diameter d and the height h , the circular concrete core with the diameter d and the height h , and the two thick steel plates make up the geometry of the circular composite column (CCC) model.



(a)

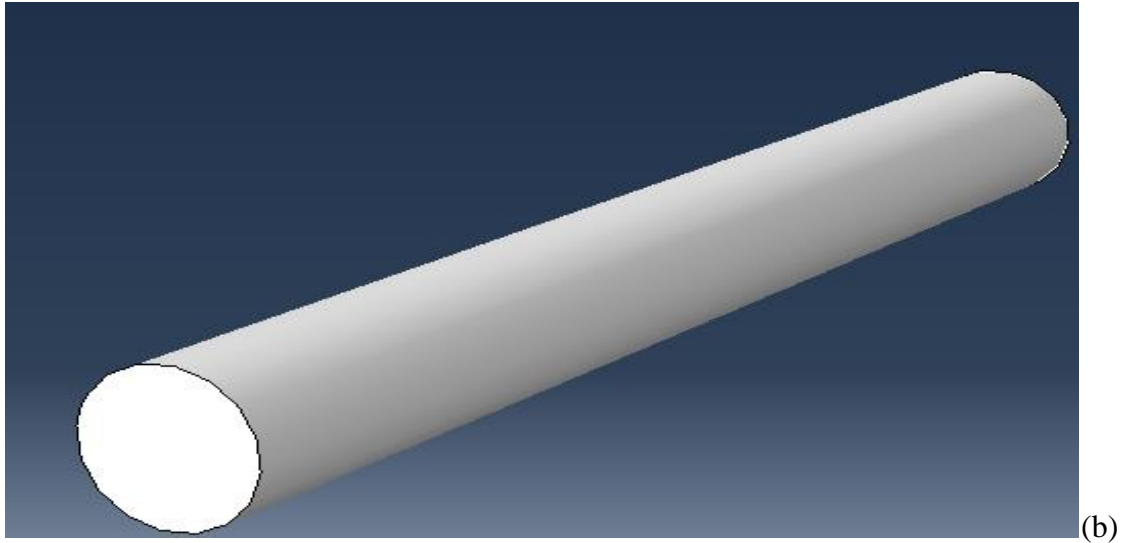


Fig 3.3 Three dimensional steel tube (a) and concrete core (b)

2. The rectangular steel tube with width b , depth d , thickness t and height h

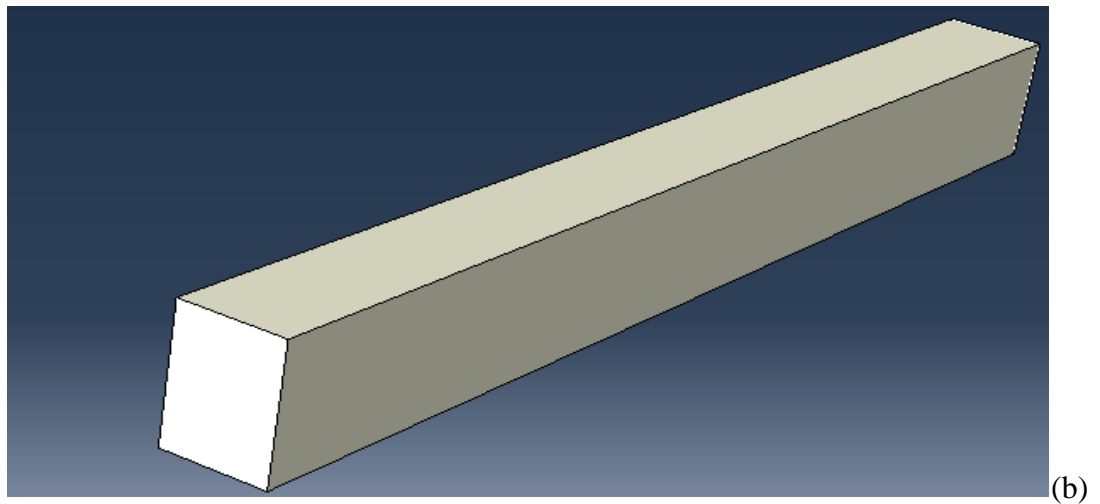
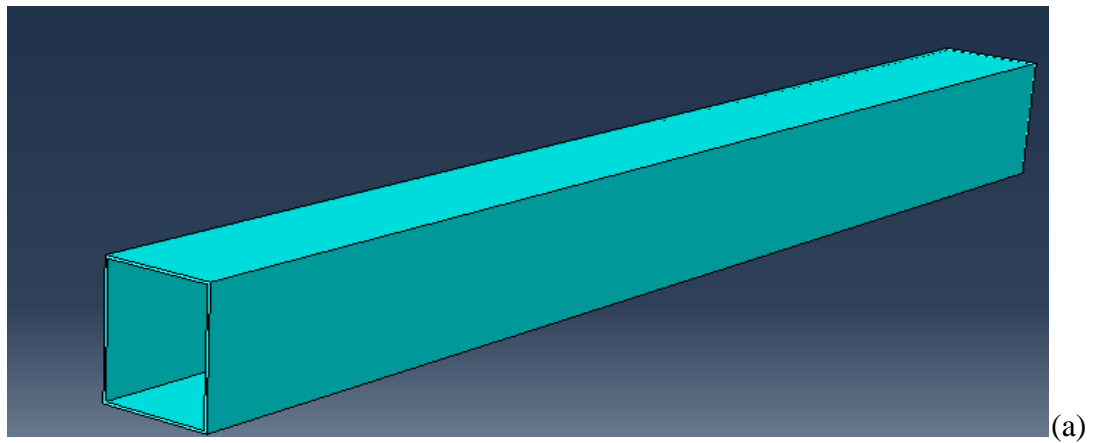


Fig. 3.4 Three dimensional rectangular steel tube (a) and concrete core (b)

3. The square steel tube with width b , depth d , thickness t and height h

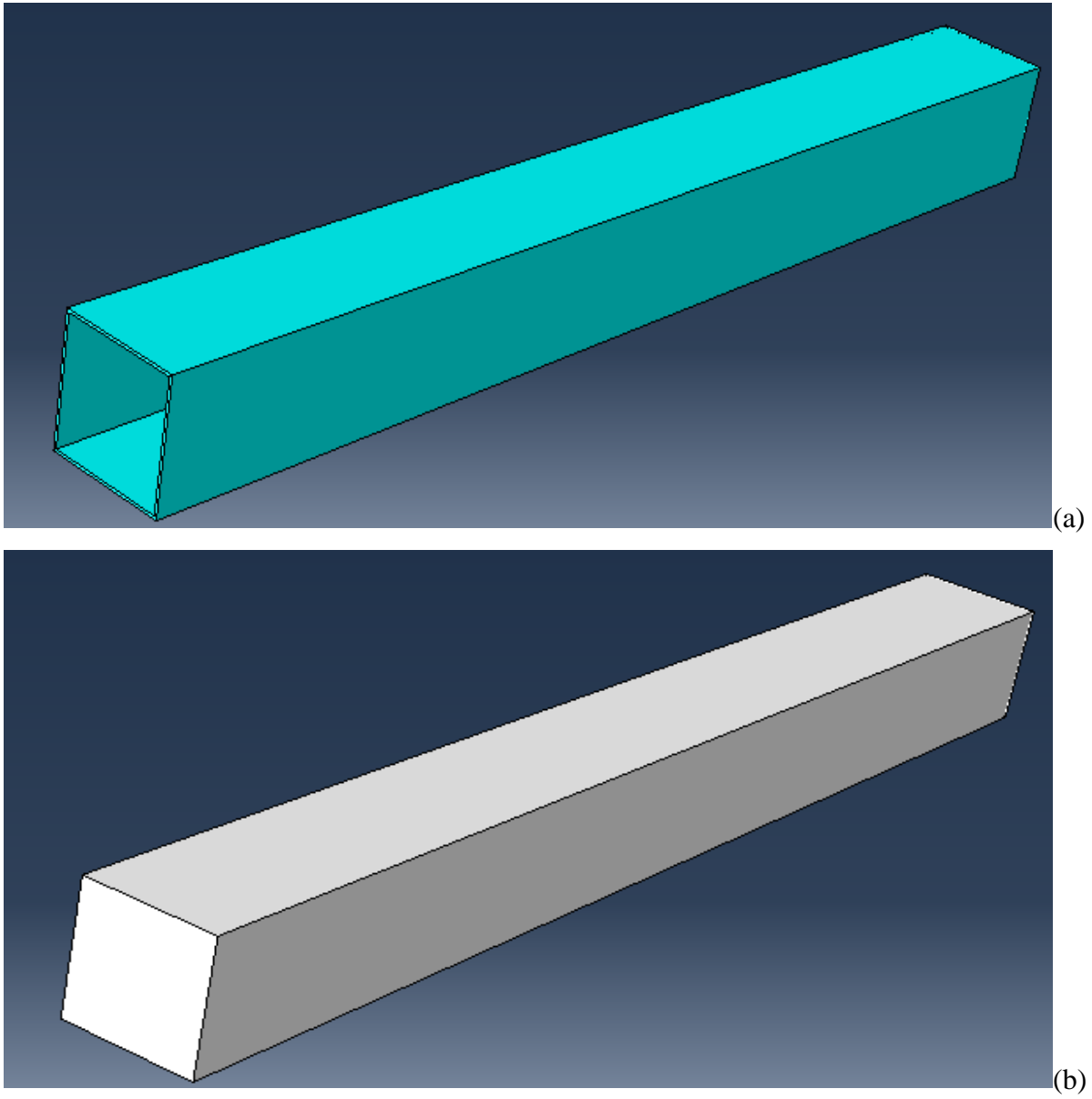


Fig.3.5 Three dimension square steel tube (a) and concrete core (b)

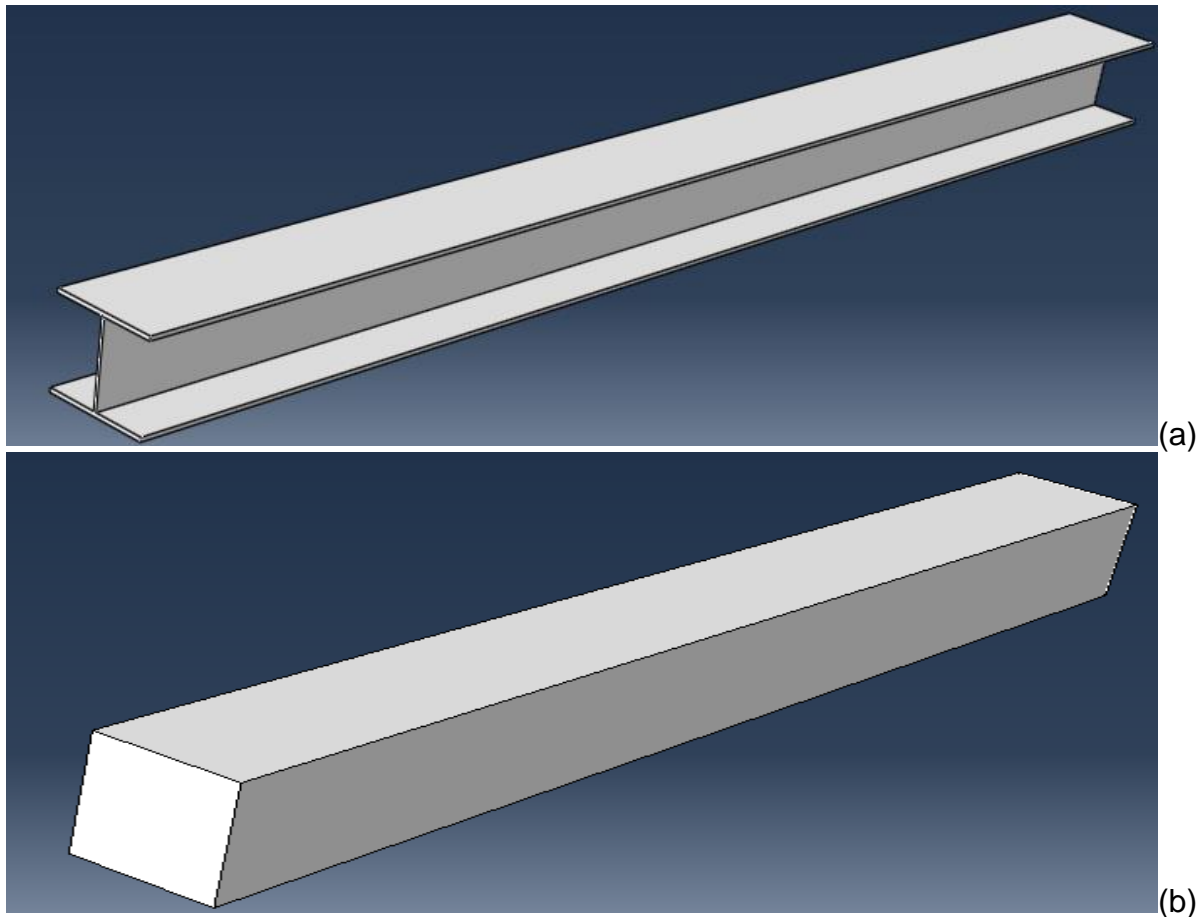
4. Encased I-section width b , depth d , thickness t and height h 

Fig.3.6 Three dimensional Encased I-section (a) and concrete core (b)

In the modelling there is no clearance exists between the concrete core and the steel tube. The rigid plate is placed at the two ends of column. The purpose of placing the thick steel plates on the top and the bottom is to simulate the real conditions of the column in an integral bridge.

As it can be seen here, the geometry of the steel tube is introduced as the three dimensional solid. This can present certain advantages and disadvantages. Among the advantages are the clear separation of the steel-concrete boundaries, and the possibility to mesh the steel tube with several layers of the finite elements which provides more data for results analysis. One of the main disadvantages is the increased computing time, and a possibility to get slightly wrong results in case of using only one layer of finite elements in the steel tube. In some of the previous studies (Ellobody et al. 2006, Hu et al. 2005, Johansson 2002, Huang et al. 2002) the circular steel tube was modeled as a three dimensional solid element.

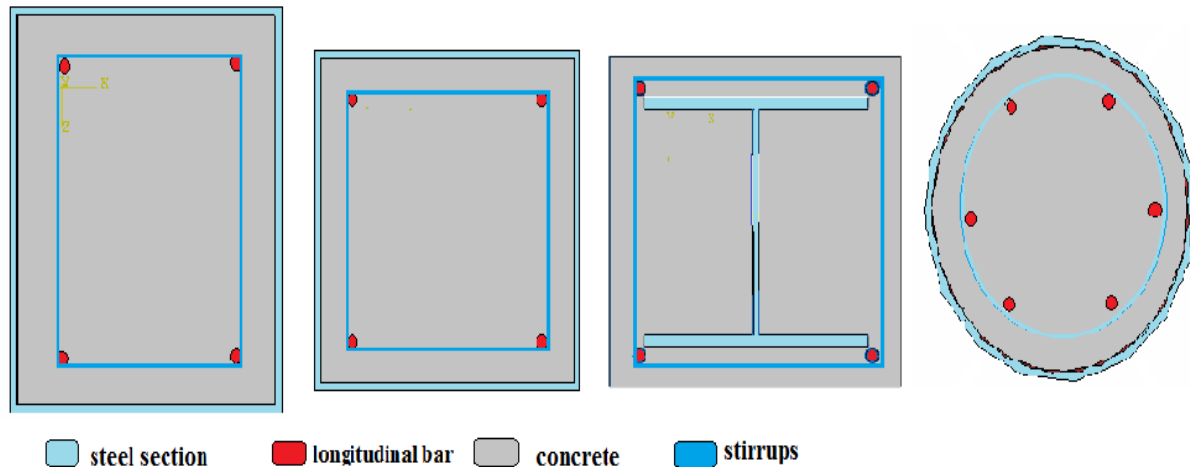


Fig.3.7 Modelling parts that used for composite column analysis

3.2.3 Material Definition

The material definition is an important part of finite element analysis, and each component should be defined carefully and all parts should be defined with appropriate material parameters.

3.2.1.1 Concrete

In the case of the concrete a nonlinear constitutive model called Concrete Damage Plasticity available in the software Abaqus 6.9 is chosen. This model is plasticity based continuum damage model. According to the Abaqus manual (6.9) this model assumes that the main two failure mechanisms are the compressive crushing and the tensile cracking of the concrete material. The evolution of the yield surface is controlled by two hardening variables, the tensile equivalent plastic strain (ϵ^{pl}) the parameters which are define by the author for the Concrete Damage.

Plasticity model are the following:

- for the plasticity, dilatation angle: 30, eccentricity 0.1, $f_b/f_{c0}=1.16$, $K=0.667$,

- Viscosity parameter = 0

- for the compressive behaviour it is taken that the material yields at the 25MPa.

- for the tensile behaviour the yield stress is taken as 2.25MPa ($0.09f_c'$).

Poisson's ratio is taken as 0.2

3.2.3.2 Steel section and reinforcement bar

Steel tube is modeled as elastic-perfectly plastic with von mises yield criterion. Due to steel tube is subjected to multiple stresses and therefore the stress-strain curve crosses elastic limit and reaches in plastic region. The nonlinear behavior of steel tube is obtained from uniaxial tension test and used in steel modeling. In this analysis poisson's ratio, density and young's modulus are taken as $\mu=0.3$, $\rho=7860\text{kg/m}^3$ and $E_s=210000\text{MPa}$ respectively. All the specimens were analyzed with the steel yield point at 355MPa and 400Mpa for reinforcement bars.

Table 3.2 summary of the mechanical properties of materials.

properties	Materials		
	steel	Reinforcement bar	concrete
Density	7860kg/m ³	7860kg/m ³	2400kg/m ³
Poisson ratio (ν)	0.3	0.3	0.2
Young's modulus (E)	210000Mpa	210,000Mpa	31,500Mpa

3.2.4 Interaction between concrete and steel

According to the Abaqus manual 6.9, there are two types of contact simulations in Abaqus/Standard:

- surface based or
- contact element based.

First the surfaces of different components that will be in contact must be created. After that pairs of surfaces which are going to be in contact must be identified. These are called contact pairs. And finally the constitutive models which describe the interactions between the various surfaces must be defined. In this work, a surface based contact is chosen, and the contacting surfaces are: the outer surface of the concrete core cylinder and the inner surface of the steel hollow cylinder. Discretization method chosen is: surface to surface, and the sliding formulation is taken as finite sliding. There are two components which define the interaction of contacting surfaces, one normal to the surfaces and one tangential. In Abaqus the default

normal interaction between the surfaces is called the 'hard contact', meaning that the surfaces can contact each other when the clearance between them becomes zero and they can transmit between each other the unlimited magnitude of pressure but cannot penetrate each other. On the other hand these surfaces can separate when the contact pressure between them becomes zero or negative. This type of normal contact was chosen in the work presented in this paper.

As for the tangential behaviour, the Abaqus uses the Coulomb friction model, where the tangential motion will be zero until the surface traction reaches a critical shear stress value, which is a function of a normal contact pressure and coefficient of friction: $\tau_{crit} = \mu \cdot \rho$. Apart from that the Abaqus uses a penalty friction formulation with an allowable elastic slip. In the analysis that is presented in this document, tangential behaviour is described by the Penalty friction formulation, described above, and the friction coefficient is taken as 0.3. By default, the maximum elastic slip is taken as 0.005 fraction of the characteristic surface dimension. Apart from the interaction between the inner surface of the steel tube, and the outer surface of the concrete core, tie constraints are also defined. In total 4 tie constraint pairs are set:

- 1) Lower surface of the upper steel plate – upper surface of the steel tube
- 2) Lower surface of the upper steel plate – upper surface of the concrete core
- 3) Upper surface of the lower steel plate – lower surface of the steel tube
- 4) Upper surface of the lower steel plate – lower surface of the concrete core

In the case of reinforced composite column two additional constraints are embedded rebars and tie of longitudinal reinforcement to the two rigid plate.

3.2.5 Loading and boundary conditions

Loads and boundary conditions must be applied to the geometry of model accurately to get the perfect result. In this analysis for each of two ends, two different types of boundary conditions were used. The nodes of the bottom end were fixed, displacement degrees of freedom in 1, 2, 3 directions (u_1, u_2, u_3) as well as rotational degrees of freedom in 1, 2, 3 directions ($\Theta_1, \Theta_2, \Theta_3$) were restrained to zero. The nodes at the top are kept free in rotational degrees of freedom in all directions and translation in the direction where the concentrated load and torsion is applied and other two direction are restrained.

The load step and displacement step were solved using static and general arithmetic with geometrical and material nonlinear methods available in the ABAQUS library. The axial load level is 40%, 50% and 60% of its axial load capacity and a constant torsion value of 60KN-m is applied at the top steel plate.

3.2.6 Meshing

In ABAQUS 6.13 meshing can be done individually on parts and then assembled or vice-versa. In this analysis parts were individually meshed and then assembled for further process. The key in finite element analysis is the appropriate selection of element type. The ABAQUS standard modules consist of a comprehensive element library that provides different types of elements catering to different situations. Meshes are composed by tri-dimensional continuum solid elements with 8 node called C3D8R, 8 node linear brick elements with reduced integration and hourglass control are used for both materials, the steel tube and the concrete core. The eight node C3D8R brick element with reduced integration is a general purpose linear brick element with only 1 integration point. In the analysis presented in this document, C3D8R, 8 node linear brick elements with reduced integration and hourglass control are used for both materials, the steel tube and the concrete core.

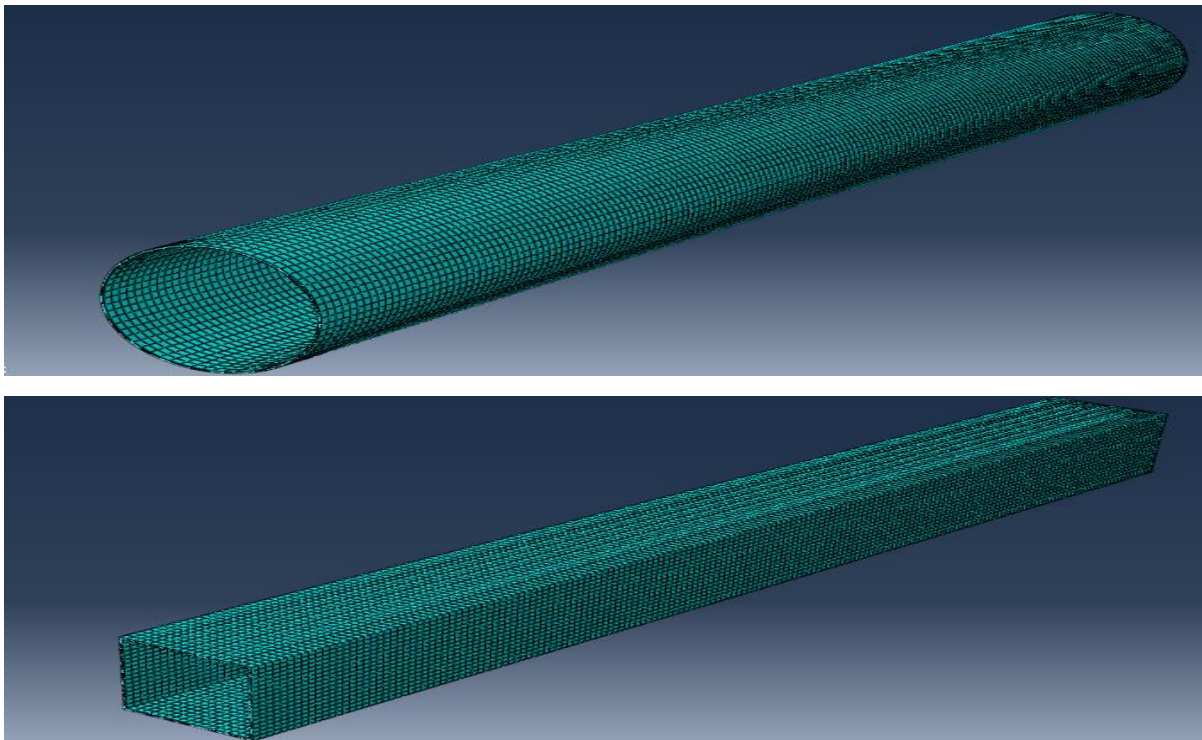


Fig.3.8 Meshing of steel tube

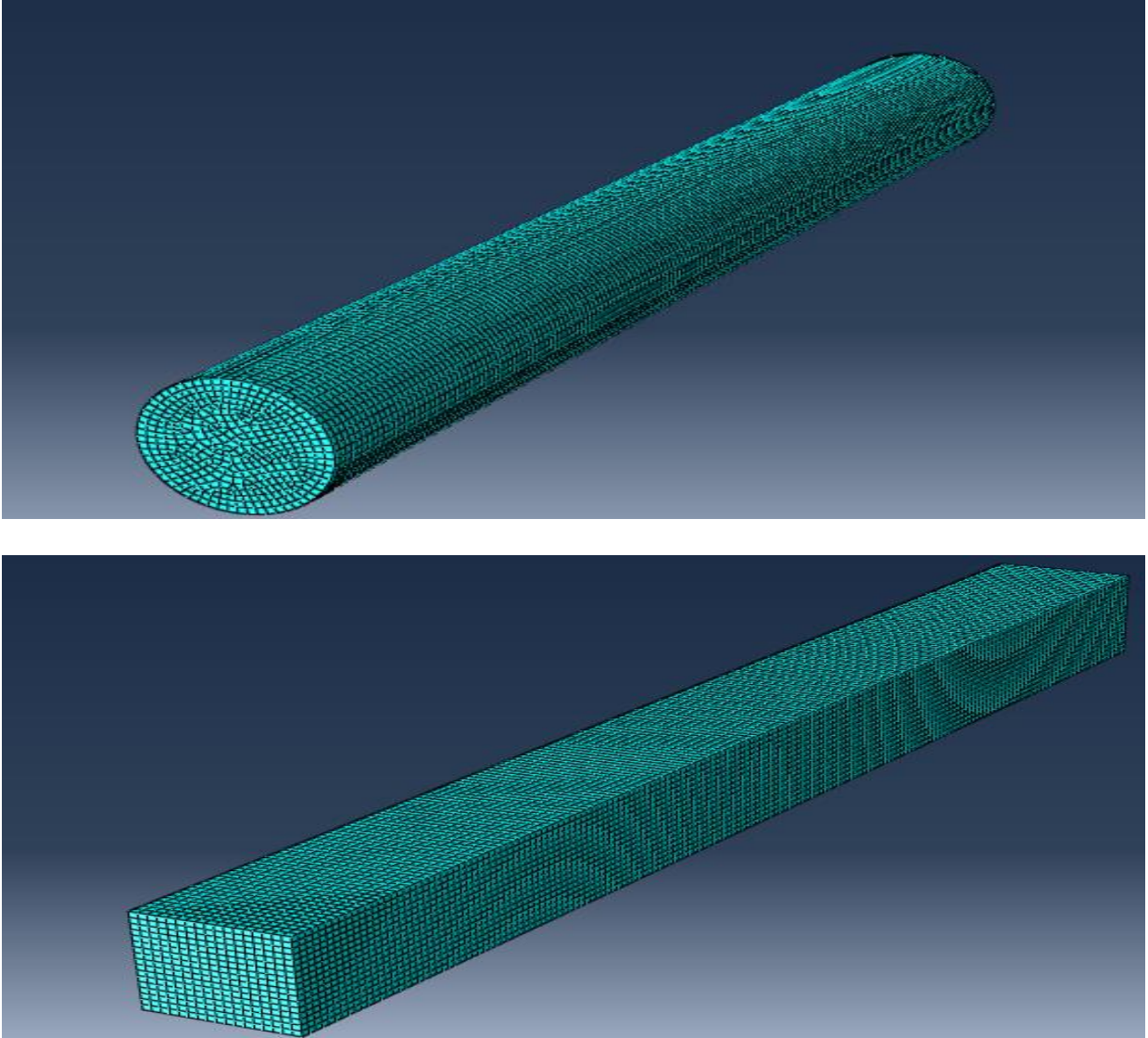


Fig.3.9 Meshing of concrete core

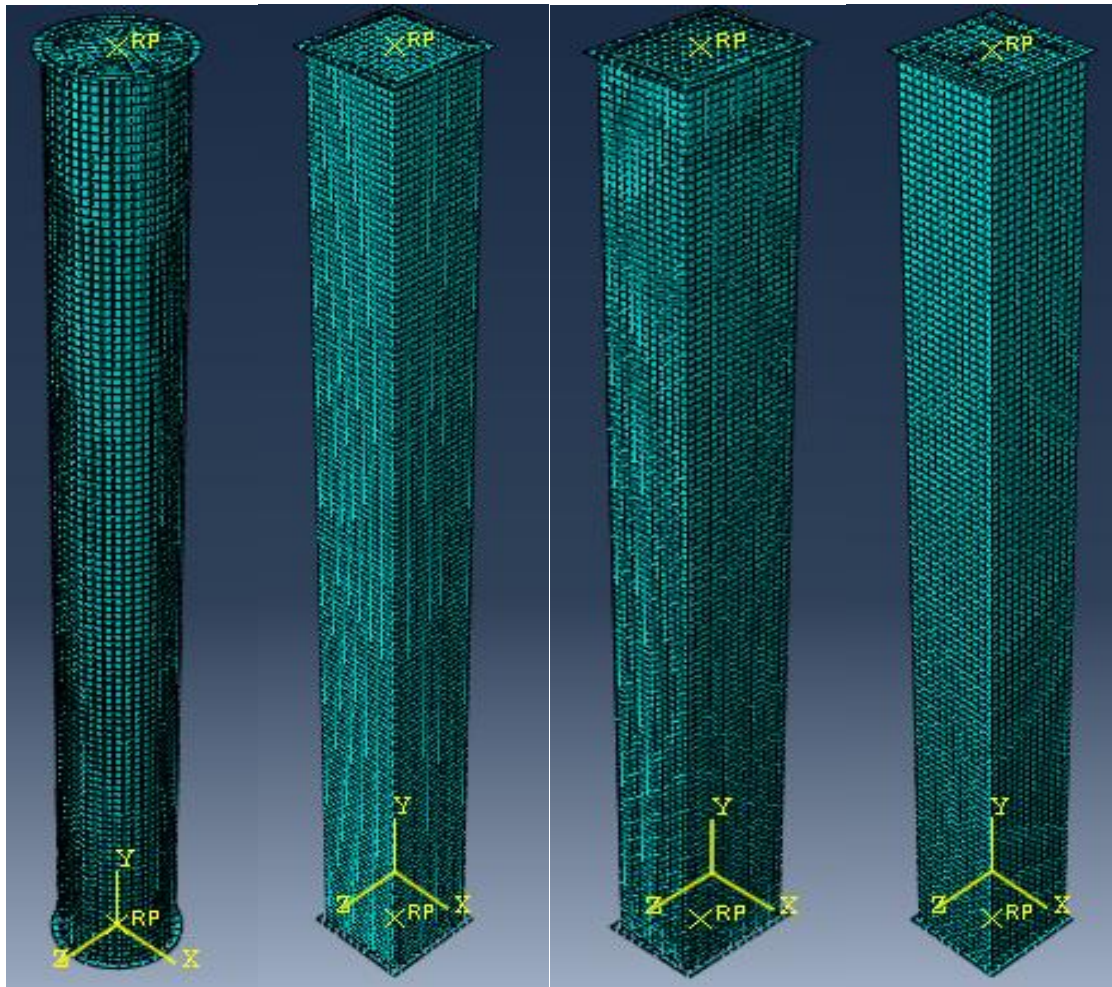


Fig 3.10 Complete mesh of composite column

3.3 Verification of FEM of the Composite Columns

The aim is to prove that the model developed in this study using the finite element program Abaqus is valid for the analysis of the circular CFT columns.

The main characteristics of the proposed model are:

- Use of the elastic- perfectly plastic material with the Von Mises yield criterion in modelling the steel tube.
- Use of the concrete damage plasticity model offered by Abaqus/CAE in modelling of concrete core.
- Modelling of both the concrete and the steel with 8 node solid elements with reduced integration C3D8R brick element.

- The loads are introduced as concentrated load and concentrated moment.
- The analysis is done in two steps – axial loading followed by Torsional loading.

The results of this model are contrasted against the theoretical results obtained which states CFST columns present higher ductility and resistance to horizontal loads than plain reinforced concrete columns, using smaller cross-section area. These features allow the use of smaller cross-section, which becomes more economic when compared to other steel-concrete composite columns (e.g. I and H steel cross sections wrapped by concrete), CFST columns exhibit higher resistance to compression and torsion.

Kawaguchi et al. tested four portal frame specimens consisting of concrete - filled square hollow section (SHS) steel tubular columns and an H-shaped steel beam with through-type diaphragms under the constant axial load and cyclic horizontal load. It is concluded that CFST frame has excellent earthquake resistance.

Lee et al. [15] theoretically studied the behavior of circular CFST columns subjected to combined compression and torsion. The results showed that the steel tube played a major role by resisting of the total torsional load, while the torsional resistance of the core concrete was not reduced even after cracking because of the restraint of the steel tube. For the core concrete, the torsional strength initially increased with the increase of the axial load, and then decreased after the axial load level reached 0.6. For the steel tube, the torsional strength decreased with the increase of the axial load. Nie et al. surveyed the torsional behavior of CFST columns under cyclic pure torsion and compression-torsion load. It was found the torsional strength would be greatly reduced under a high axial load level.

CHAPTER 4

RESULTS AND DISCUSSIONS

4.1 General

Analysis of different section of composite column done using abaqus and behavior of composite column under axial load only and under axial and torsion load is determined. The FEM output was then examined to determine the effect of different levels of axial loads on behavior under torsion loading, high stress zone and the following discussion covers the results of abaqus software.

4.2 Effect of combined action of Axial and Torsion loads

Effect of combined action of axial and torsion load on composite column is analyzed based on behavior of column analysis under axial load only and adding torsion moment to the respective axial load. Different section of composite column (rectangular, square, circular and Encased I-section) with the different section of steel tube is analyzed and effect of torsion on the column is studied by using abaqus software. The effect of combined action of axial load and Torsion is identified in terms of evaluating the rotation, compression and distribution of stress. Based on this the following results obtained and discussed in detail.

4.2.1 Behavior of Composite Column

4.2.1.1 Behavior of Composite Column Under Axial Load Only

Different section of composite column, Rectangular Composite Column (RCC), Square Composite Column (SCC), Circular Composite Column (CCC) and Encased I-section under 40% of its axial capacity is loaded by 2221.36 KN, 2238 KN, 2377.18 KN and 2017 KN respectively.

Table 4.1 Summary of the applied axial load

Composite Column	Axial Capacity(KN)	P1 (40%) (KN)	P2 (50%) (KN)	P3 (60%) (KN)
RCC	5553.4	2221.36	2776.7	3332.04
SCC	5595	2238	2797.5	3357
CCC	5942.95	2377.18	2971.475	3565.77
Encased I-secn	5042.47	2017	2521.2	3025.5

During Axial loading of composite column specimens, abaqus software output are used and the significant events were noticed which are as follow.

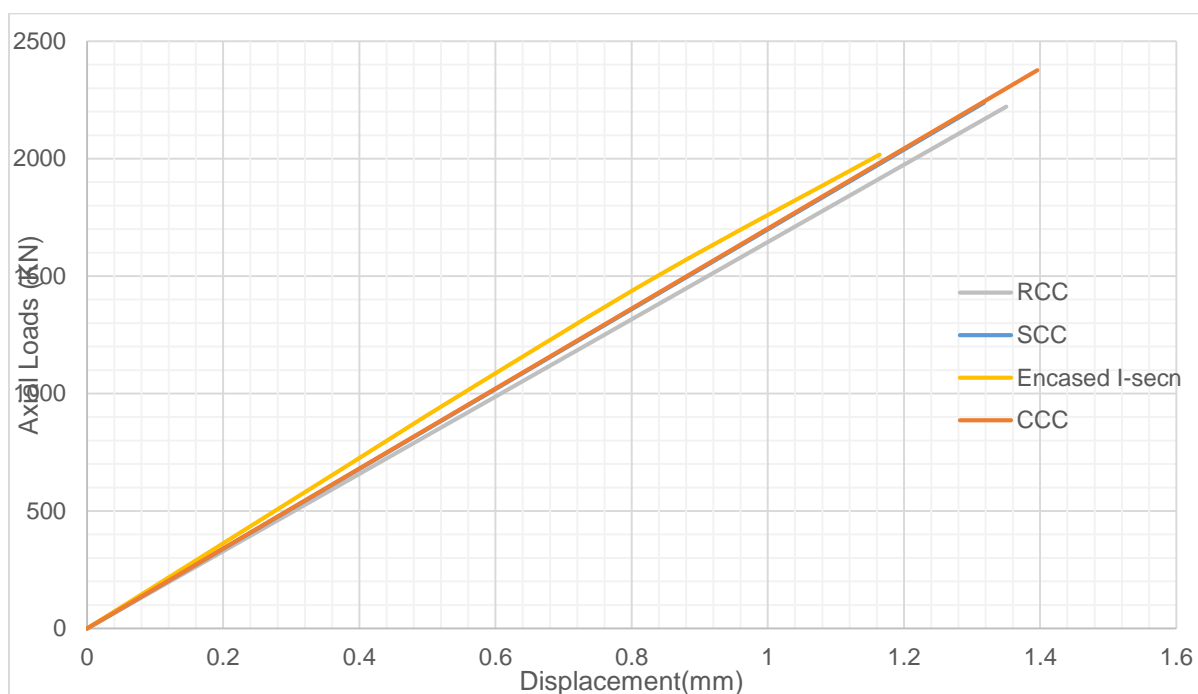


Fig 4.1 Axial load vs Compression at 40% of Axial Capacity of composite column

Axial loads of 40% of ultimate axial capacity of rectangular composite column, square composite column, circular composite column and encased I – section 2221.36 KN, 2238KN,

2377.18KN and 2017KN are applied respectively at the top center of each composite column. Using Abaqus software the corresponding deflection/compression of composite column was plotted.

At the initial loading of 40% of ultimate axial capacity for each composite column section encased I-section show better performance in terms of compression while square composite column and circular composite column shows same performance and the rectangular composite column shows higher compression than other cross section.

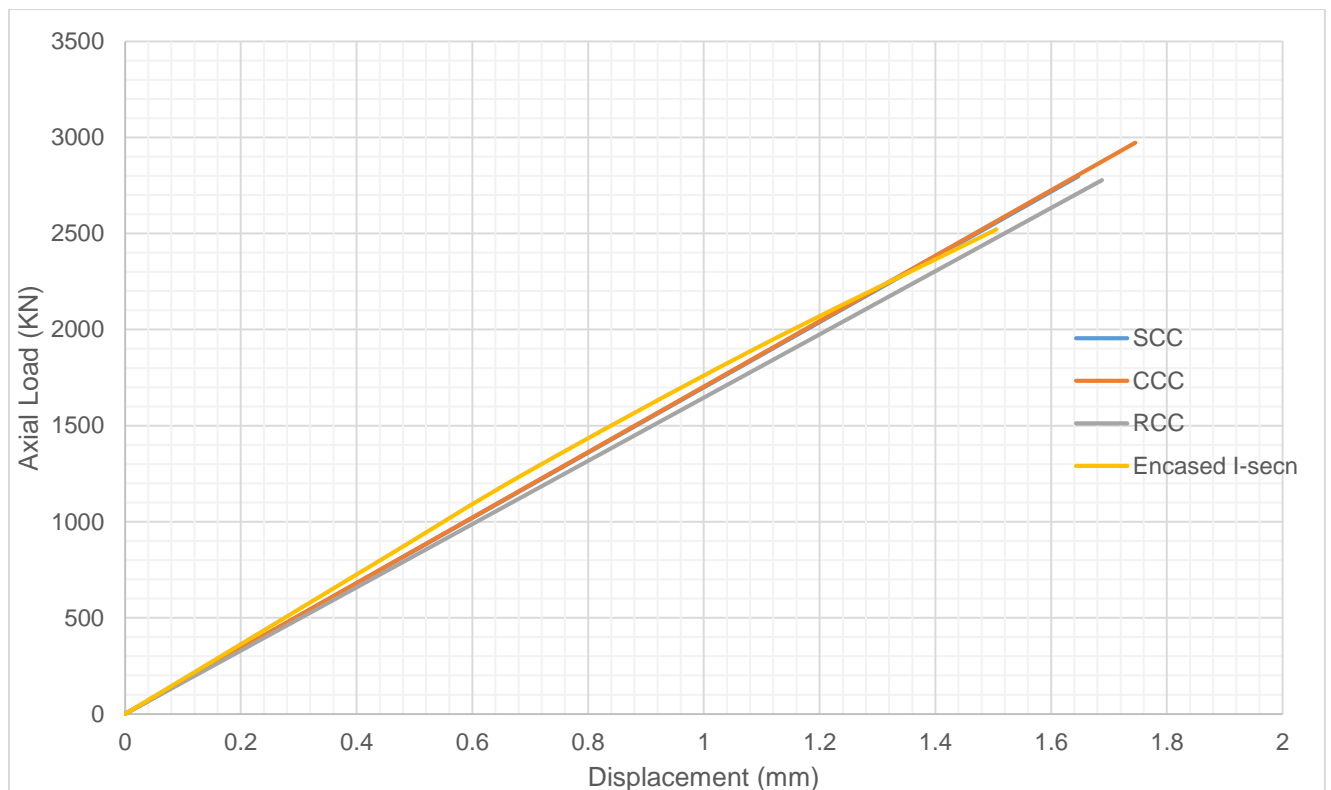


Fig 4.2 Axial load vs Compression at 50% of Axial Capacity of composite column

As the applied load on each composite column reaches 50% of its axial load capacity rectangular composite column, square composite column, circular composite column and encased I-section is subjected to 2776.7 KN, 2797.5 KN, 2971.5 KN and 2521.2 KN respectively. When the applied load is increased (to 50% of axial capacity), encased I-section composite column shows better performance at first stage of loading and starts to compress/deflect more than circular composite column and square composite column but less than rectangular composite column at final stage of loading.

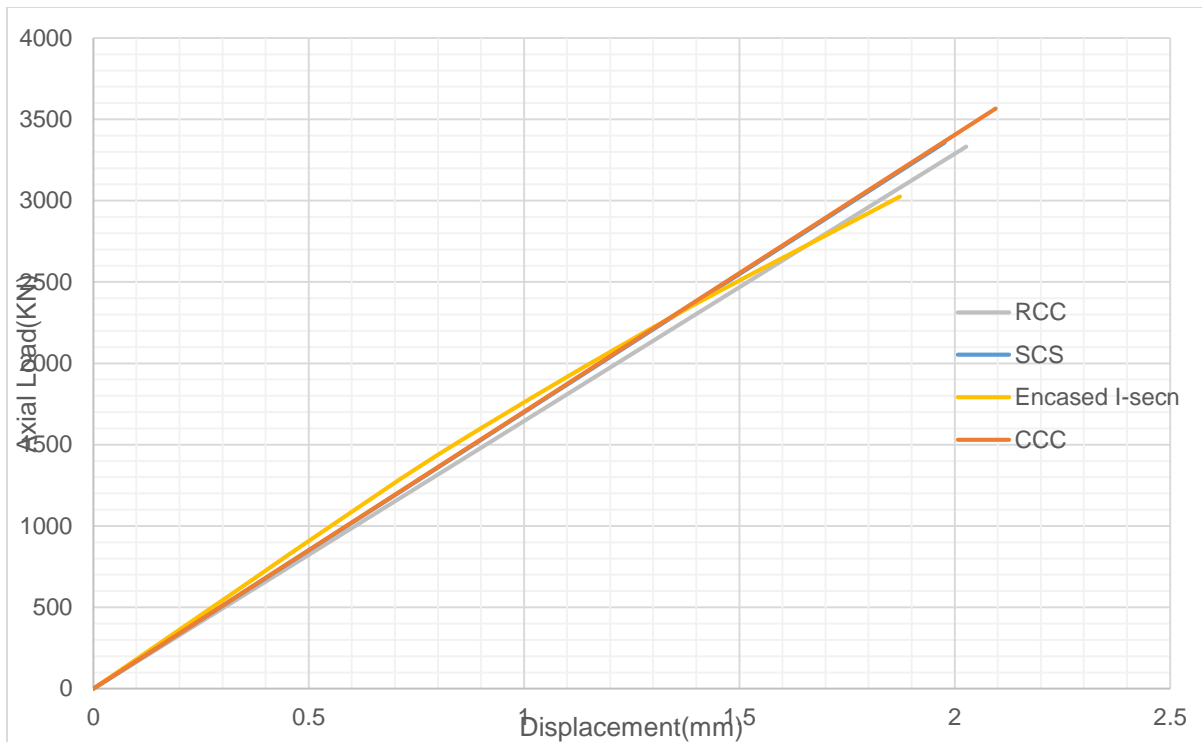


Fig 4.3 Axial load vs Compression at 60% of Axial Capacity of composite column

When the concentrated load applied reaches 60% of ultimate axial capacity for each composite column rectangular composite column, square composite column, circular composite column and encased I-section subjected to 3332.04 KN, 3357 KN, 3565.77 KN and 3025.5 KN respectively. At this stage of loading the performance of encased I-section in terms of compression is better at first stage of loading and starts to compress more than other cross section at the middle stage of loading

As the concentrated load applied on composite increases square composite column and circular composite column shows similar condition through all loading and rectangular composite column compresses more than other cross section but as the applied load increases the encased I-section compresses more.

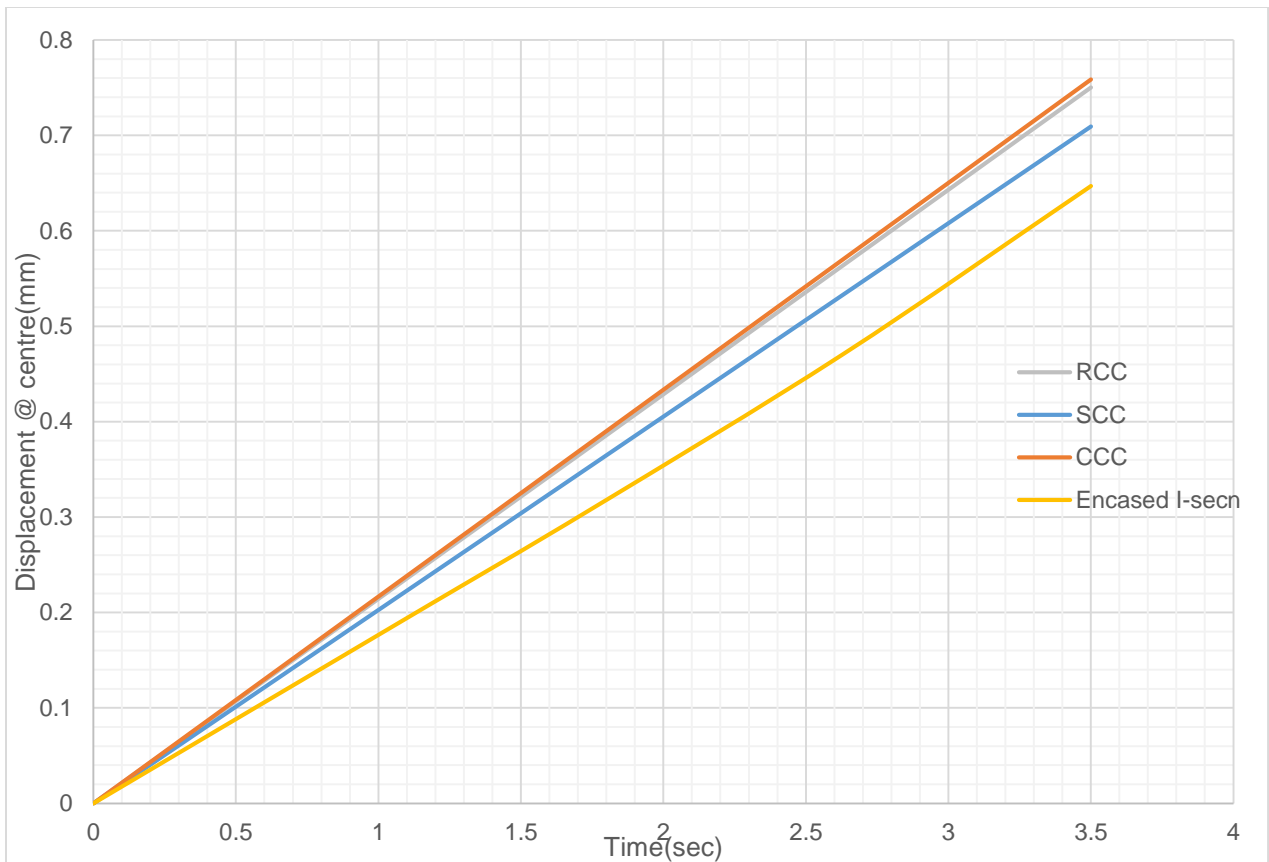


Fig 4.4 Compression at the center of composite column-40%P

At the first trial of loading (40% of ultimate axial capacity) on each cross section of composite column the rate at which compression of composite column transferred to the center of composite column is checked at center using the Abaqus software and the above figure is plotted. As it is seen from the graph above the compression/deflection in circular composite column reaches its center early than other cross section of composite column and in encased I-section the distribution of compression at the center of the section lately distributed.

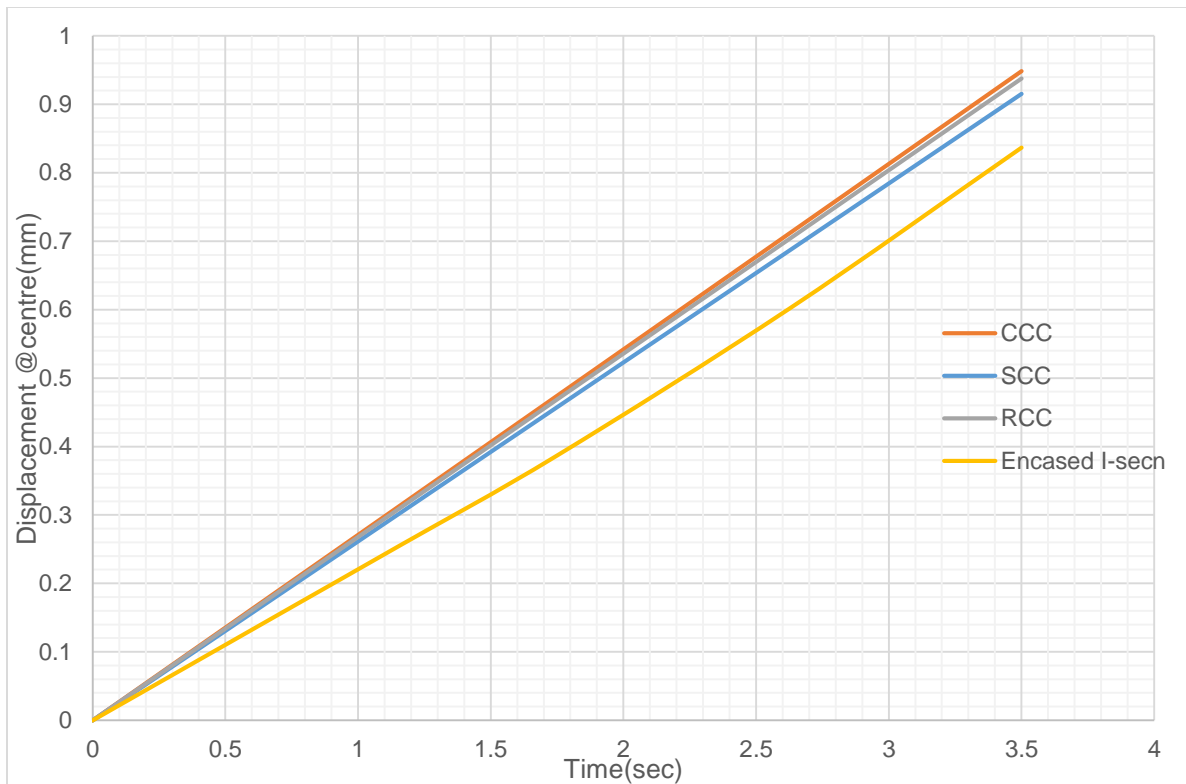


Fig 4.5 Compression at the centre of composite column-50%P

When the concentrated load applied on composite column is about 50% of its ultimate axial capacity for each cross section of composite column, the distribution of compression/deflection is similar to that when the applied load is 40% of its ultimate axial capacity. At first stage of loading circular composite column, rectangular composite column and square composite column shows similar distribution of compression.

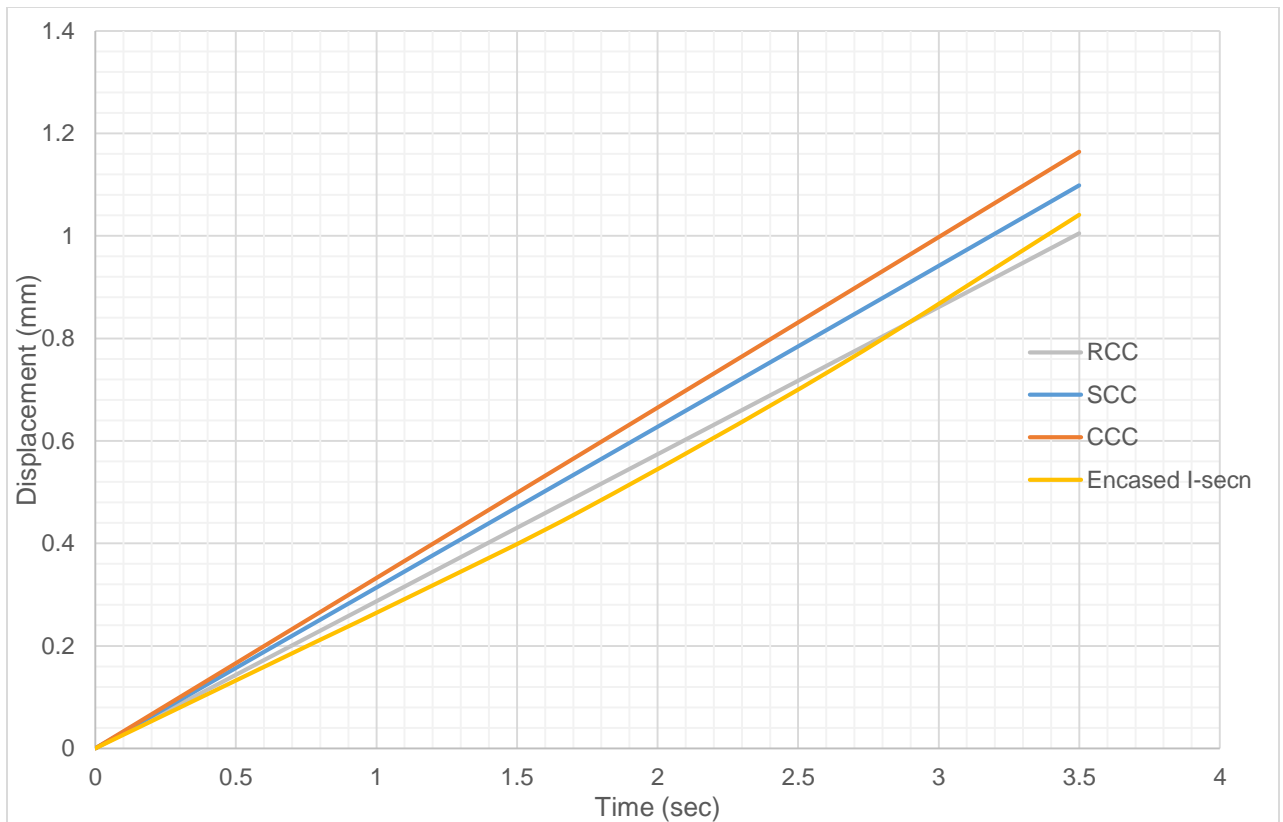


Fig 4.6 Compression at the center of composite column-60%P

As the concentrated load applied on composite column increased to about 60% of its ultimate axial capacity the distribution of compression to the center is fast as it is in the case of 40% & 50% of its axial capacity in circular composite column while in square composite column it starts to distribute fast next to circular composite column as the applied load reaches 60% of its axial capacity.

At the first stage of loading the distribution of compression to the center of the section in rectangular composite column is faster than encased I-section composite column but at the final stage of loading the compression in encased I-section starts to distribute to the center faster than rectangular composite column cross section.

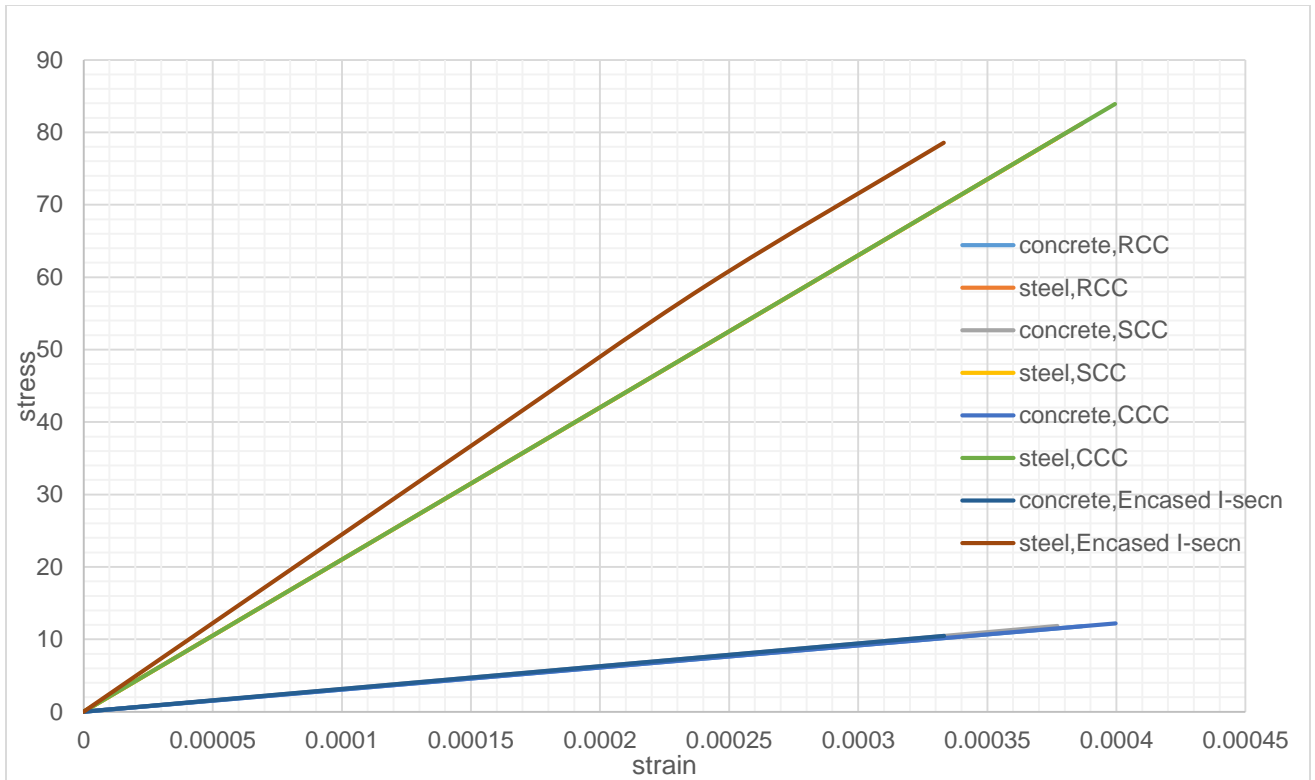


Fig 4.7 Stress – strain diagram – 40%P

The stress and strain of steel and concrete section of rectangular composite column, square composite column, circular composite column and encased I-section are drawn based on the resulted from abaqus analysis. As it can be seen from the above figure the stress-strain of steel and concrete of rectangular, square and circular cross section shows similar while stress-strain of steel in encased I-section is higher than concrete filled steel tube section stress-strain of concrete in encased I-section is approximately similar to the other cross section.

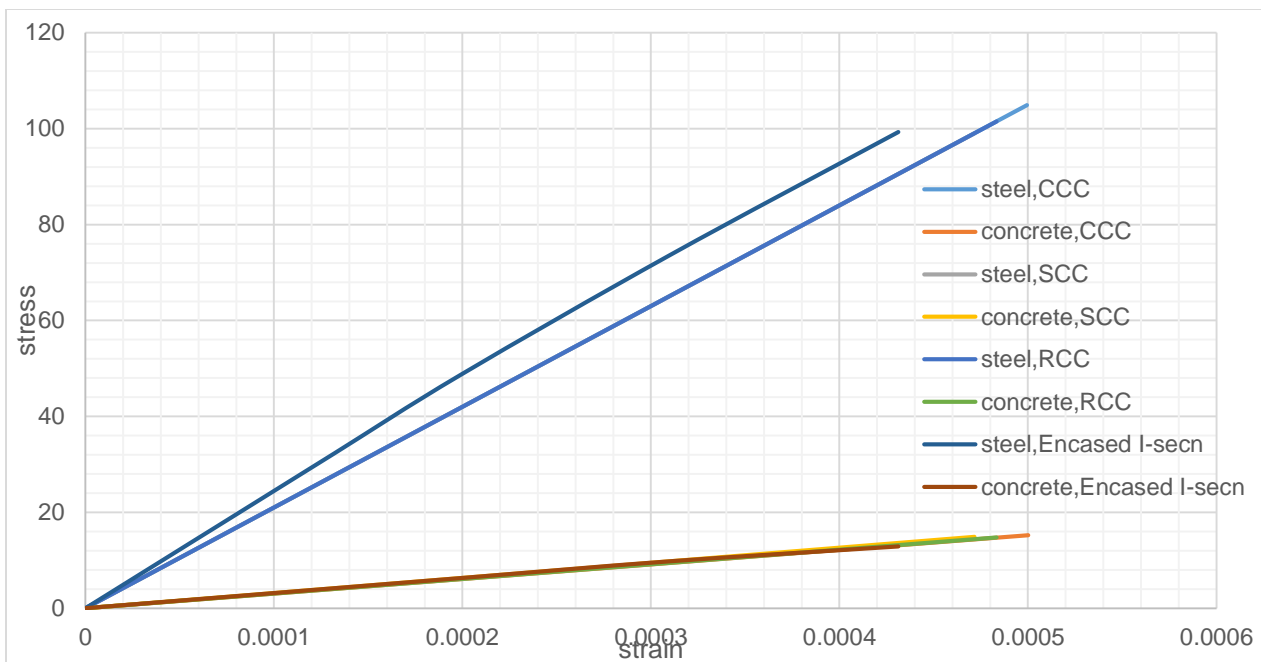


Fig.4.8 Stress – strain diagram – 50%P

As the applied load reaches 50% of its ultimate axial capacity the stress-strain diagram of concrete and steel is similar to that of when the applied load is 40% of axial capacity.

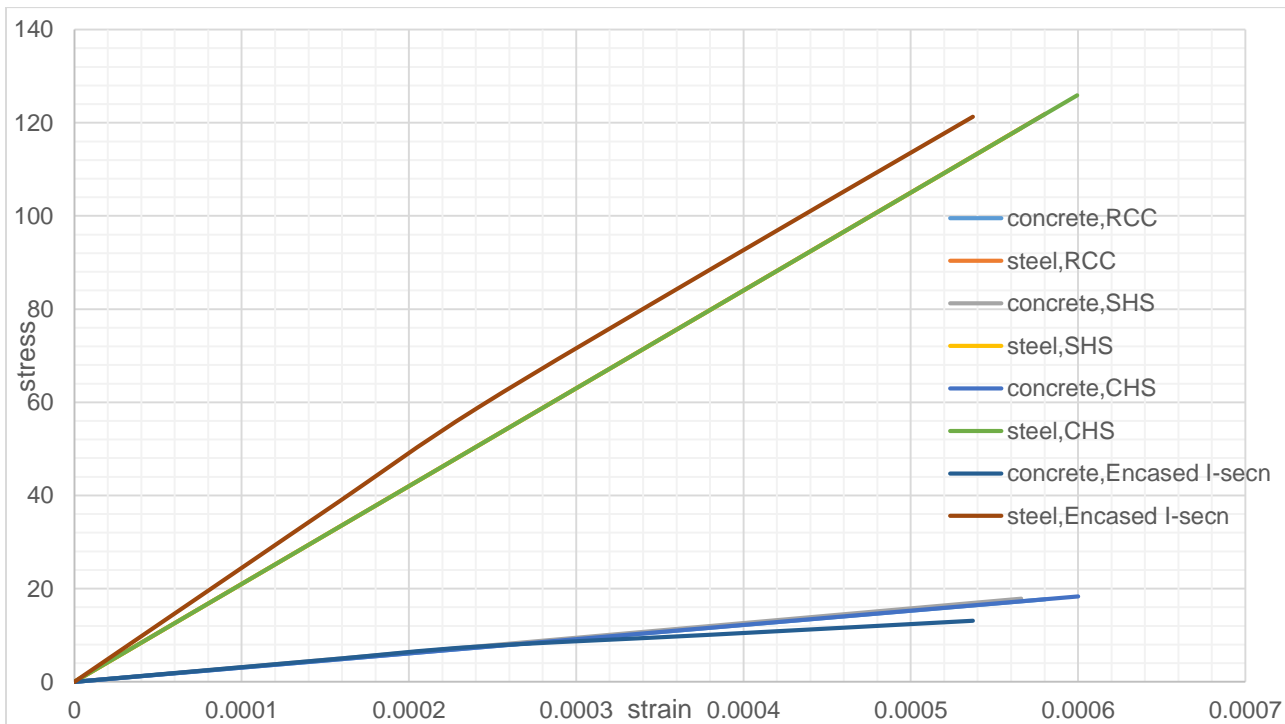
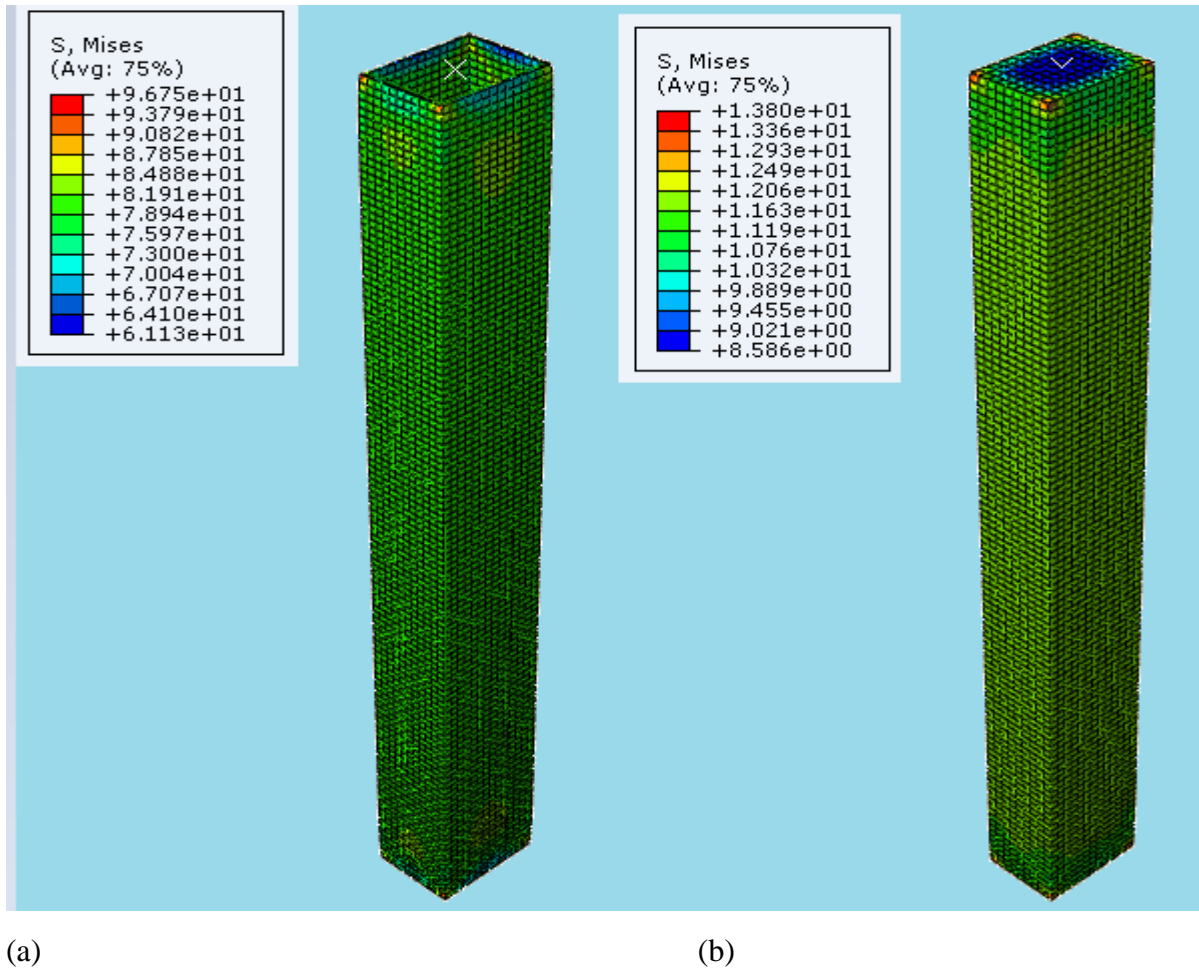
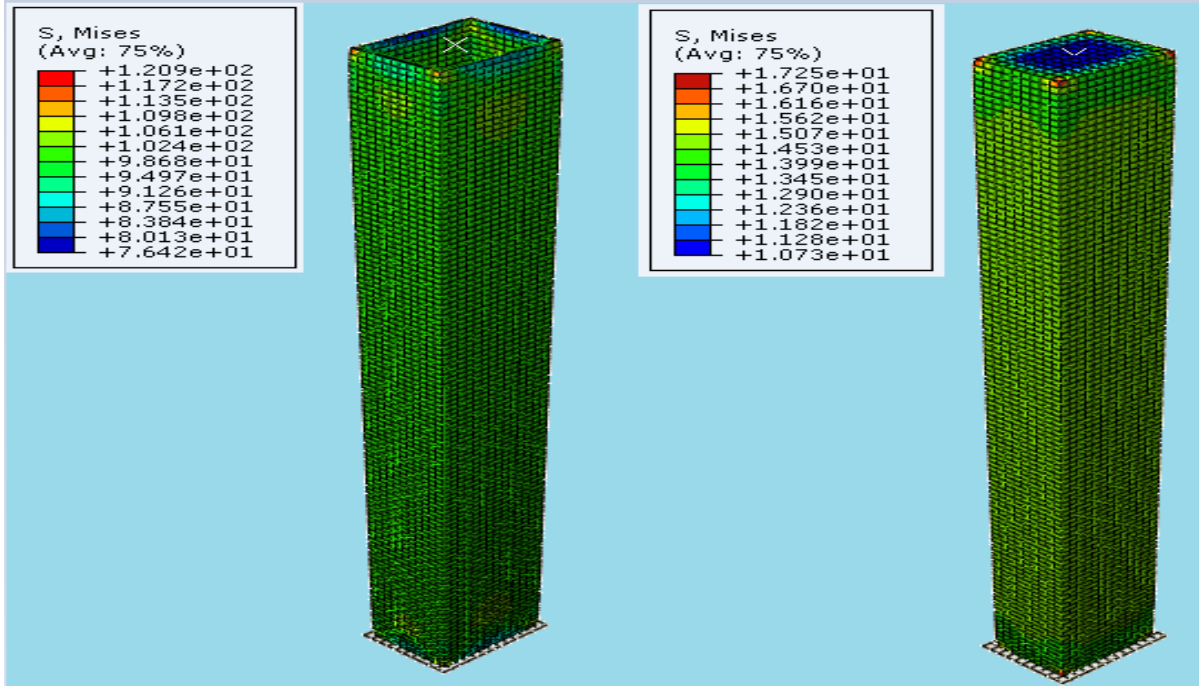


Fig. 4.9 Stress – strain diagram – 60%P

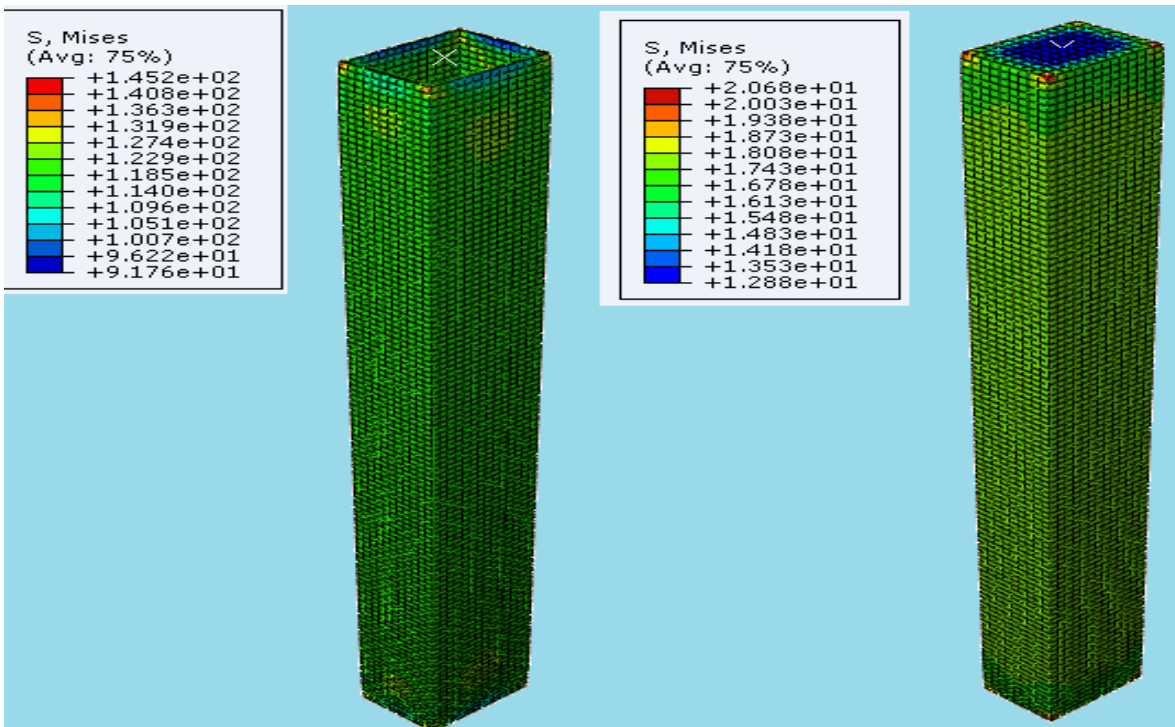
Increasing the concentrated load to 60% of its ultimate axial capacity of rectangular, square, circular and encased I-section composite column, from the abaqus results on the figure 4.9 shows that the stress-strain of steel and concrete is similar to that when the applied load is 40% & 50% of axial capacity except stress-strain of concrete in encased I-section composite column which shows lower stress strain diagram.





(c)

(d)



(e)

(f)

Fig.4.10 Stress of steel and concrete of RCC @ 40%P (a & b),@50%P (c & d) and @ 60%P (e & f) respectively

Different axial load 40%, 50% and 60% of its ultimate axial capacity of Rectangular Composite Column of about 2221.36KN, 2776.7KN and 3332.04 KN is applied at the top center of composite column using rigid plate and analyzed using ABAQUS software. From the results obtained using abaqus software stress distribution of different elements of composite column is shown in the figure 4.10. Under these introduced concentrated load steel tube experiences stress of about 79, 99 and 118 while concrete has 11, 14 and 18 stresses.

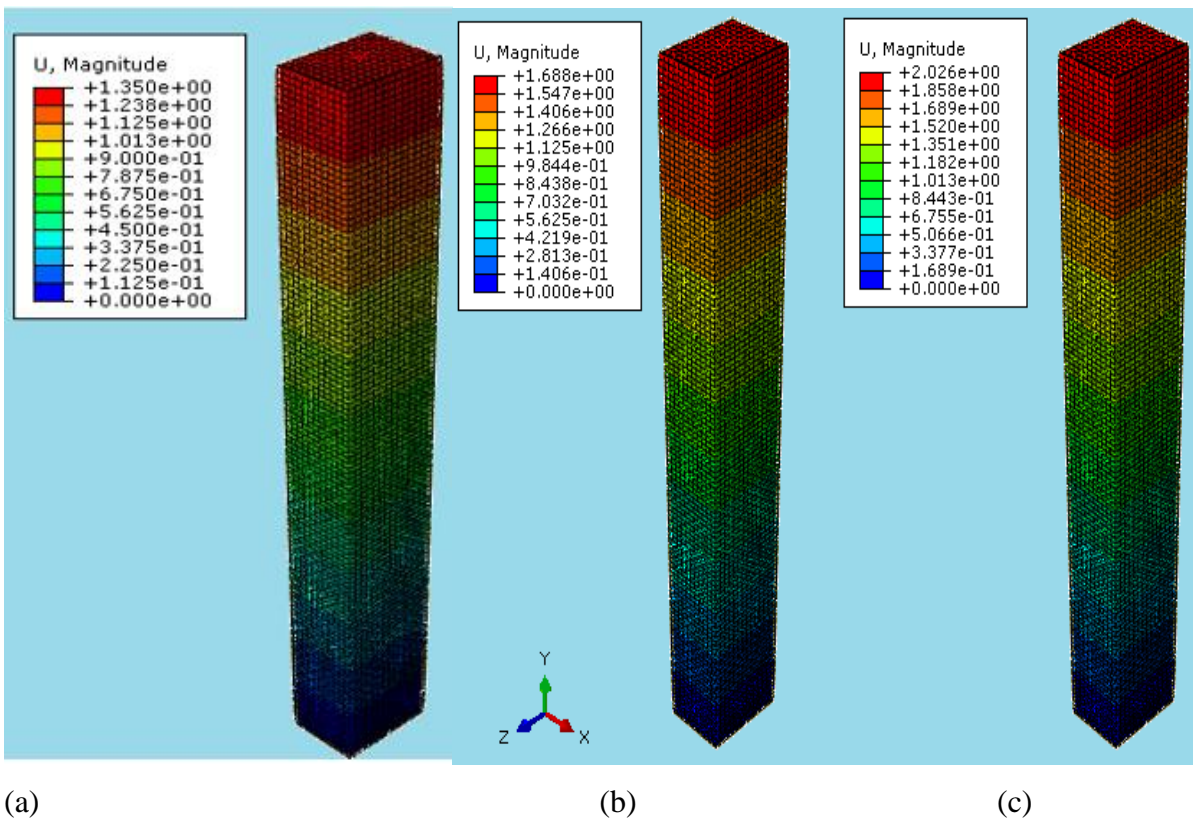
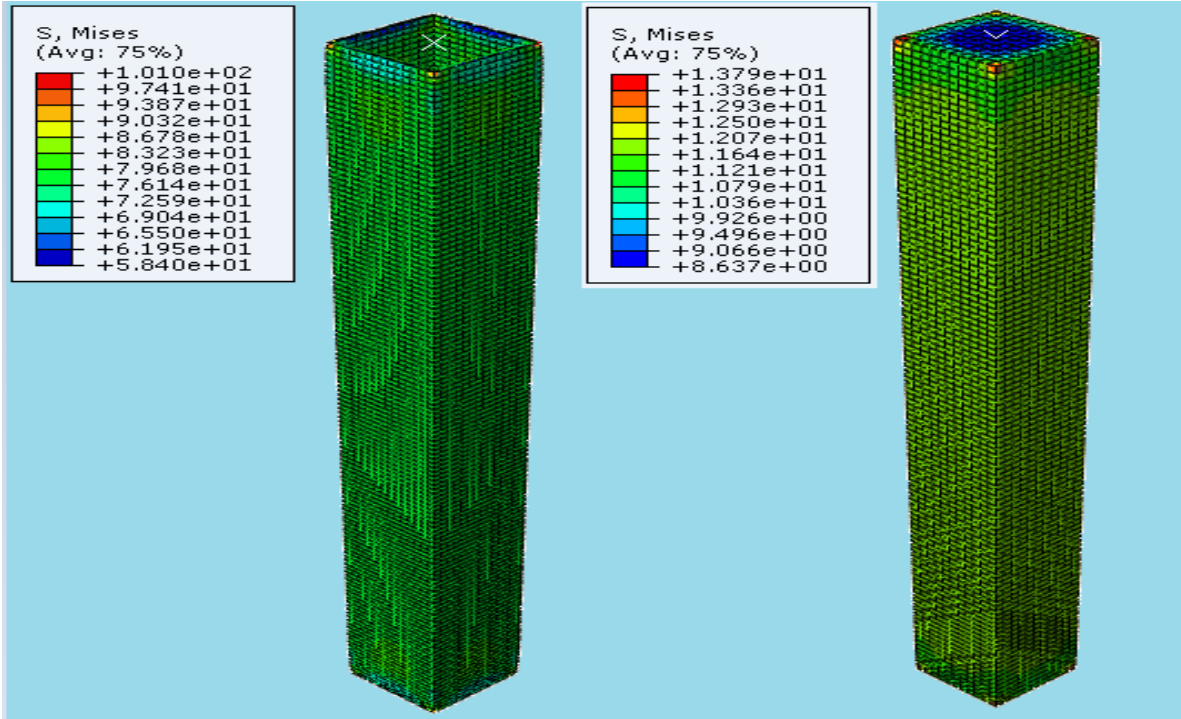
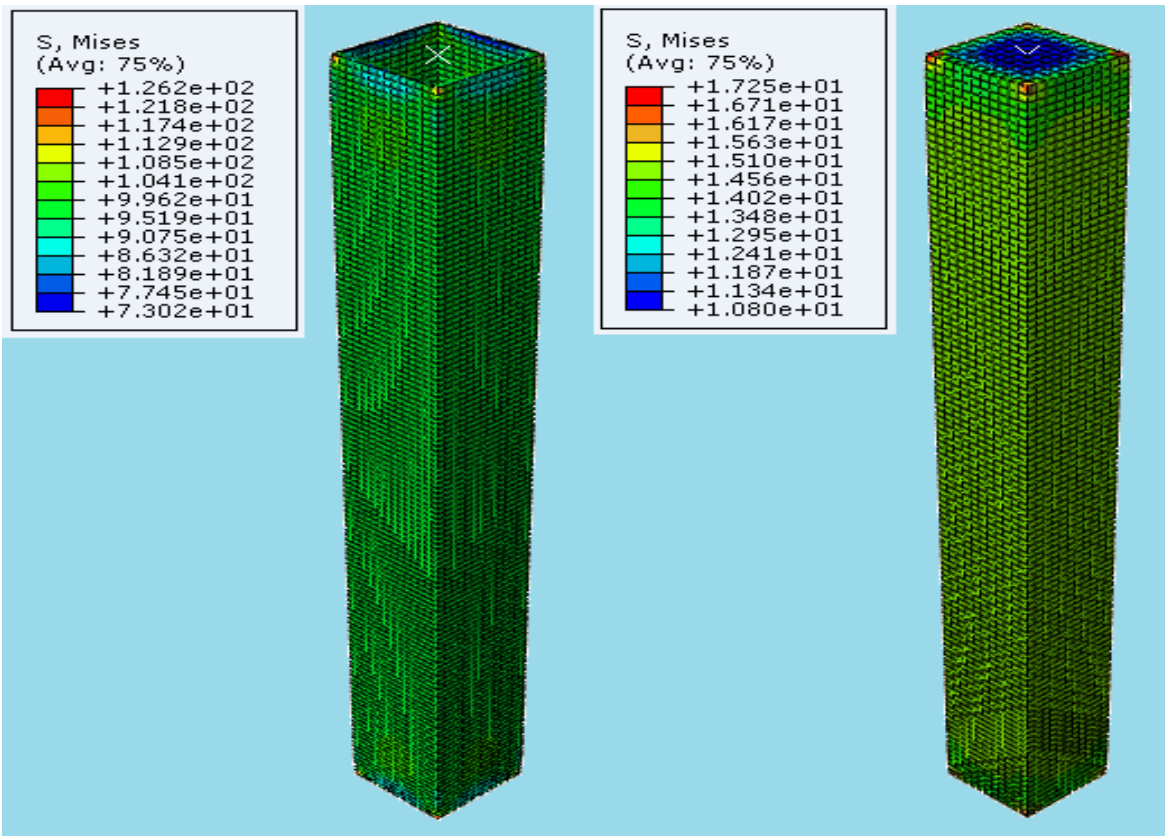


Fig 4.11 Displacement/Compression of RCC @ 40% (a), 50% (b) and 60% (c) of axial capacity Due applied concentrated load of about 40%, 50% and 60% of ultimate axial capacity of rectangular composite column compression of the column is seen in the direction of applied loads. Under these concentrated load the distribution of compression is high at the top while it is approximately equal to zero at the bottom of the section. As it can be seen from the figure above, which is drawn from the abaqus results the compression of the column increases as the applied load increases which is about 1.35mm, 1.69mm and 2.02mm at 40%P, 50%P and 60%P respectively.



(a)

(b)



(c)

(d)

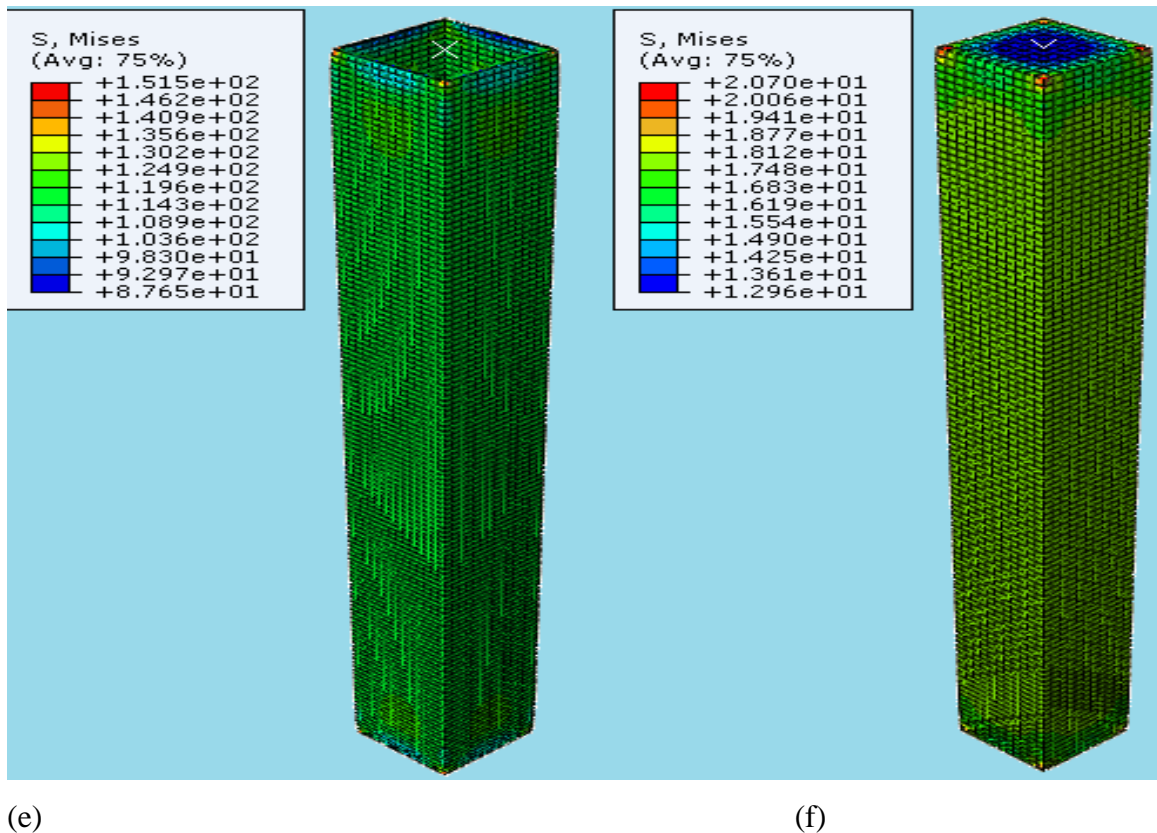
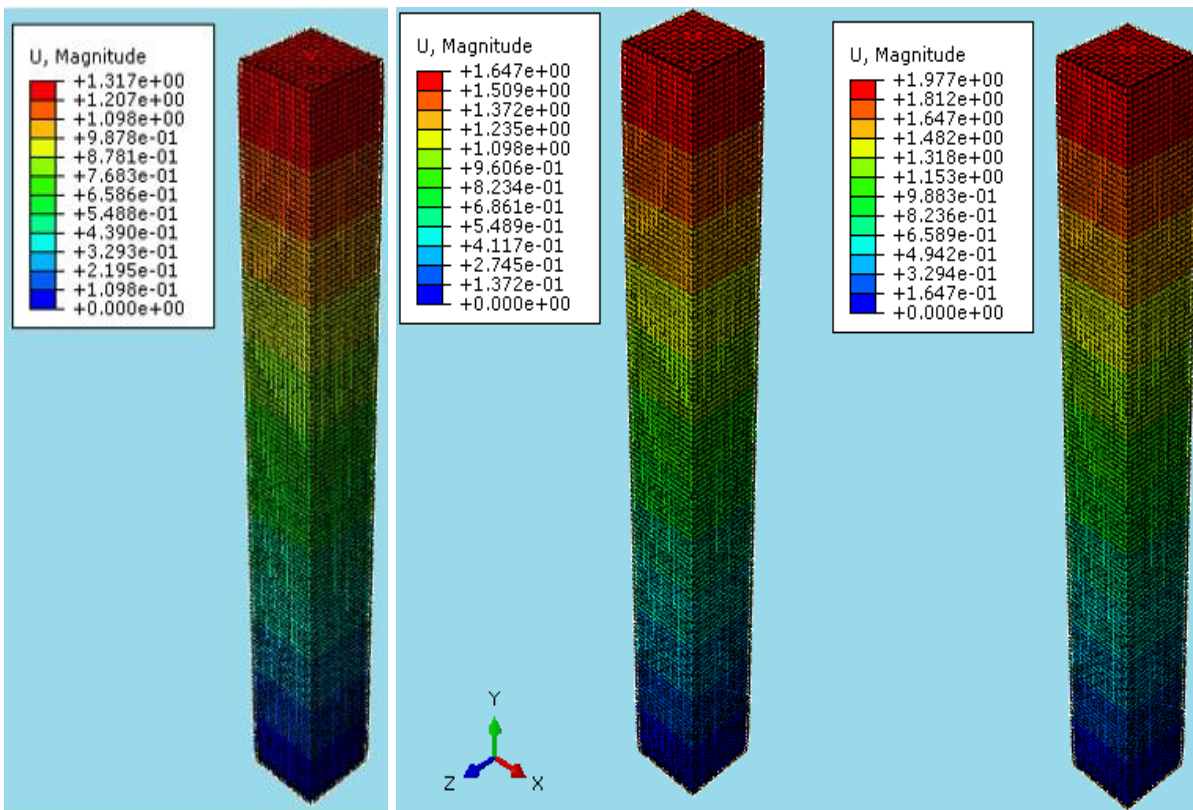


Fig.4.12 Stress of steel and concrete of SCC @ 40%P (a & b),@50%P (c & d) and @ 60%P (e & f) respectively.

The other section of composite column which is analyzed using abaqus analysis is square composite column. The concentrated load of about 40%P, 50%P, and 60%P which is 2238 KN, 2797.5 KN and 3357 KN respectively applied and the stress distribution in steel and concrete material is calculated using abaqus software.

From the figure 4.12 the stress distribution of steel section is approximately 80, 100 and 125 while concrete stress is 12, 15 and 17.5 as the applied concentrated load is 40%P, 50%P and 60%P respectively. From the results obtained, it is clear that the stress distribution steel and concrete material in rectangular and square composite column is similar.

As it can be seen from the figure, the stress distribution in the concrete core is high at the corner of the column where it has direct contact to the steel tube while it is low at the center of concrete core.

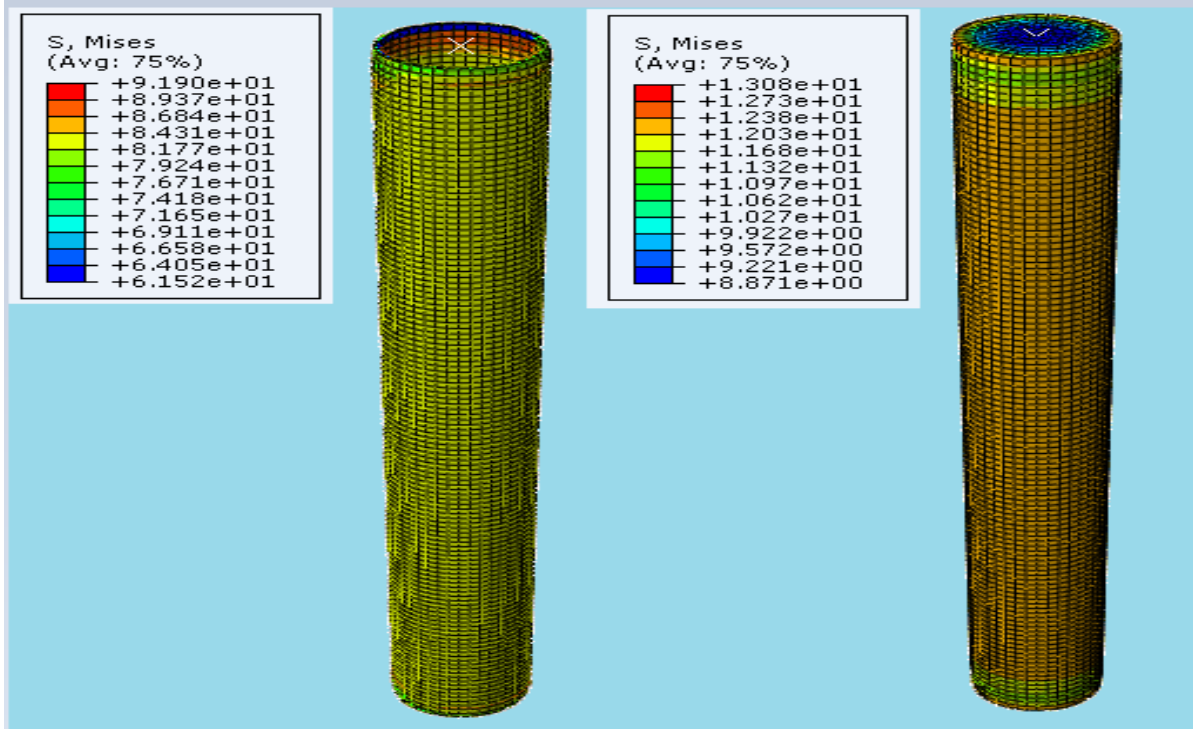


(e)

(f)

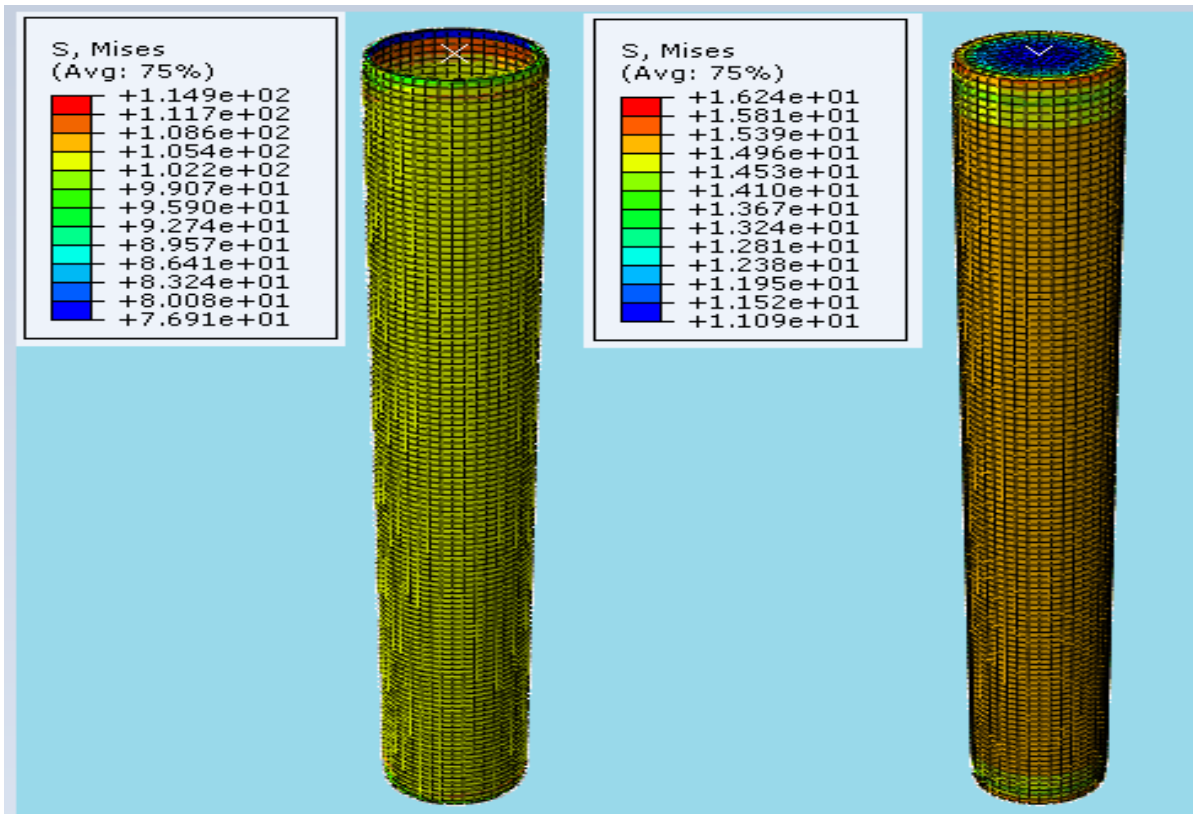
Fig 4.13 Displacement/Compression of SCC @ 40% (a), 50% (b) and 60% (c) of axial capacity

When concentrated load of about 40%, 50% and 60% of ultimate axial capacity of square composite column is applied compression of the column is seen in the direction of applied loads. Under these concentrated load the distribution of compression is high at the top while it is approximately equal to zero at the bottom of the section. As it can be seen from the figure above, which is drawn from the abaqus results the compression of the column increases as the applied load increases which is about 1.32mm, 1.65mm and 2.0mm at 40%P, 50%P and 60%P respectively. Comparing the compression happened in the two rectangular and square composite column, the compression of square composite column is lower than the rectangular cross section.



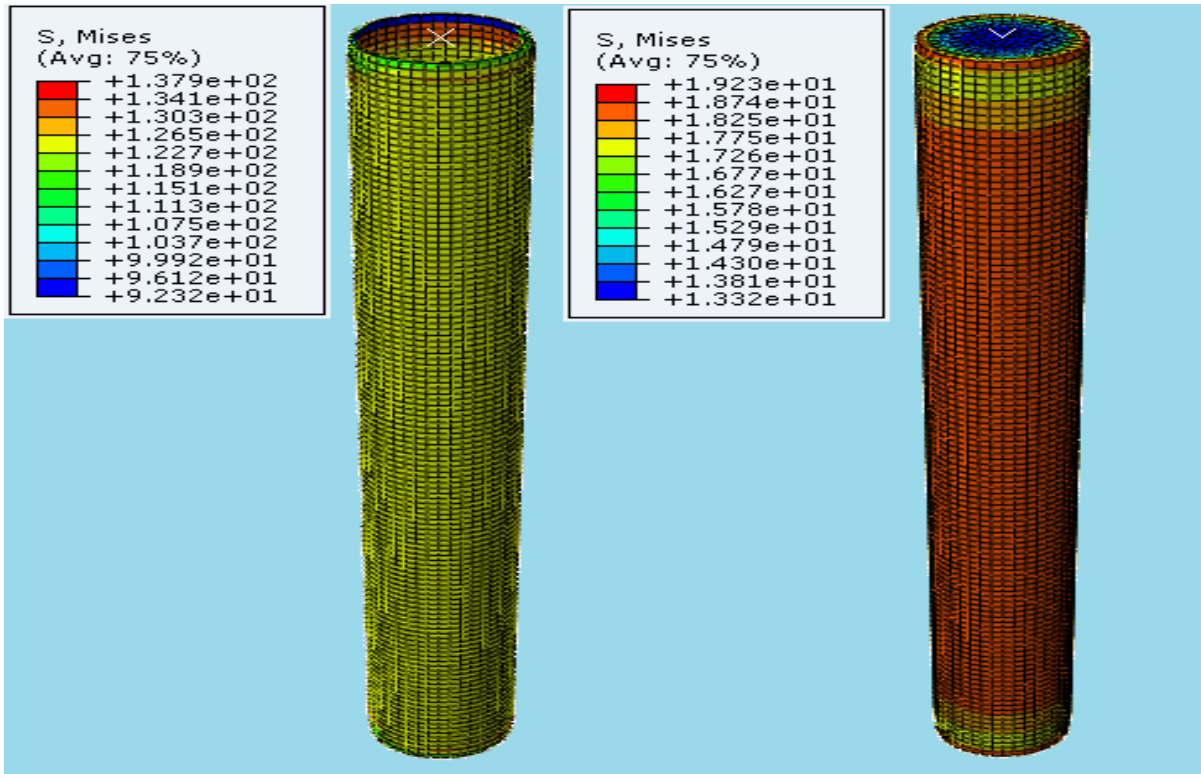
(a)

(b)



(c)

(d)



(e)

(f)

Fig.4.14 Stress of steel and concrete of CCC @ 40%P (a & b),@50%P (c & d) and @ 60%P (e & f) respectively

Concentrated load of 40%P, 50%P and 60%P (where P is axial load capacity of circular composite column) applied on circular composite column and the stress distribution of steel and concrete material of composite column is drawn in the figure 4.14. As it can be seen from the figure stress of steel is about 82, 102, and 122 while stress of concrete section is 12, 15 and 18 as concentrated load of about 2377.18 KN, 2971.475 KN and 3565.77 KN respectively.

The stress distribution of concrete is high on the outside of concrete section where it has contact with steel and it is lower at the center of steel core but the stress distribution of steel is higher than the concrete material.

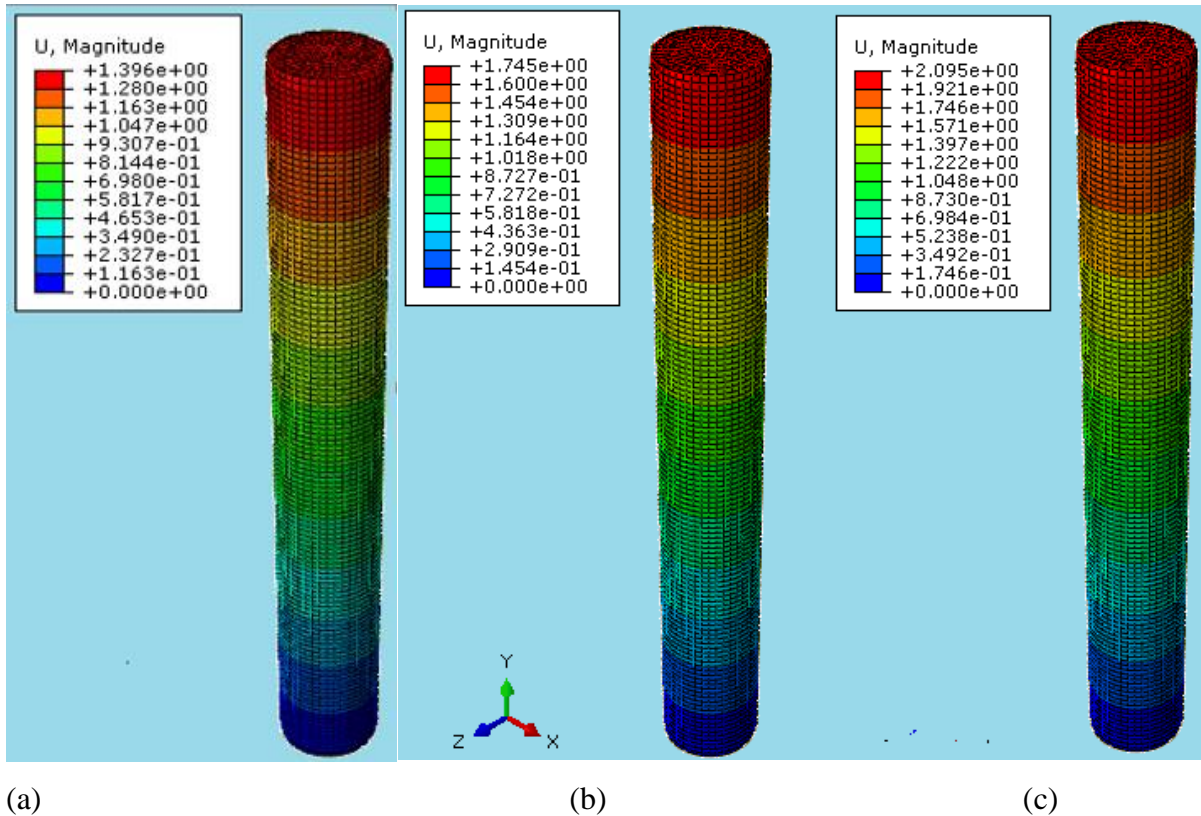
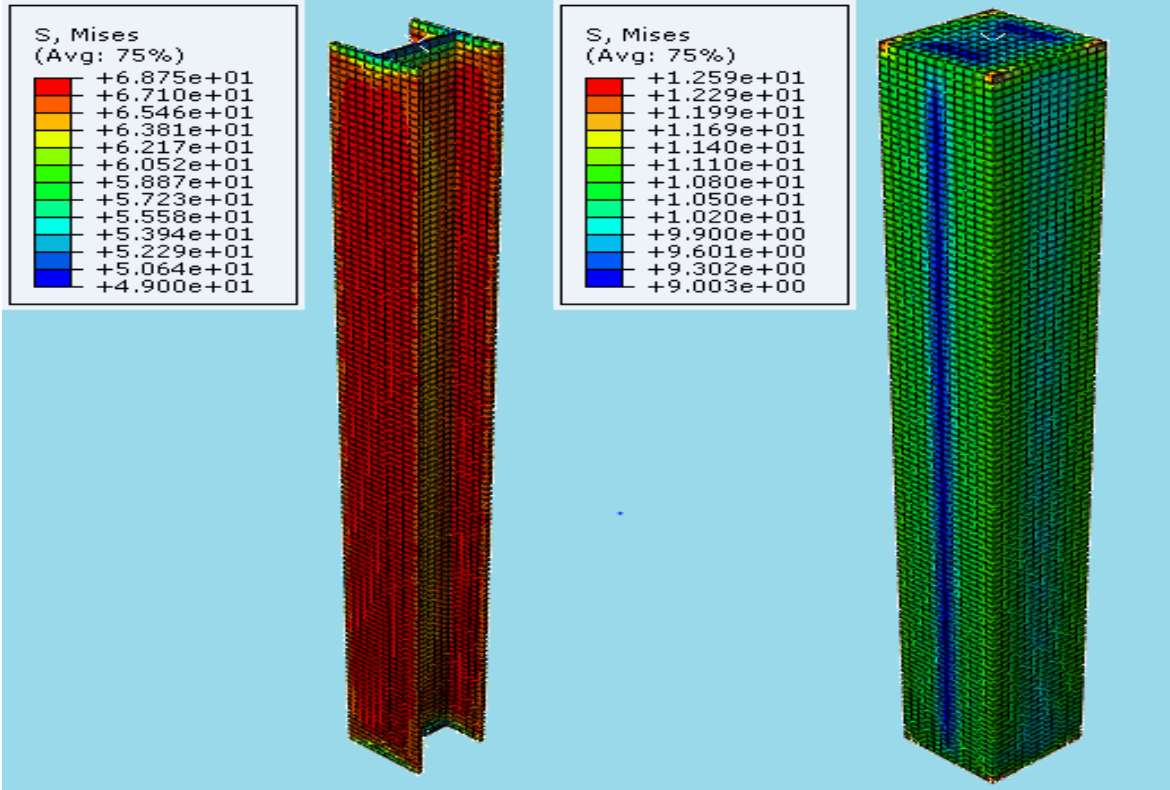


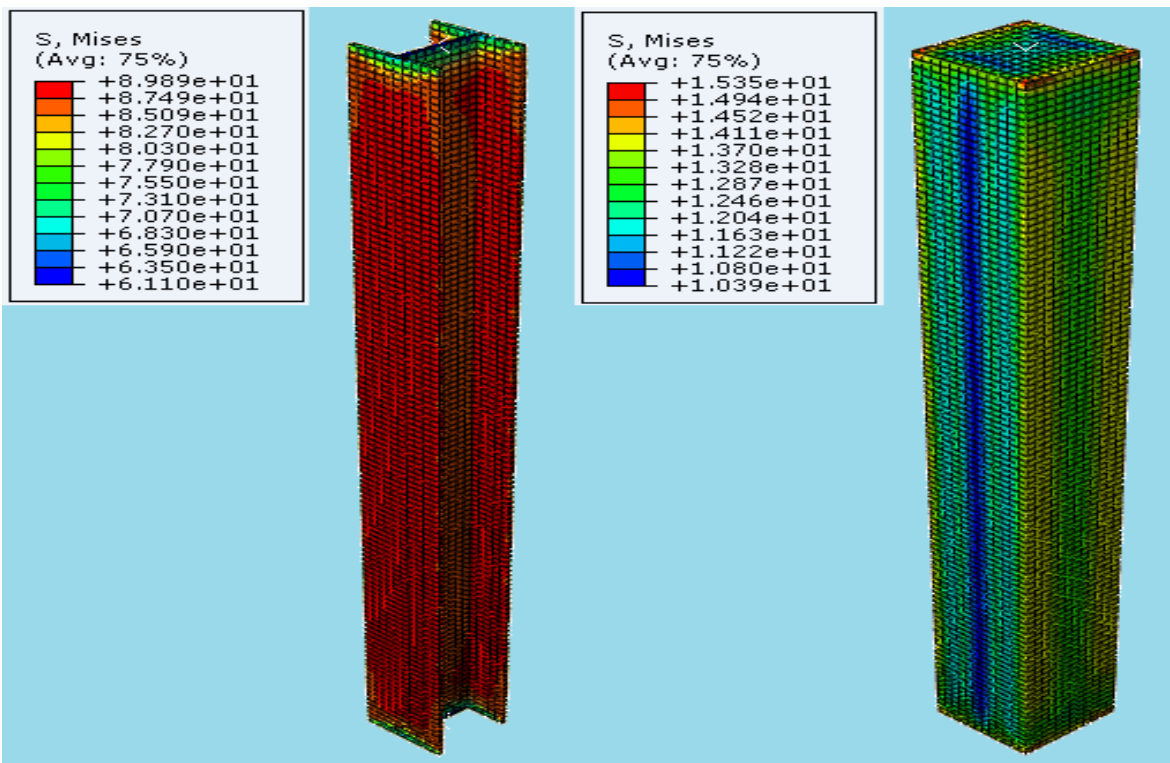
Fig 4.15 Displacement/Compression of CCC @ 40% (a), 50% (b) and 60% (c) of axial capacity

The compression of composite column are high at the top nearly where concentrated load applied and it is distributed from the top to the lower portion of the section. The concentrated load applied on circular composite section is about 40%P, 50%P and 60%P results in compression of about 1.4mm, 1.7mm and 2.1mm respectively which is approximately equal to zero at the bottom of the column.



(a)

(b)



(c)

(d)

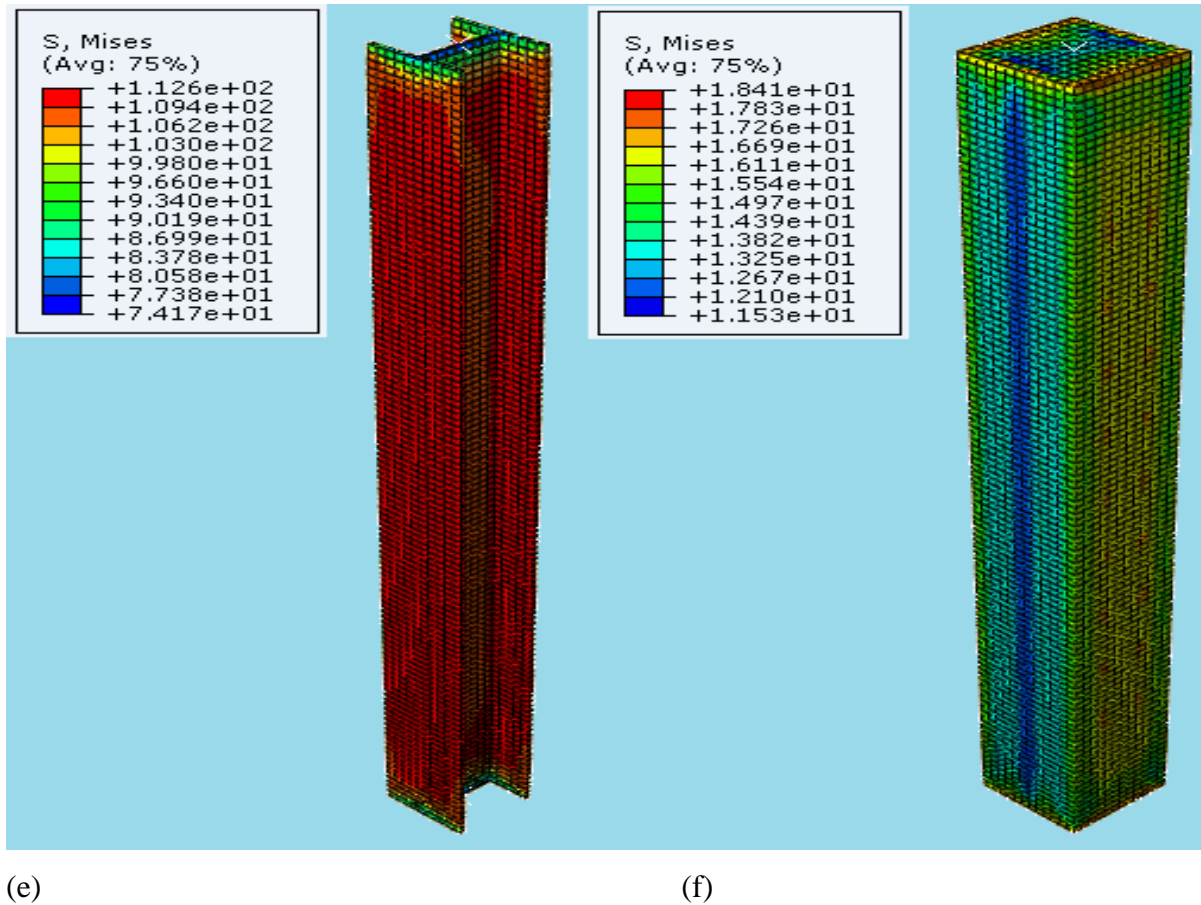


Fig.4.16 Stress of steel and concrete of Encased I-section @ 40%P (a & b),@50%P (c & d) and @ 60%P (e & f) respectively

In the case of encased I-section composite column the stress distribution of steel and concrete material due to the applied concentrated load of about 40%P, 50%P and 60%P which is about 2017 KN, 2521.2 KN and 3025.5 KN respectively is lower than other cross-section of composite column based on the results obtained from the abaqus analysis. The stress of steel material is about 65, 87 and 111 while that of concrete is about 11, 12, 15 respectively with the applied load.

Unlike in the other cross-section of composite column, the stress distribution in the concrete section along the steel tube is lower while in other cross section of composite column stress distribution in concrete material is high along the steel tube or in areas of concrete which has direct contact with the steel tube.

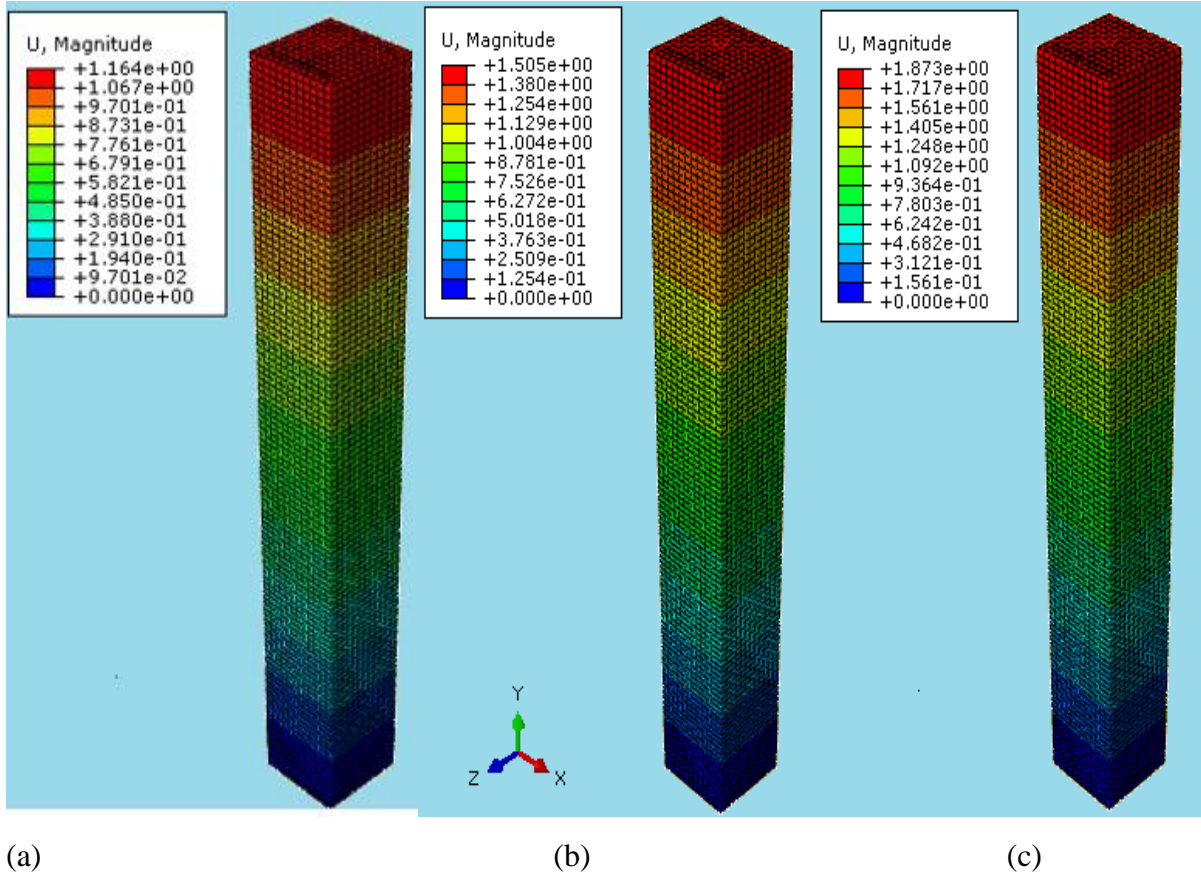


Fig 4.17 Displacement/Compression of CCC @ 40% (a), 50% (b) and 60% (c) of axial capacity

The compression of encased I-section of composite column which is subjected to about 40%P, 50%P and 60%P calculated by abaqus and the result is drawn on the figure 4.17 below. The compression of about 1.16mm, 1.5mm and 1.87mm are seen at the top of encased I-section due the applied concentrated load of about 2017KN, 2521.2KN and 3025.5KN respectively. As it can be seen from the results the compression of encased I-section due applied of 40%P, 50%P and 60%P is less than other cross-section (rectangular, square and circular) under the same condition of loading.

4.2.1.2 Behavior of Composite Column Under Axial Load and Torsion

For the behavior analysis under torsion and axial concentrated load, each section of composite column have approximately equal area of steel and concrete section and are subjected to a constant torsion with their 40% , 50%, 60% of its axial capacity.

Table 4.2 Summary of the applied axial load and Torsion

Composite Column section	Axial Capacity(KN)	P1 (40%) (KN)	P2 (50%) (KN)	P3 (60%) (KN)	T (KN.m)
RCC	5553.4	2221.36	2776.7	3332.04	60
SCC	5595	2238	2797.5	3357	60
CCC	5942.95	2377.18	2971.475	3565.77	60
Encased I-secn	5042.47	2017	2521.2	3025.5	60

Based on the load from table 4.2 each section of composite column is analysed by Abaqus software and the following output is obtained and each result is discussed in detail.

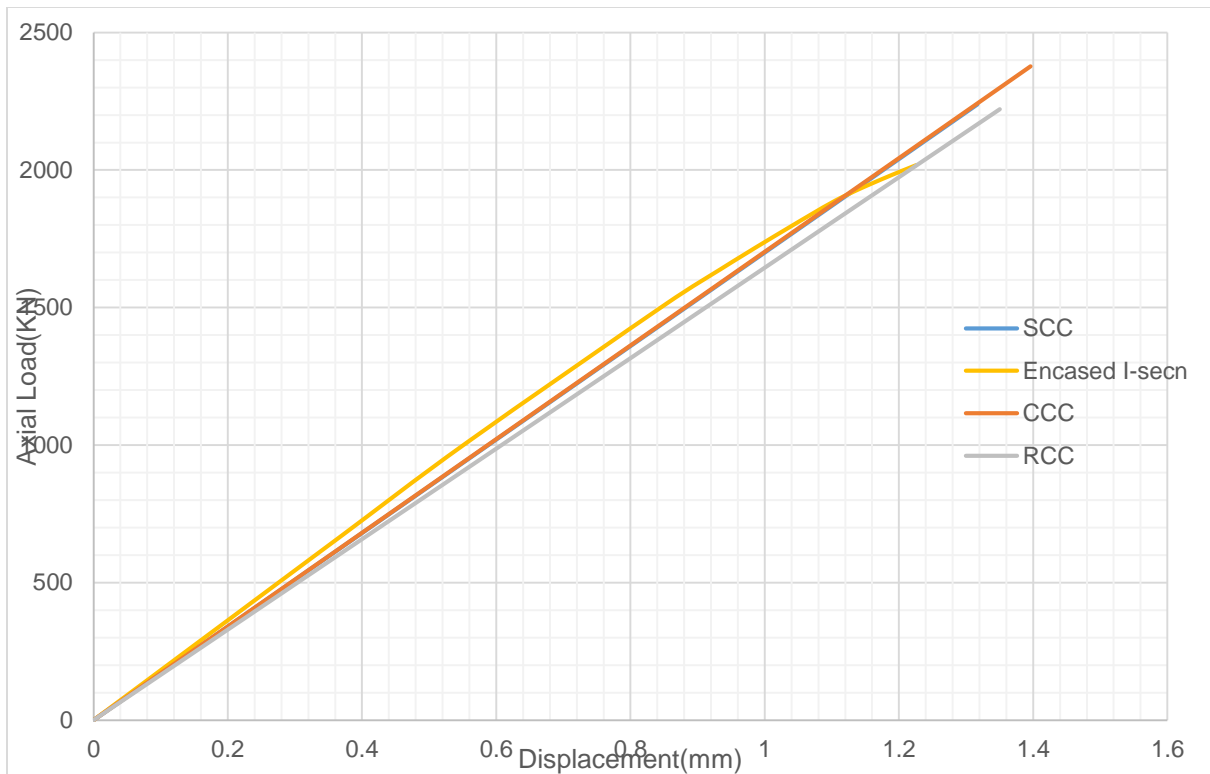


Fig 4.18 Axial load vs displacement @ 40% P

Axial concentrated loads of about 40% of ultimate axial capacity of rectangular composite column, square composite column, circular composite column and encased I – section with the magnitude of 2221.36 KN, 2238KN, 2377.18KN and 2017KN are applied respectively at the top center on each composite column with constant Torsion of about 60 KN-m. Using Abaqus software the corresponding deflection/compression of composite column is plotted in the figure 4.18. In this case keeping the concentrated as it is and adding torsion load at the top of the column.

At the initial stage of loading of 40% of ultimate axial capacity for each composite column section and constant torsion, encased I-section show better performance in terms of compression but it starts to show parabolic increasing in compression while square composite column and circular composite column shows same linear performance and the rectangular composite column shows higher compression than other cross section. Comparing encased I-section subjected to concentrated load and Torsion and Encased I-section subjected to

concentrated load only, compression/deflection increases when torsion is applied than in cases concentrated load is applied.

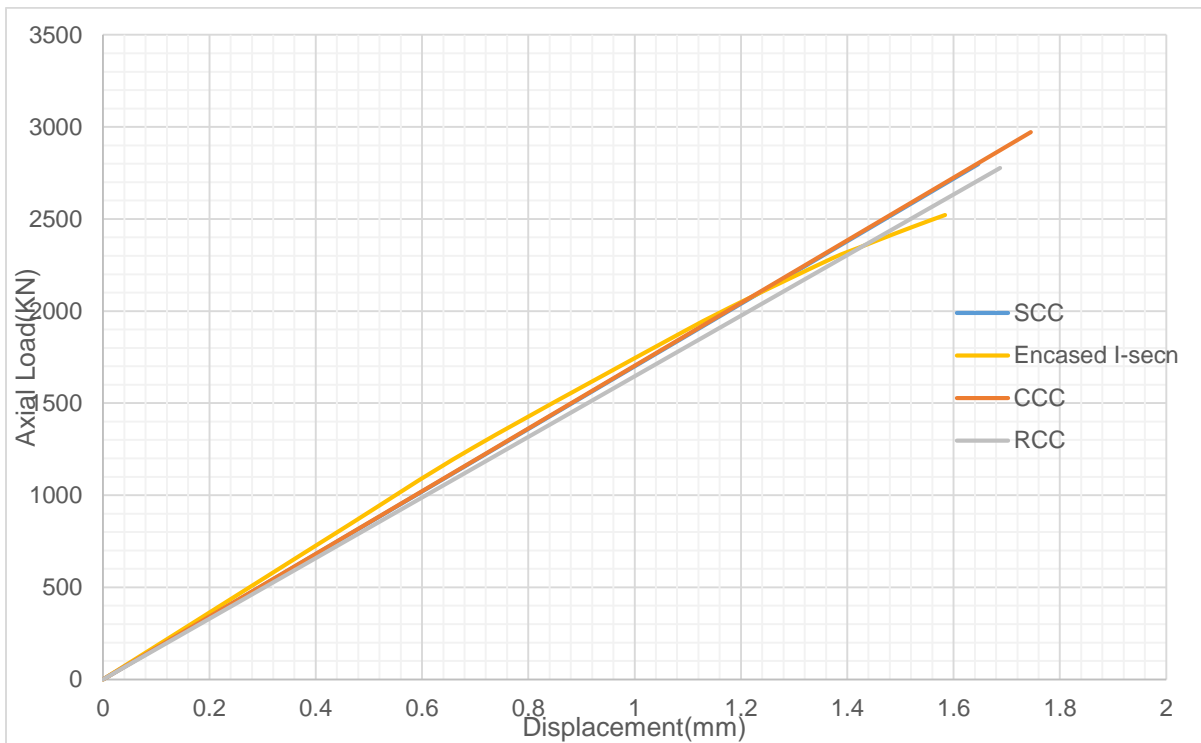


Fig 4.19 Axial load vs displacement @ 50% P

As the applied load on each composite column reaches 50% of its axial load capacity, rectangular composite column, square composite column, circular composite column and encased I-section is subjected to 2776.7 kN, 2797.5 kN, 2971.5 kN and 2521.2 kN respectively and a constant torsion about 60 kN-m is applied. When the applied load is increased (to 50% of axial capacity) from 40%P, encased I-section composite column shows lower performance in terms of compression than circular composite column and square composite column and rectangular composite column. Data obtained from abaqus result analysis on fig 4.19 shows the decreasing in strength of encased I-section does not linear as in other cross section.

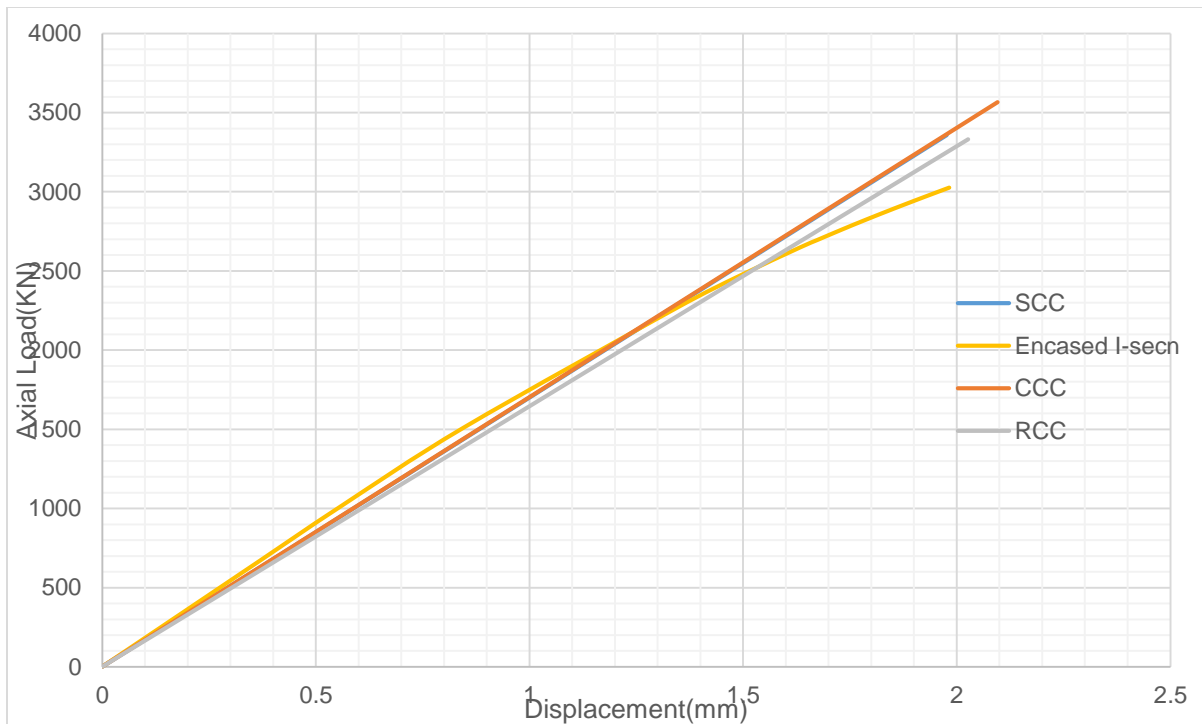


Fig 4.20 Axial load vs displacement @ 60% P

When the concentrated load applied reaches 60% of ultimate axial capacity for each composite column rectangular composite column, square composite column, circular composite column and encased I-section subjected to 3332.04 KN, 3357 KN, 3565.77 KN and 3025.5 KN respectively and keeping torsion constant.

As the concentrated load applied on composite increases square composite column and circular composite column shows similar condition through all loading and rectangular composite column compresses more than other cross section but as the applied load increases the encased I-section compresses more. As it can be seen from abaqus result adding torsion load on column with concentrated load does not have much effect on compression of rectangular composite column, square composite column and circular composite column but encased I-section increases in compression as torsion applied on it.

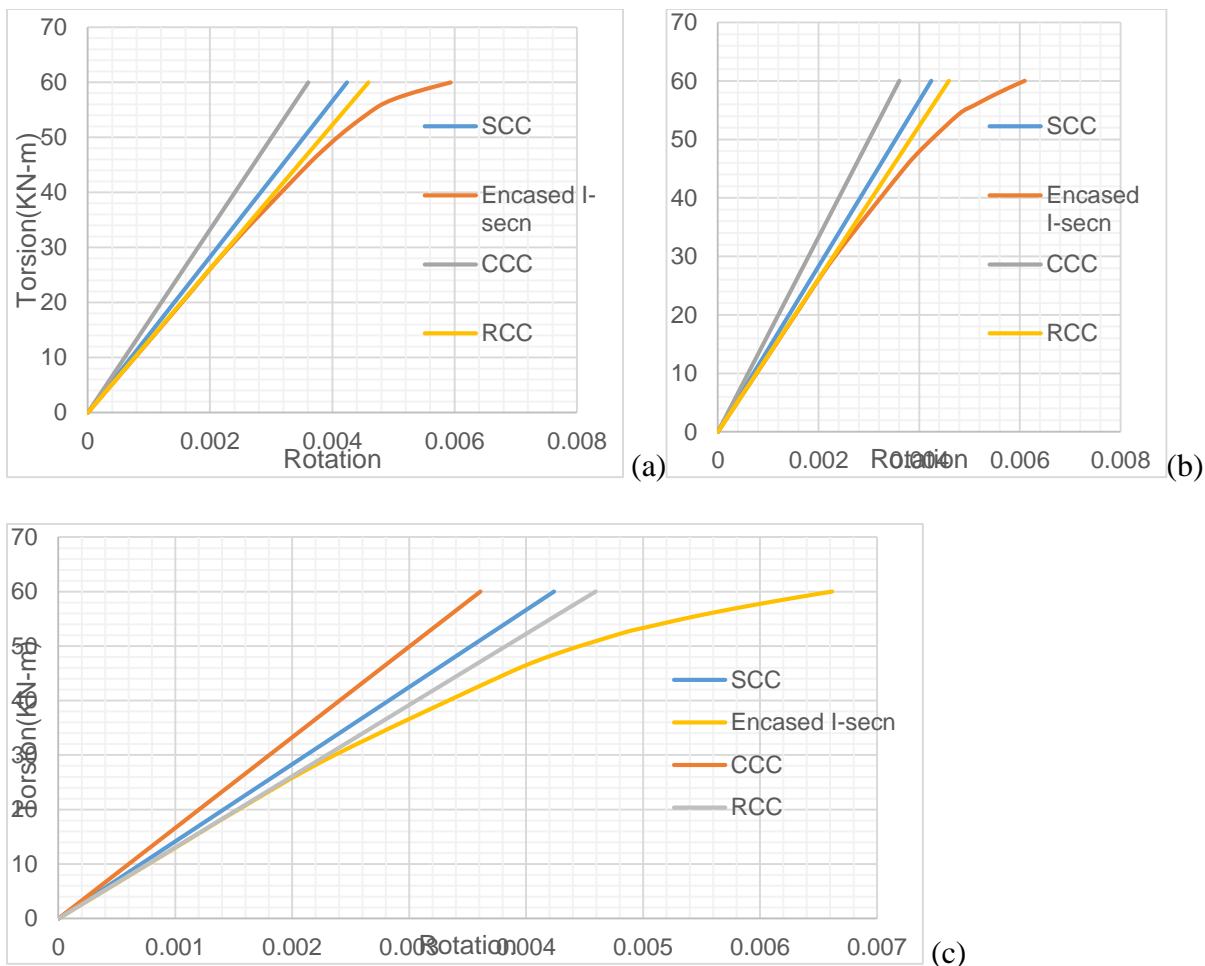
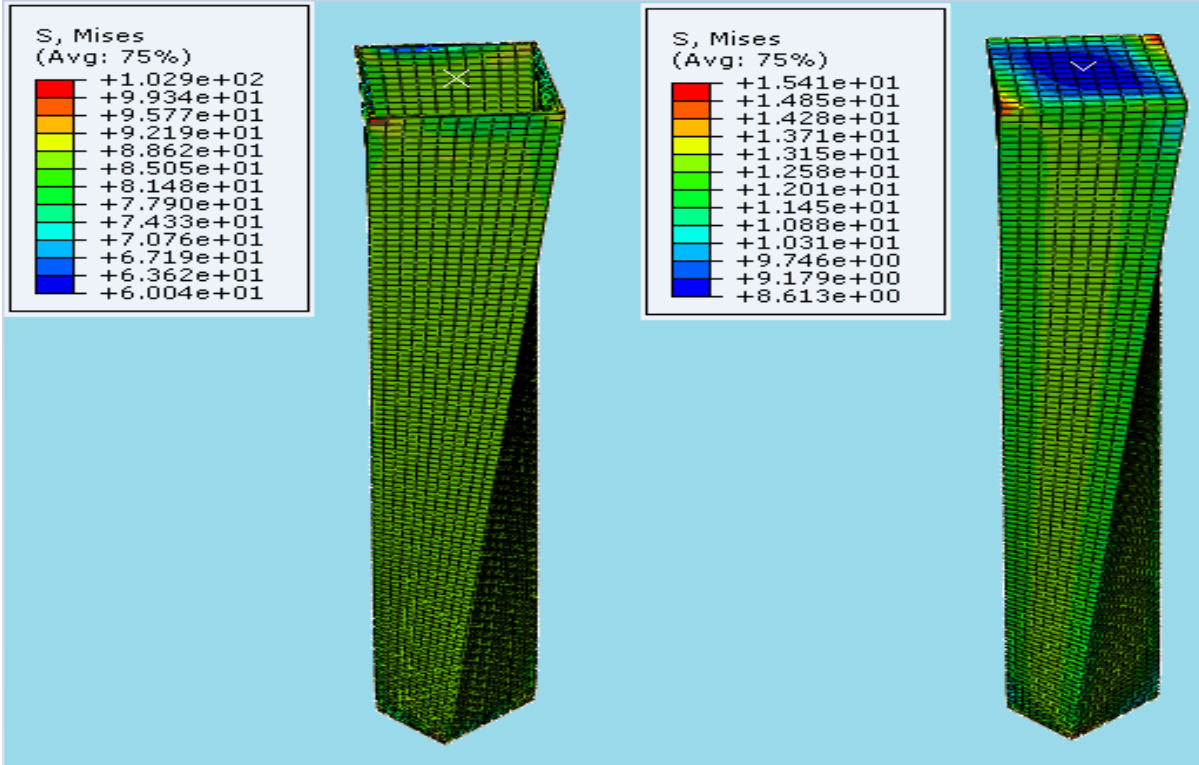


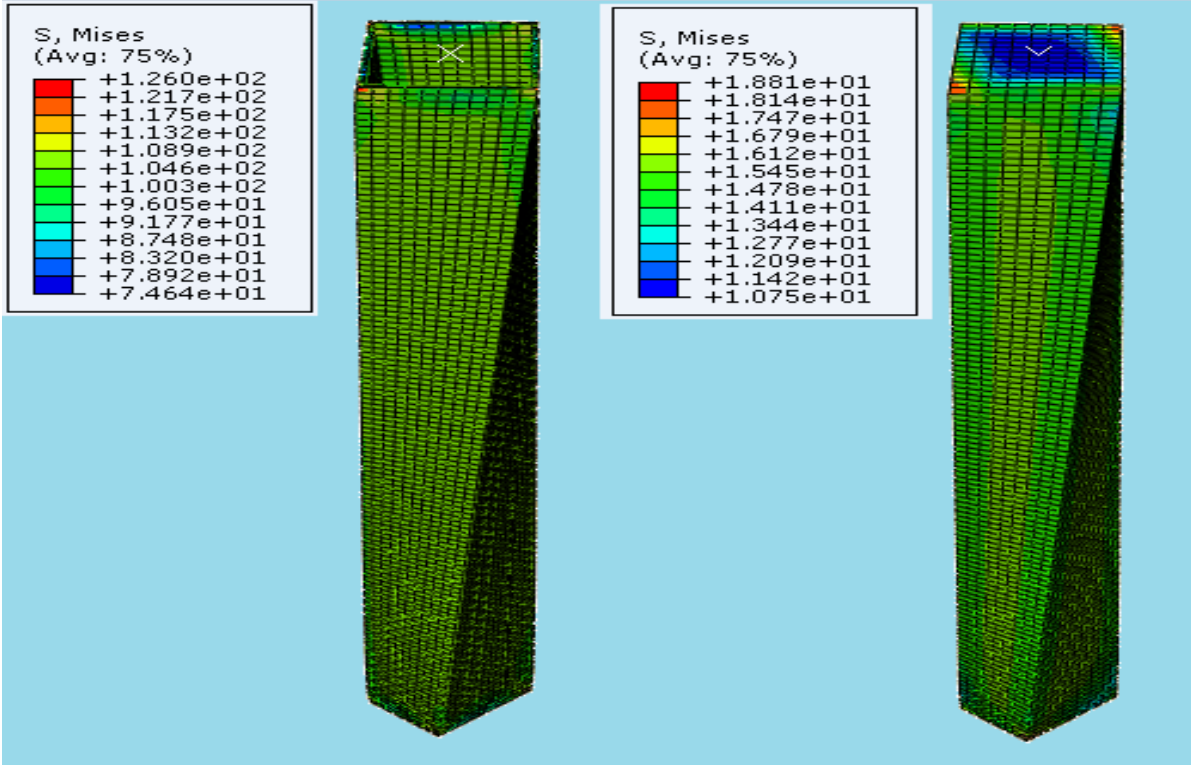
Fig 4.21 Torsion vs rotation of composite column as Axial Load is 40%P(a), 50%P(b), 60%(c)

Effect of axial load on composite column in terms of rotation is plotted on the figure below from the abaqus analysis result. Increasing the axial load from 40%-60% of the axial capacity of composite column by keeping torsion constant, the rotation of composite column does not change due changing or increasing of axial load. Increasing the axial load on column does not have effect to increase the rotation of column under constant Torsion.



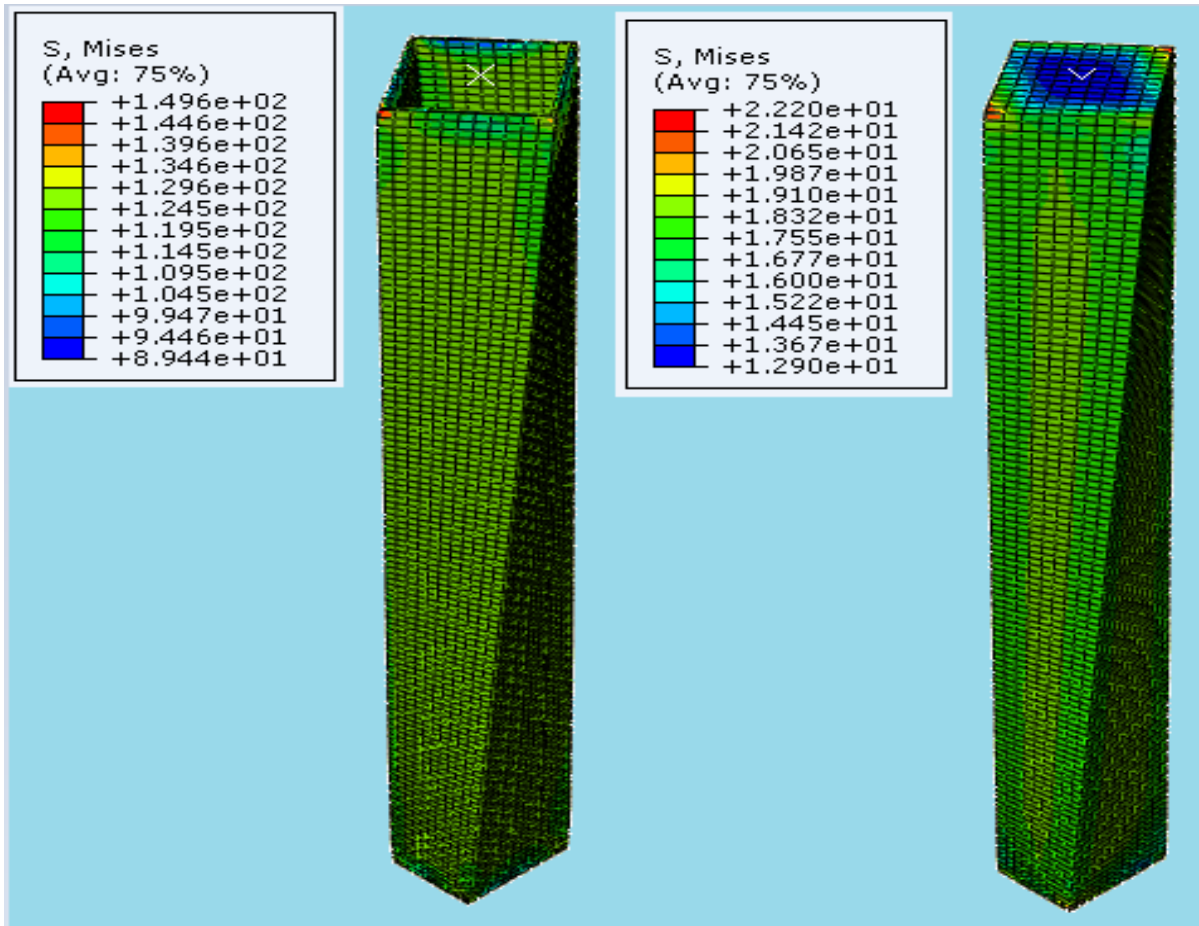
(a)

(b)



(c)

(d)



(e)

(f)

Fig.4.22 Stress of steel and concrete of RCC @ 40%P (a & b),@50%P (c & d) and @ 60%P (e & f) respectively with constant Torsion.

Different axial load 40%, 50% and 60% of its ultimate axial capacity of Rectangular Composite Column of about 2221.36KN, 2776.7KN and 3332.04 KN and a constant torsion of about 70KN-m is applied at the top center of composite column using rigid plate and analyzed using ABAQUS software. From the results obtained using abaqus software stress distribution of different elements of composite column is shown in the figure 4.22. Under these introduced concentrated load steel tube experiences stress of about 82, 100 and 125 while concrete has 12,16 and 18 stresses.as it can be seen there is an increase in stresses on both material and is due to application of torsion in addition to the concentrated loads.

From the figure below, it shows that as the concentrated axial load increases with keeping the Torsion constant, the twisting of column decreases.

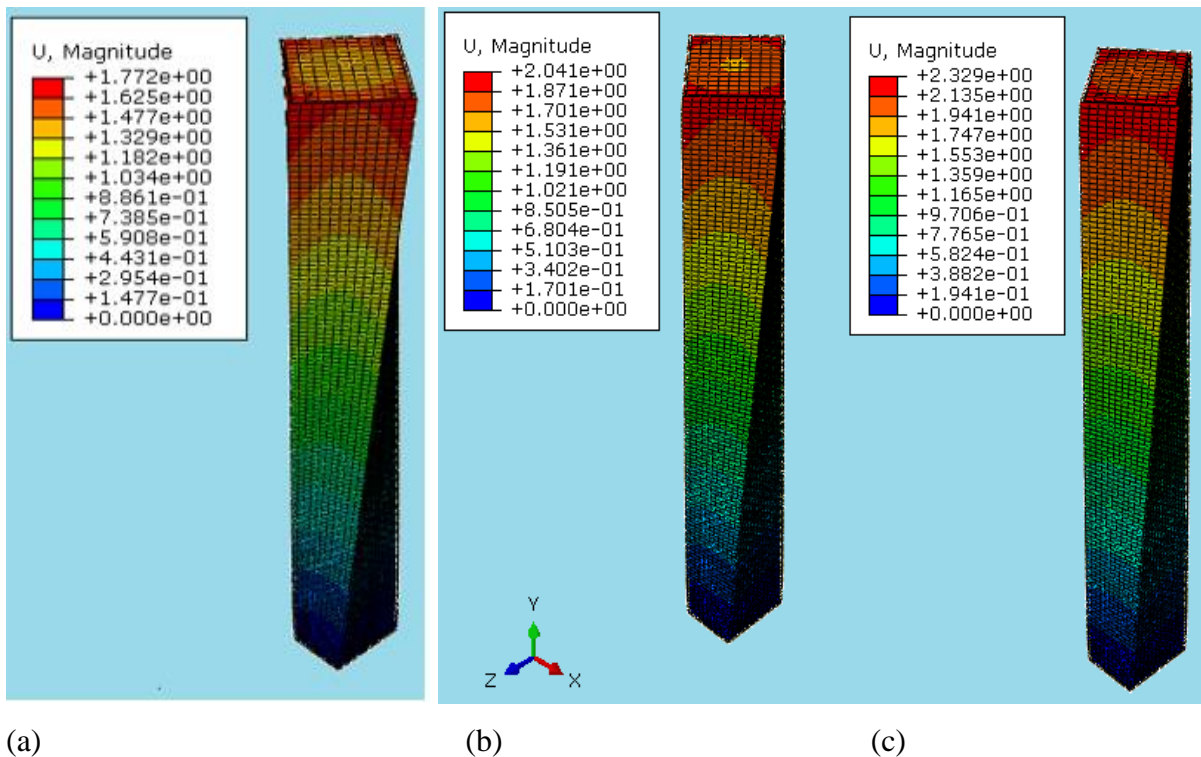
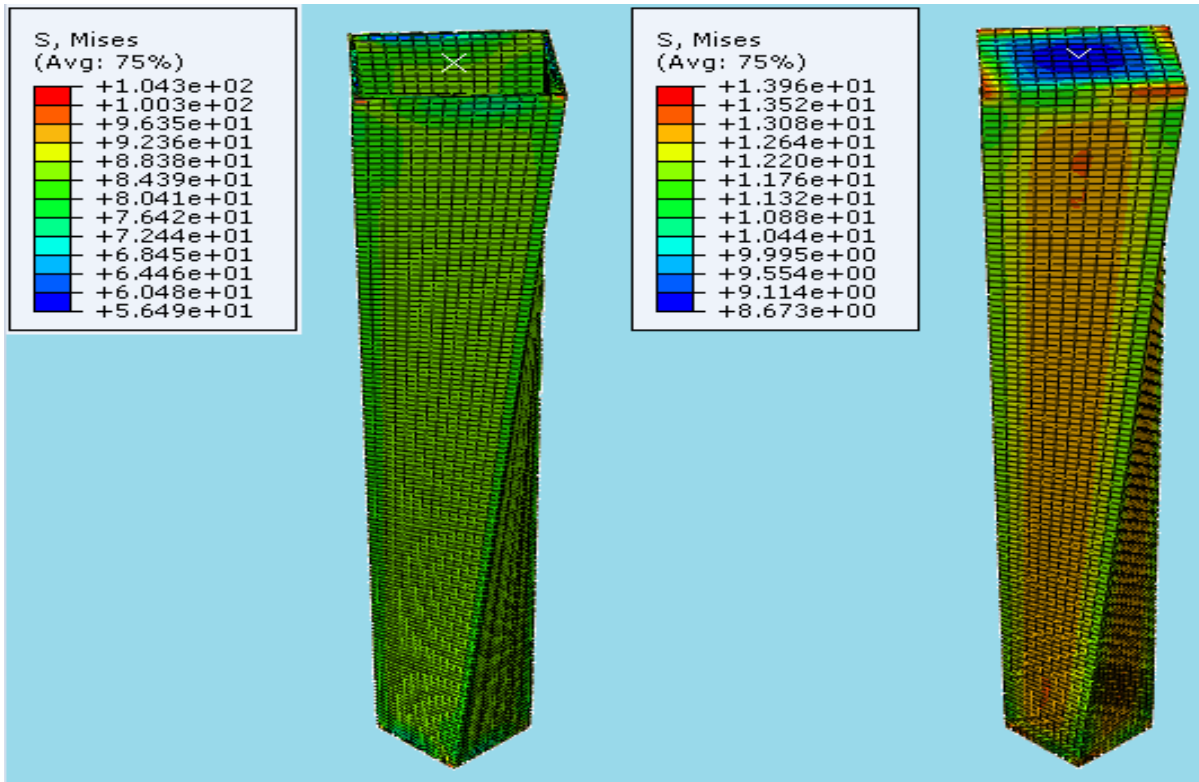


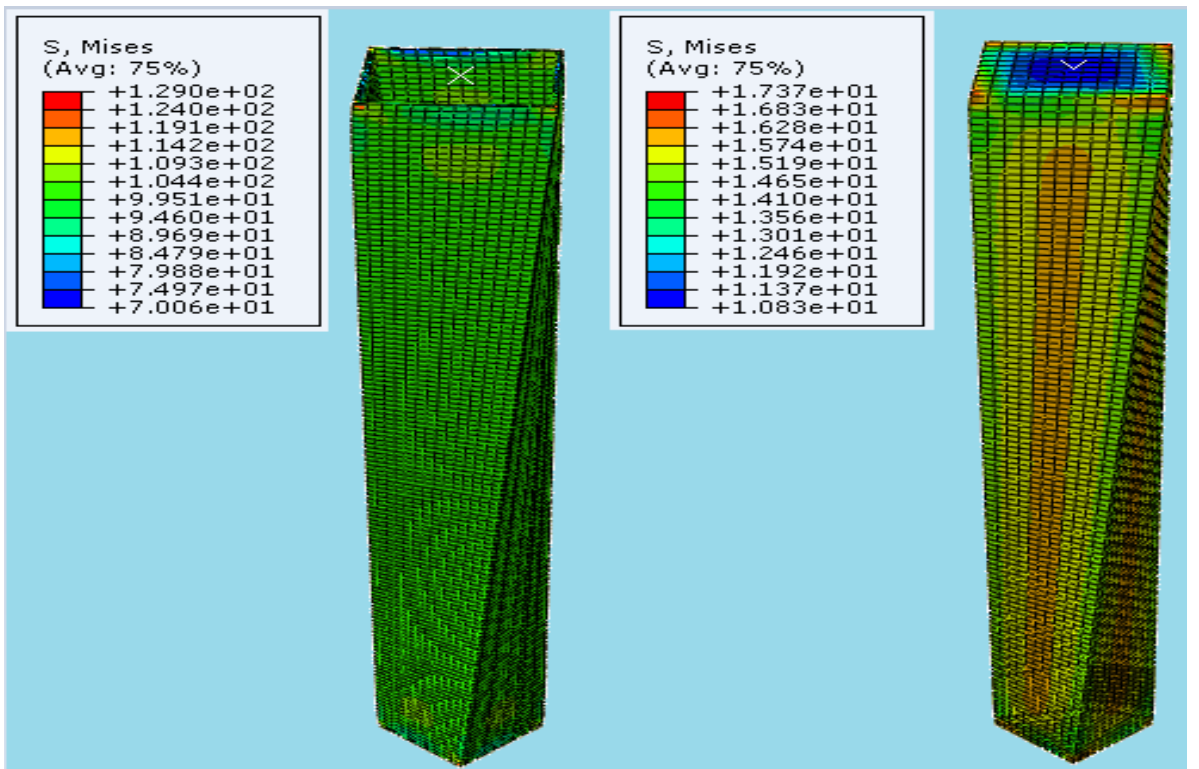
Fig 4.23 Displacement/Compression of RCC @ 40% (a), 50% (b) and @ 60% (c)

Due applied concentrated load of about 40%, 50% and 60% of ultimate axial capacity of rectangular composite column which is 2221.36KN, 2776.7KN and 3332.04 KN respectively and a constant torsion of about 60KN-m is applied. Using the results from abaqus displacement of the column is shown in figure 4.23. The application of torsion in addition to the concentrated load results in increasing the displacement of the column. The distribution of compression is high at the top while it is approximately equal to zero at the bottom of the section. Due to application of torsion with concentrated load, As it is seen on the figure, the compression of the column is about 1.8mm, 2.04mm and 2.33mm at 40%P, 50%P and 60%P and constant torsion respectively.



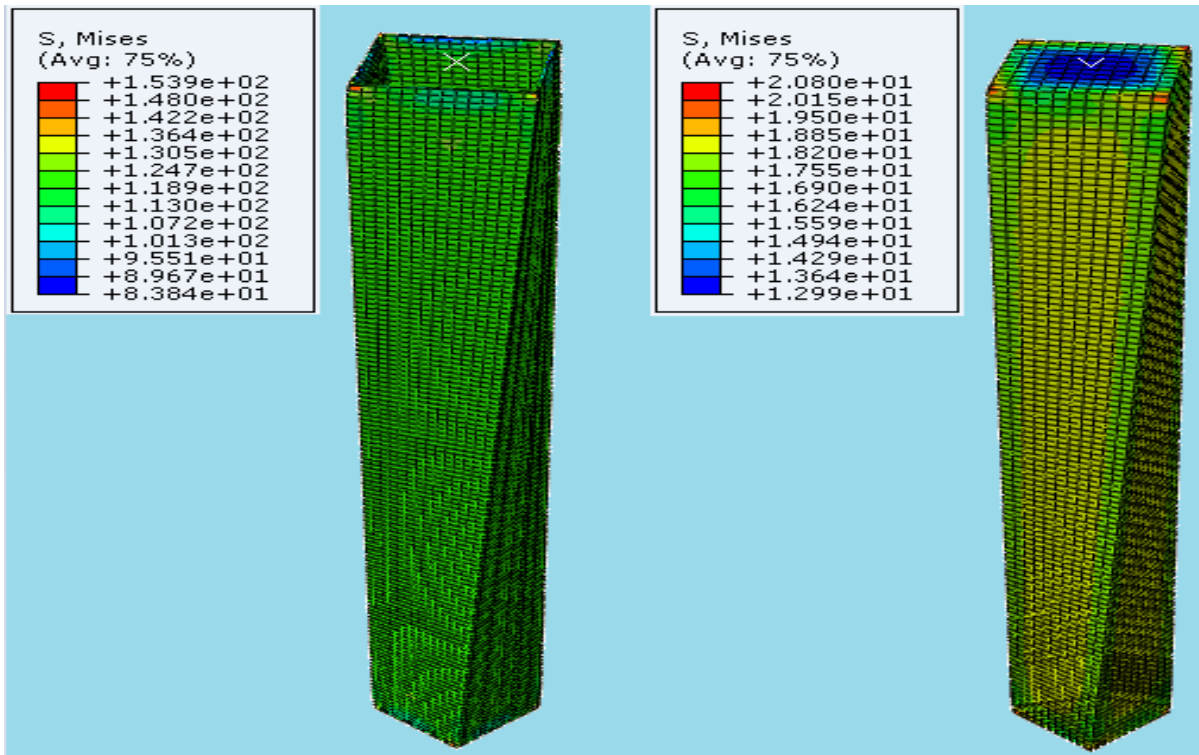
(a)

(b)



(c)

(d)



(e)

(f)

Fig.4.24 Stress of steel and concrete of SCC @ 40%P (a & b),@50%P (c & d) and @ 60%P (e & f) respectively with constant Torsion.

Keeping the concentrated load of about 40%P, 50%P, and 60%P which is 2238 KN, 2797.5 KN and 3357 KN respectively and adding a constant torsion of about 60KN-m is applied and the stress distribution in steel and concrete material is calculated using abaqus software.

From the figure 4.24 the stress distribution of steel section is approximately 85, 105 and 125 while concrete stress is 12.2, 15 and 18.2 as the applied concentrated load is 40%P, 50%P and 60%P respectively with a constant Torsion. From the results obtained, it is clear that the stress distribution steel and concrete material in rectangular and square composite column is similar.

As it can be seen from the figure, the stress distribution in the concrete core is high at the corner of the column where it has direct contact to the steel tube while it is low at the center of concrete core. It is also clear that, the twisting of square composite column decreases as the concentrated load decreases.

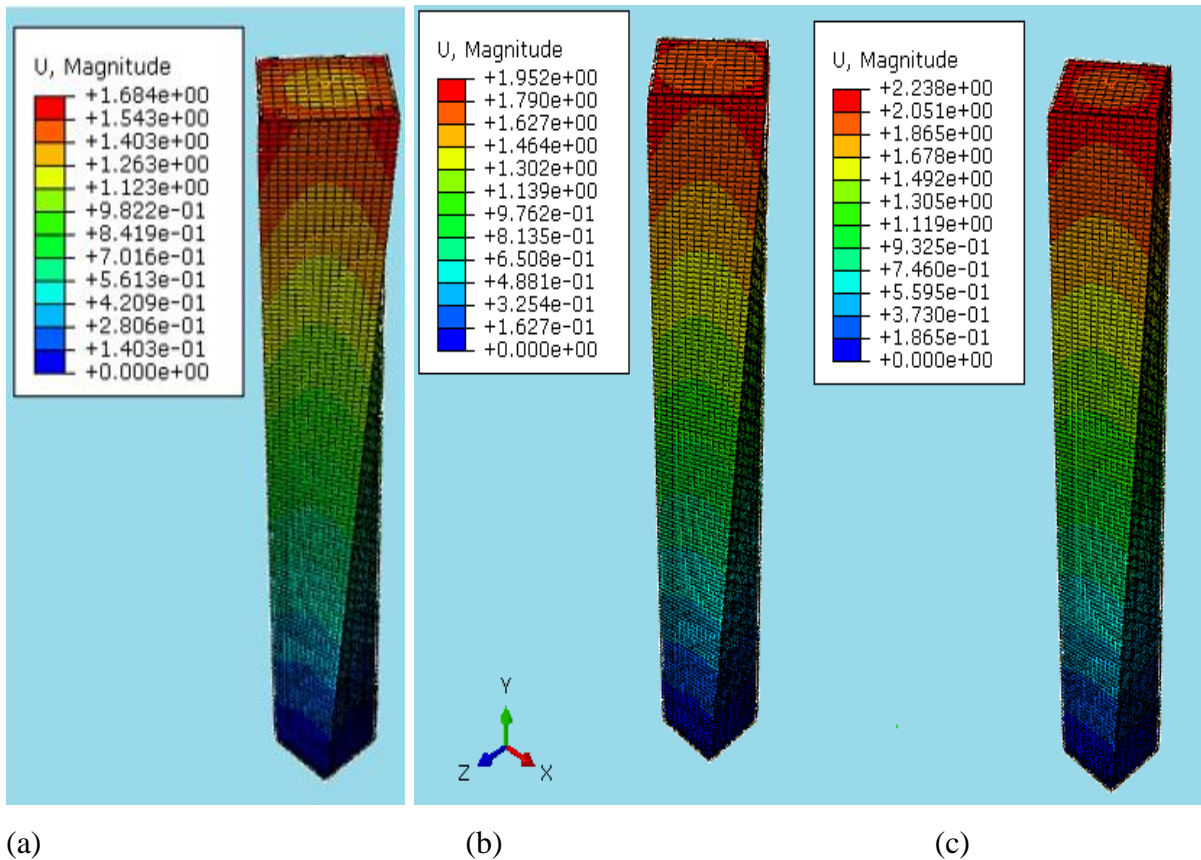
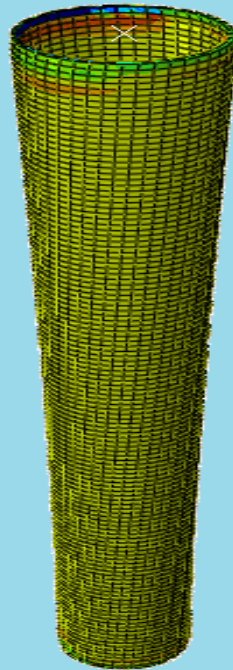
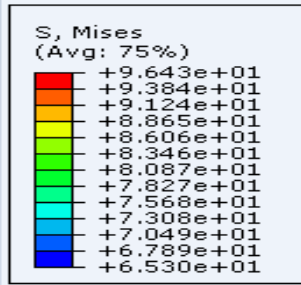
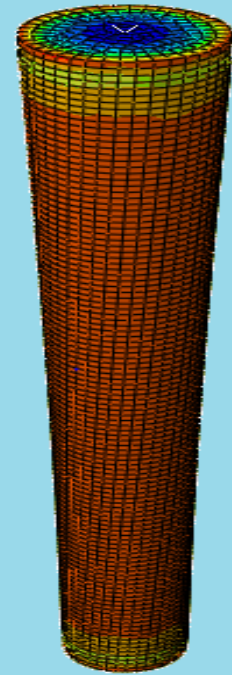
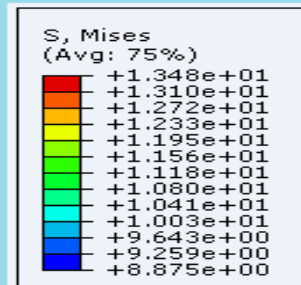


Fig 4.25 Displacement/Compression of SCC @ 40% (a), 50% (b) and @ 60% (c)

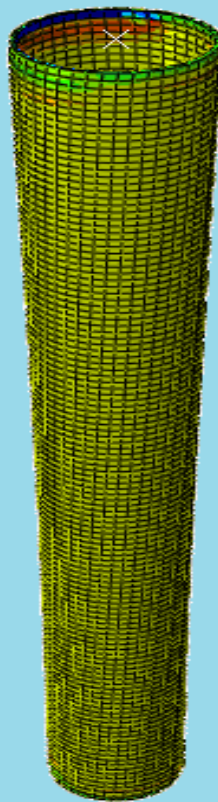
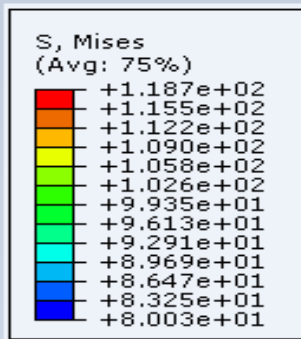
When concentrated load of about 40%, 50% and 60% of ultimate axial capacity of square composite column in addition to constant load of about 60KN-m is applied, displacement of the column is seen on the figure 4.25. Under these concentrated load and torsion, the distribution of compression is high at the top while it is approximately equal to zero at the bottom of the section. As it can be seen from the figure above, which is drawn from the abaqus results the compression of the column increases as the applied load increases which is about 1.68mm, 1.95mm and 2.24mm at 40%P, 50%P and 60%P with constant torsion respectively. Comparing the compression happened in the two rectangular and square composite column, the compression of square composite column is lower than the rectangular cross section.



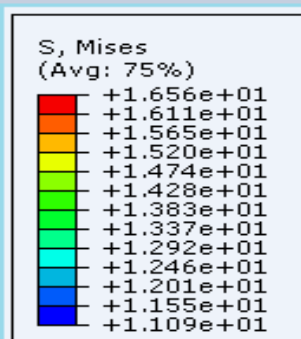
(a)



(b)



(c)



(d)

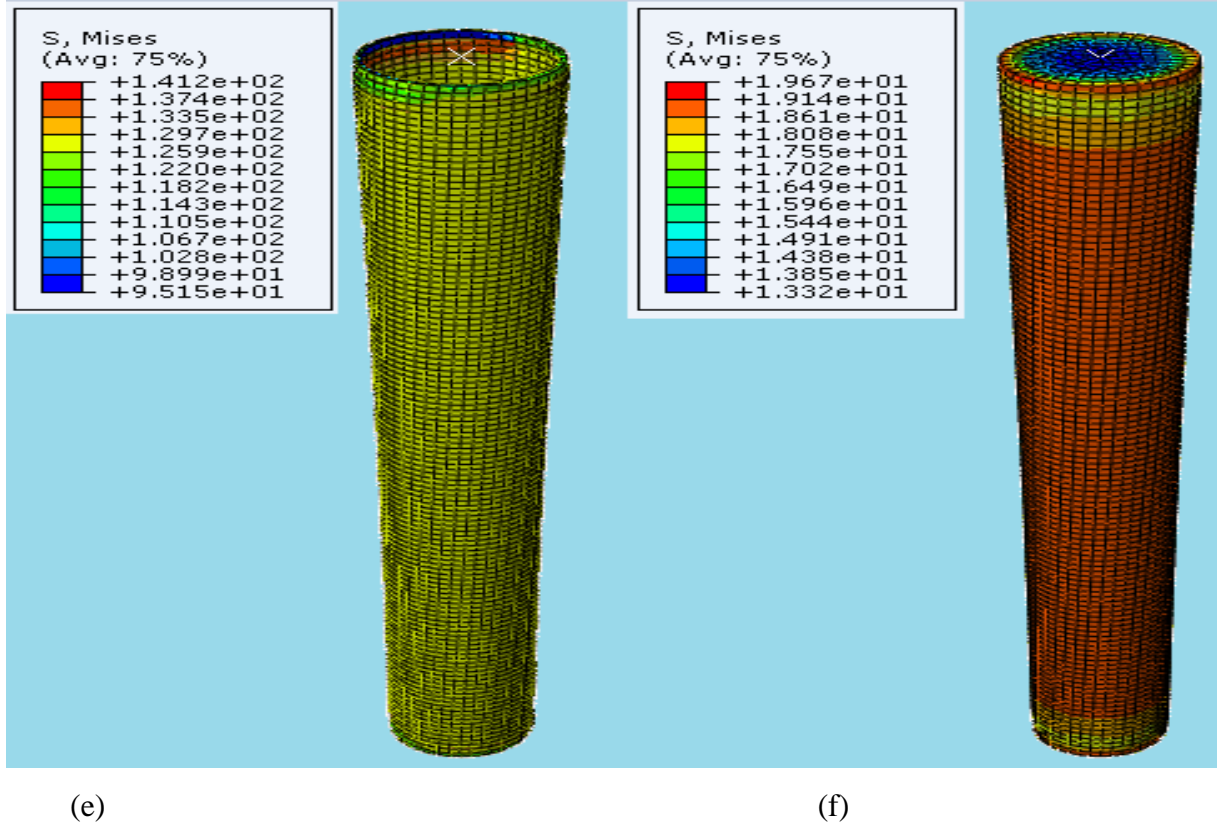


Fig.4.26 Stress of steel and concrete of CCC @ 40%P (a & b), @50%P (c & d) and @ 60%P (e & f) respectively with constant Torsion.

Concentrated load of about 40%P, 50%P and 60%P (where P is axial load capacity of circular composite column) and a constant torsion of about 60KN-m applied on circular composite column and the stress distribution of steel and concrete material of composite column is drawn in the figure 4.26. As it can be seen from the figure stress of steel is about 86, 106, and 126 while stress of concrete section is 13, 16 and 19 as concentrated load of about 2377.18 KN, 2971.475 KN and 3565.77 KN with constant torsion applied respectively.

The stress distribution of concrete is high on the outside of concrete section where it has contact with steel and it is lower at the center of steel core but the stress distribution of steel is higher than the concrete material.

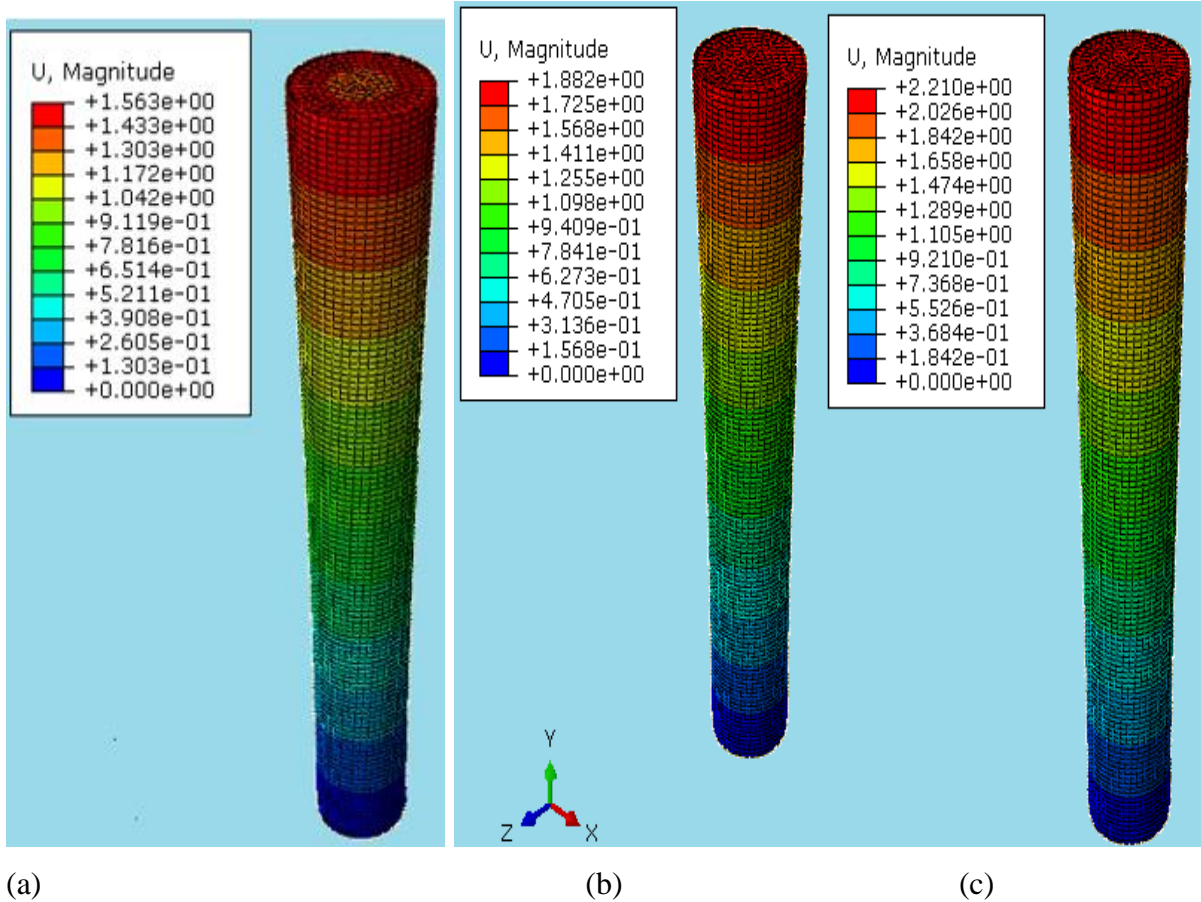
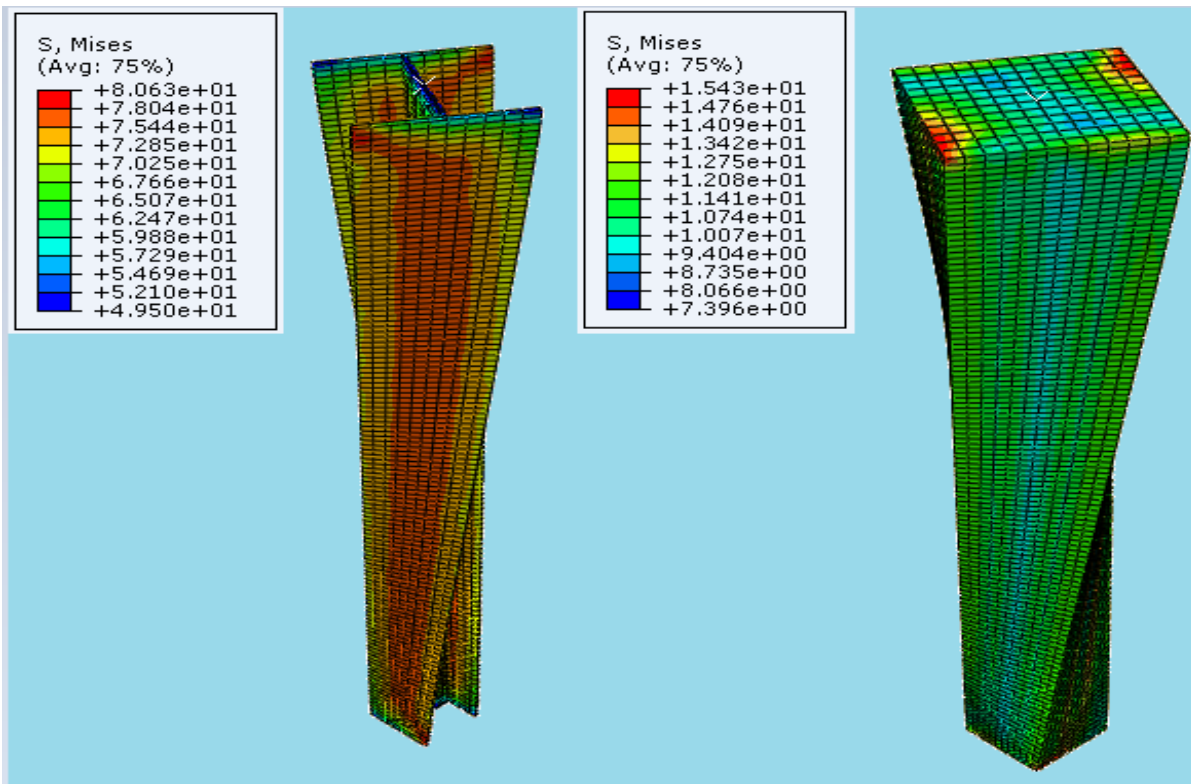


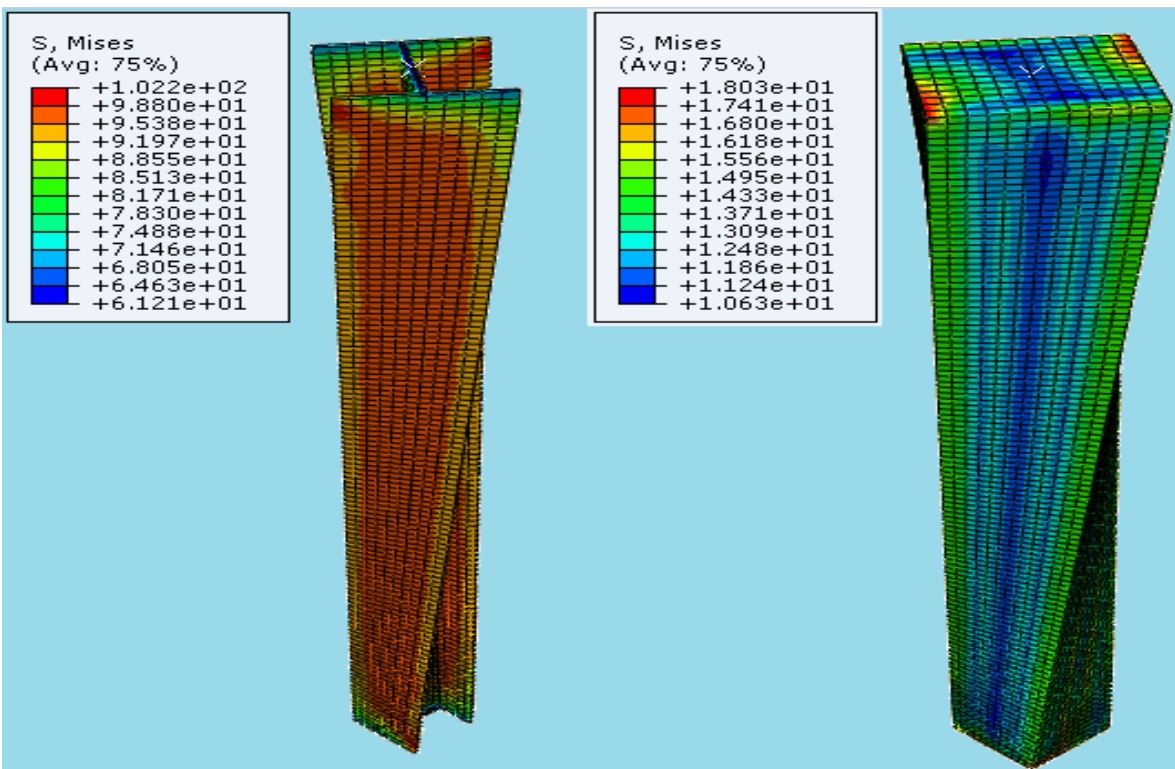
Fig 4.27 Displacement/Compression of SCC @ 40% (a), 50% (b) and @ 60% (c)

Keeping the concentrated load applied, a constant torsion of about 60KN-m is applied. The compression of composite column are high at the top nearly where concentrated load applied and it is distributed from the top to the lower portion of the section. The concentrated load applied on circular composite section is about 40%P, 50%P and 60%P with constant torsion results in compression of about 1.56mm, 1.9mm and 2.2mm respectively which is approximately equal to zero at the bottom of the column.



(a)

(b)



(c)

(d)

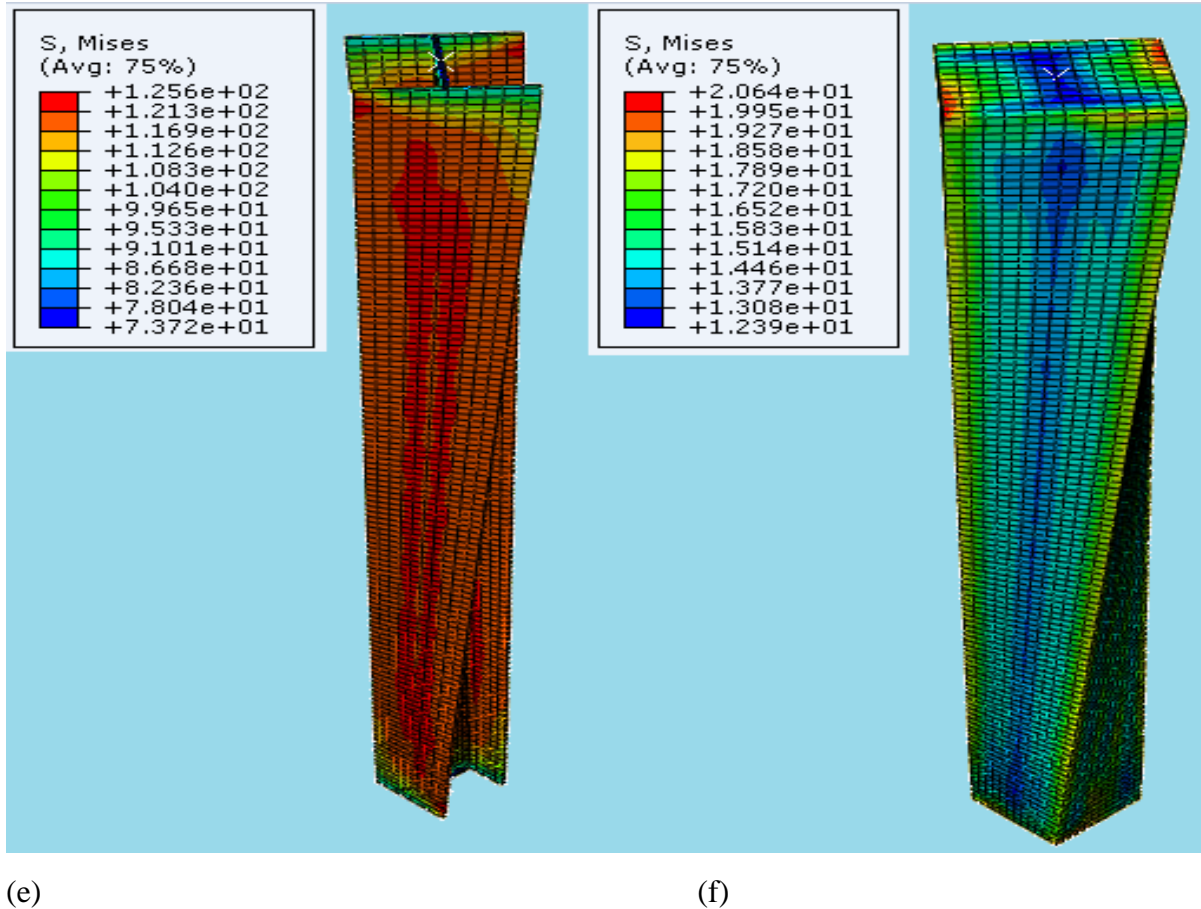


Fig.4.28 Stress of steel and concrete of Encased I-section @ 40%P (a & b),@50%P (c & d) and @ 60%P (e & f) respectively with constant Torsion.

In the case of encased I-section composite column, the stress distribution of steel and concrete material due to the applied concentrated load of about 40%P, 50%P and 60%P which is about 2017 KN, 2521.2 KN and 3025.5 KN respectively with constant torsion of about 60KN-m is lower than other cross-section of composite column based on the results obtained from the abaqus analysis. The stress of steel material is about 76, 95 and 117 while that of concrete is about 12, 15, 17 respectively with the applied load.

Unlike in the other cross-section of composite column, the stress distribution in the concrete section along the steel tube is lower while in other cross section of composite column stress distribution in concrete material is high along the steel tube or in areas of concrete which has direct contact with the steel tube. As it is seen on the figure twisting of encased I-section is high than other cross section and increasing the concentrated load decreases twisting of column

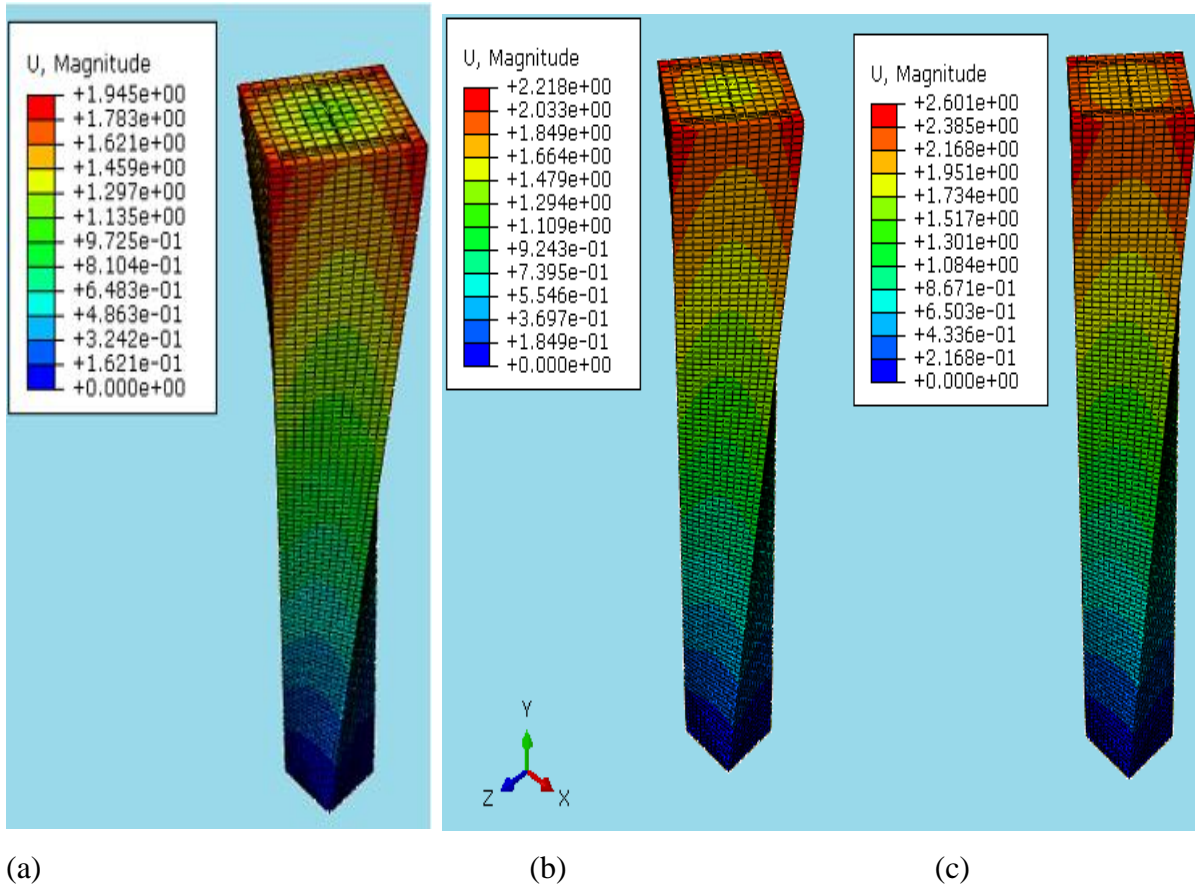


Fig 4.29 Displacement/Compression of SCC @ 40% (a), 50% (b) and @ 60% (c)

The compression of encased I-section of composite column which is subjected to about 40%P, 50%P and 60%P and a constant torsion of about 60KN-m is calculated by abaqus and the result is drawn on the figure 4.29 below. The compression of about 1.95mm, 2.22mm and 2.6mm are seen at the top of encased I-section due the applied concentrated load of about 2017KN, 2521.2KN and 3025.5KN and constant Torsion of about 60KN-m respectively. As it can be seen from the results the compression of encased I-section due applied of 40%P, 50%P and 60%P and constant T is higher than other cross-section (rectangular, square and circular) under the same condition of loading.

4.2.1.3 Behavior of CFST section without longitudinal reinforcement under Torsion

When Circular CFST, Rectangular CFST and Square CFST subjected to 40%, 50% and 60% of its axial capacity and constant Torsion with the same cross section and loading but without providing longitudinal reinforcement is analyzed using Abaqus software,

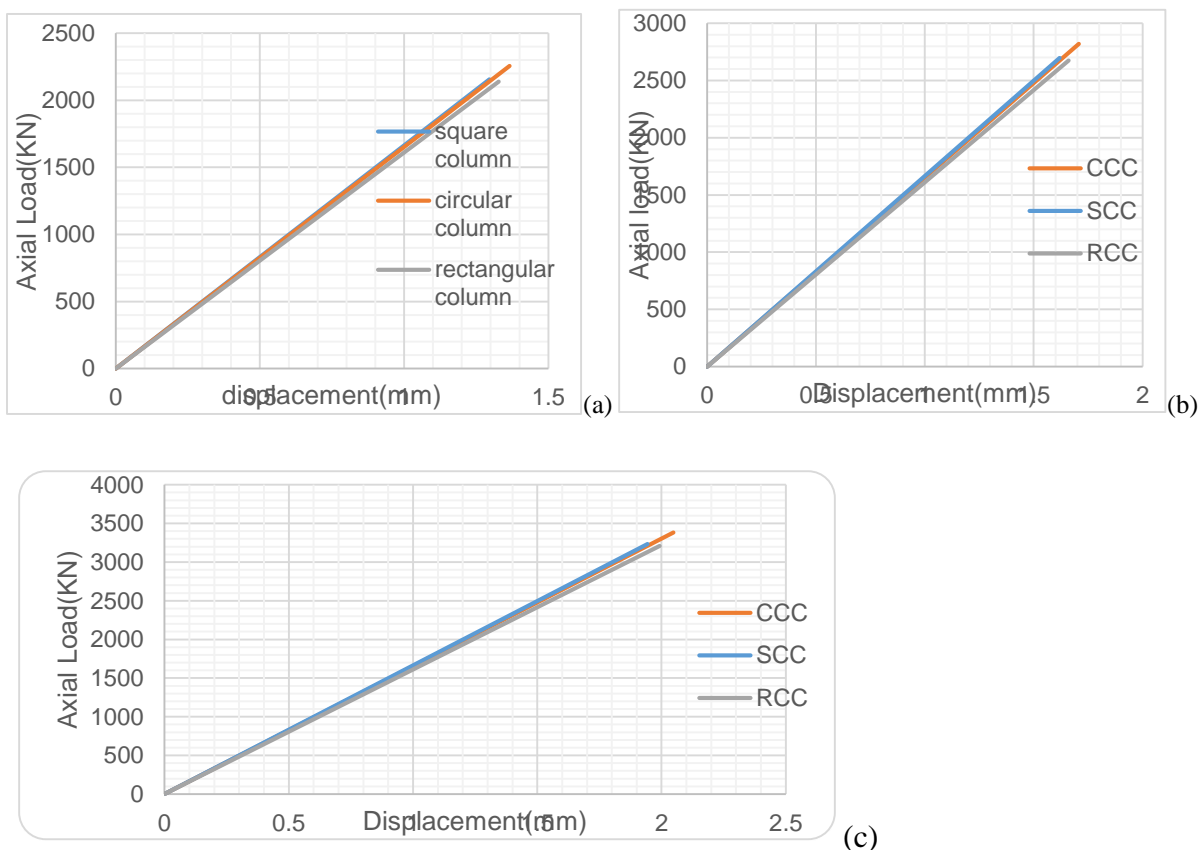


Fig 4.30 Axial Load vs displacement @ 40%P(a), @50%P(b) & @60%P(c) and constant T.

Different section of concrete filled steel tube (CFST) composite column subjected to 40%P, 50%P and 60%P with constant Torsion without providing longitudinal reinforcement is analyzed and from the results obtained the figure 4.30 is drawn. All the three composite column, rectangular composite column, square composite column and circular composite column is subjected to 40%,50% and 60% of their respective axial capacity with constant torsion of about 60kN-m. These result is compared to the results obtained using similar cross section and loading figure 4.18-4.20 which obtained from the analysis done by providing longitudinal reinforcement. As it is seen from the two results, Compression increases in column

without longitudinal reinforcement than in column in which longitudinal reinforcement is provided.

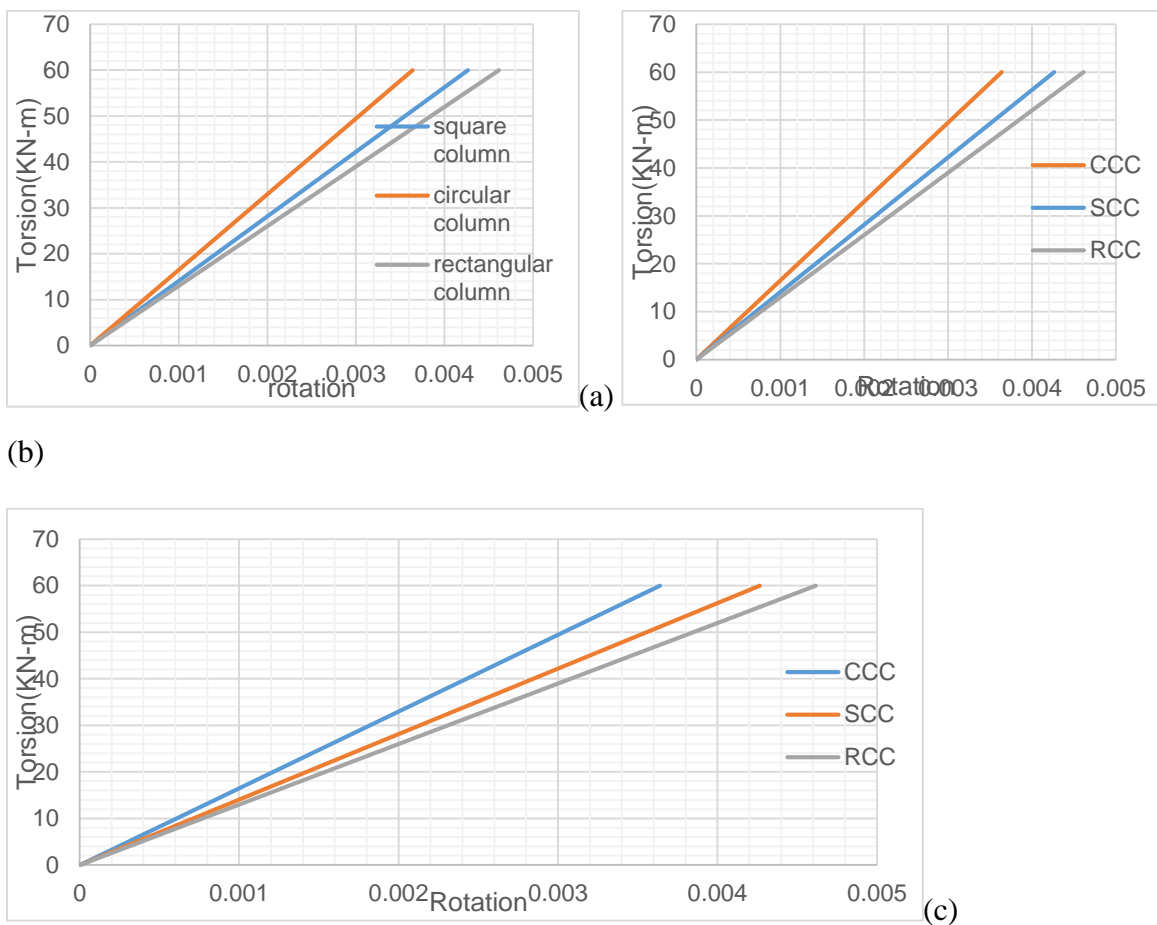
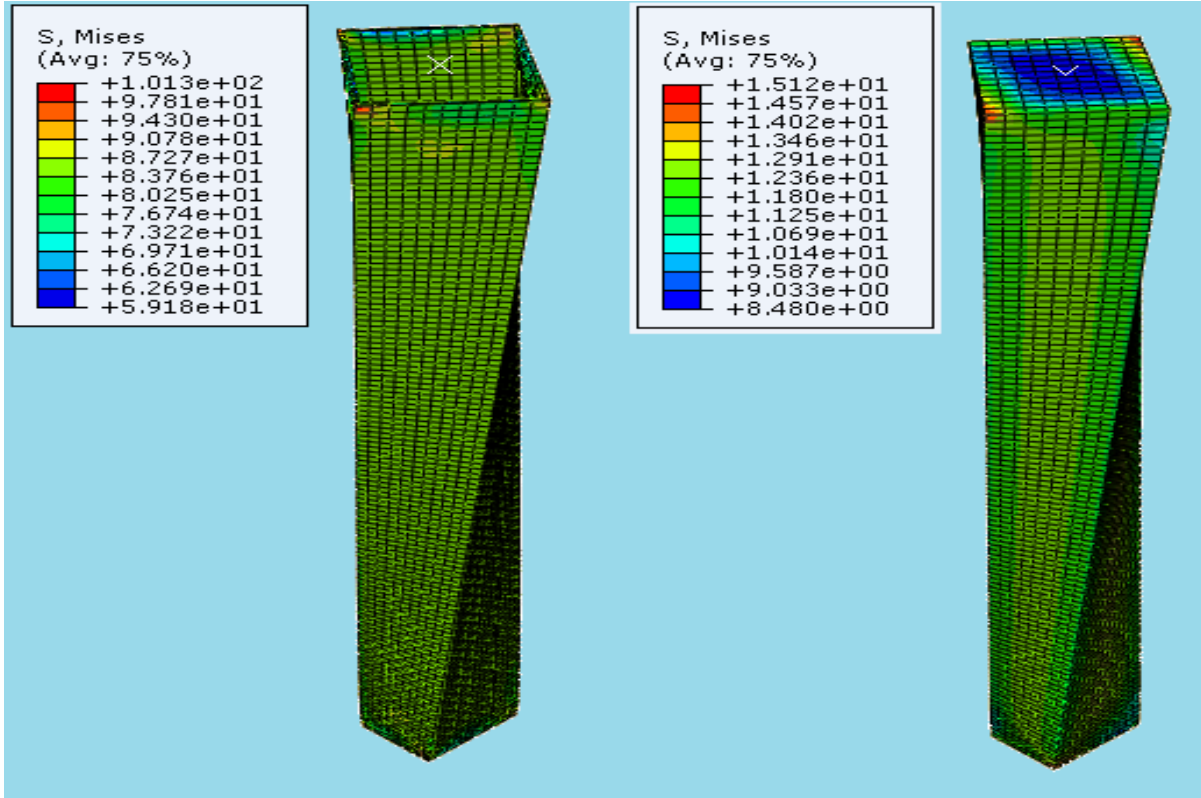


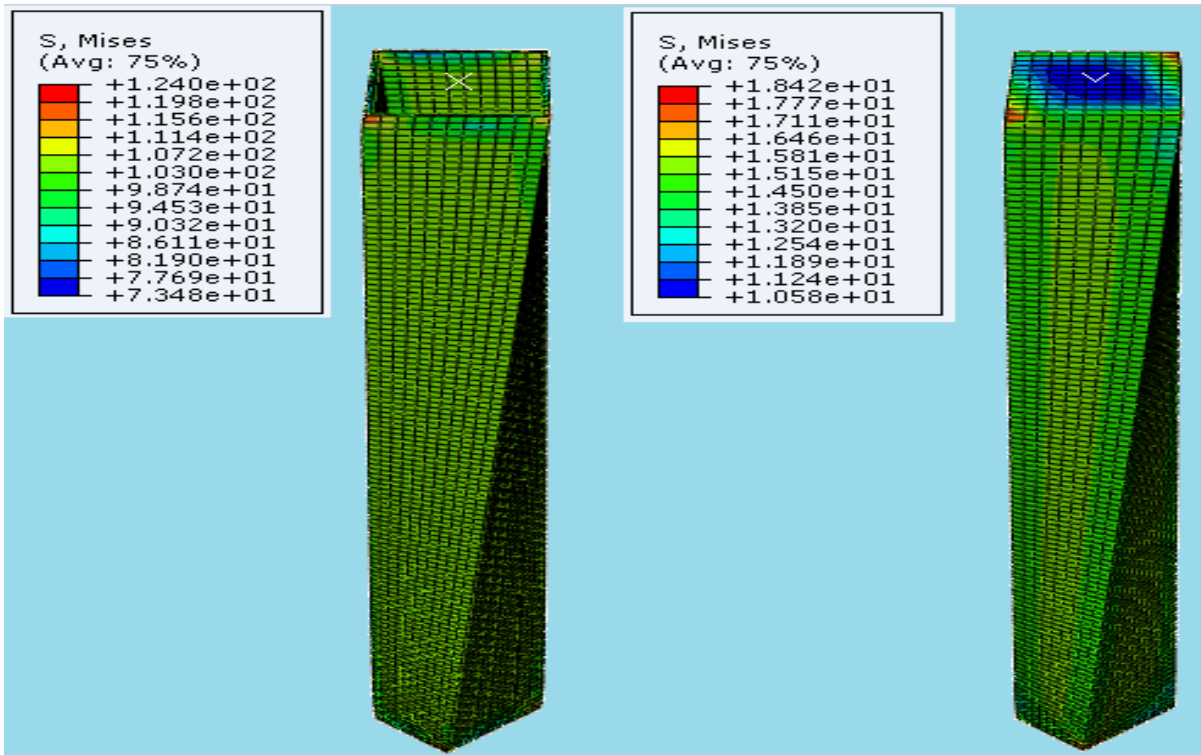
Fig 4.31 Torsion vs Rotation @ 40%P (a), @50%P (b) and 60%P (c) Axial load with constant T.

When the rotation of the composite column subjected to 40%P, 50%P and 60%P with constant Torsion without providing longitudinal reinforcement is checked to that composite column provided with longitudinal reinforcement the rotation of column is high in column without longitudinal reinforcement than on the column with longitudinal reinforcement.as it can be seen on the figure 4.31 rotation of rectangular composite is high than circular composite column and square composite column under the same condition of axial loading and constant torsion.



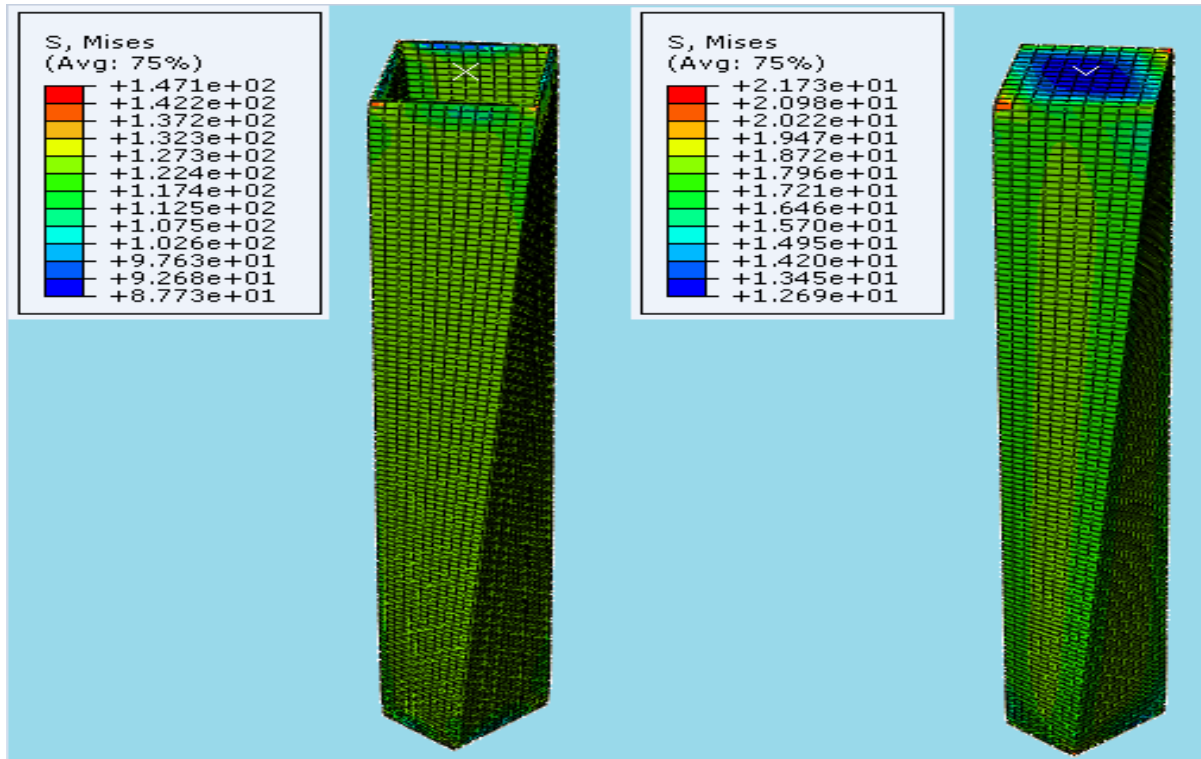
(a)

(b)



(c)

(d)

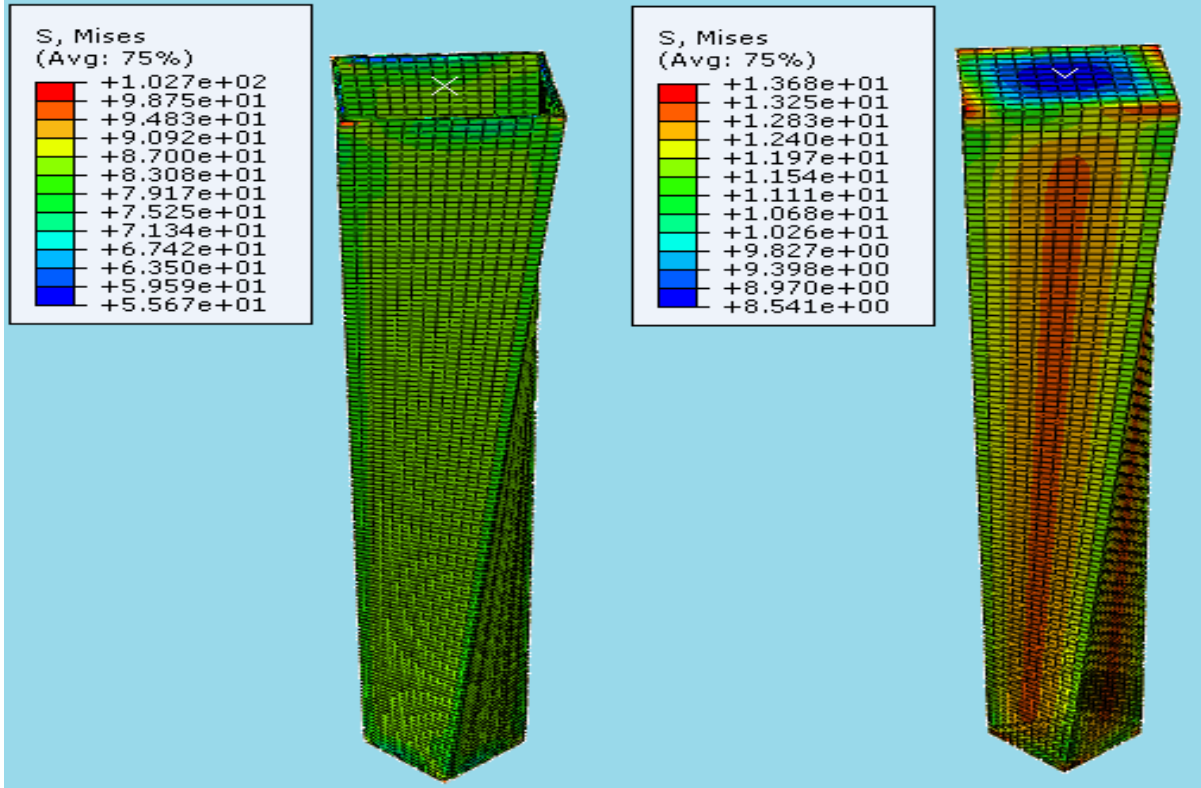


(e)

(f)

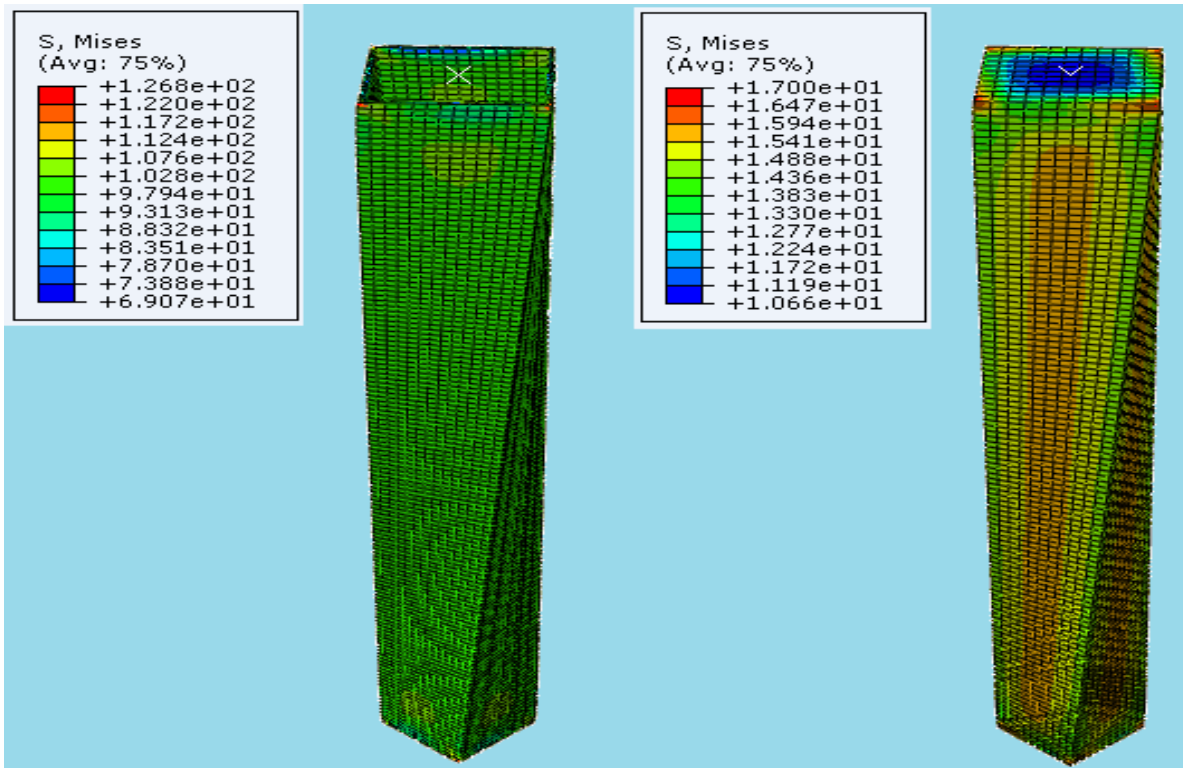
Fig.4.32 Stress of steel and concrete of RCC without longitudinal reinforcement @ 40%P (a & b),@50%P (c & d) and @ 60%P (e & f) respectively with constant Torsion.

The stress distribution of rectangular composite column doesn't that much affected by the absence of longitudinal reinforcement. The stress distribution of steel material is about 84, 103 and 127 while that of concrete is about 12.5, 15 and 18 as the subjected load is 40%P, 50%P and 60% respectively with keeping torsion constant as the concentrated load increases.



(a)

(b)



(c)

(d)

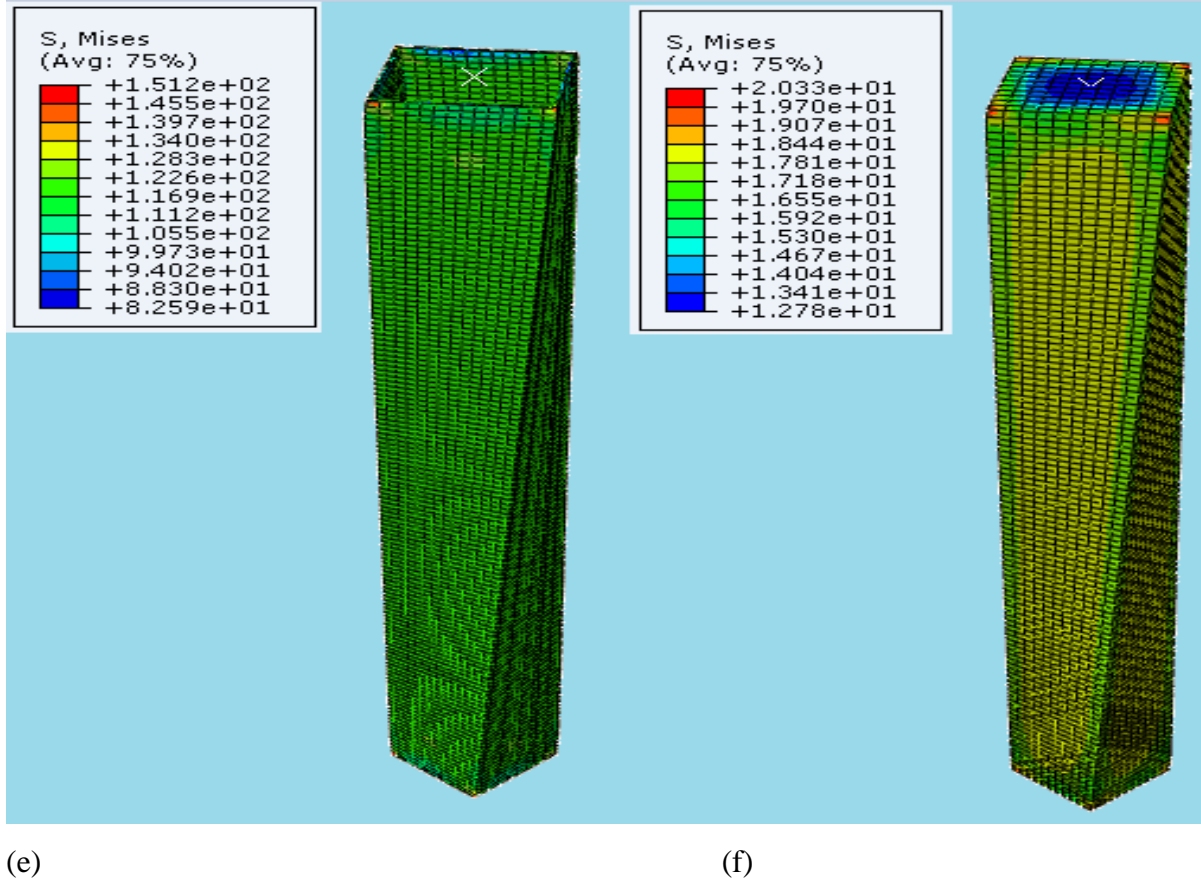
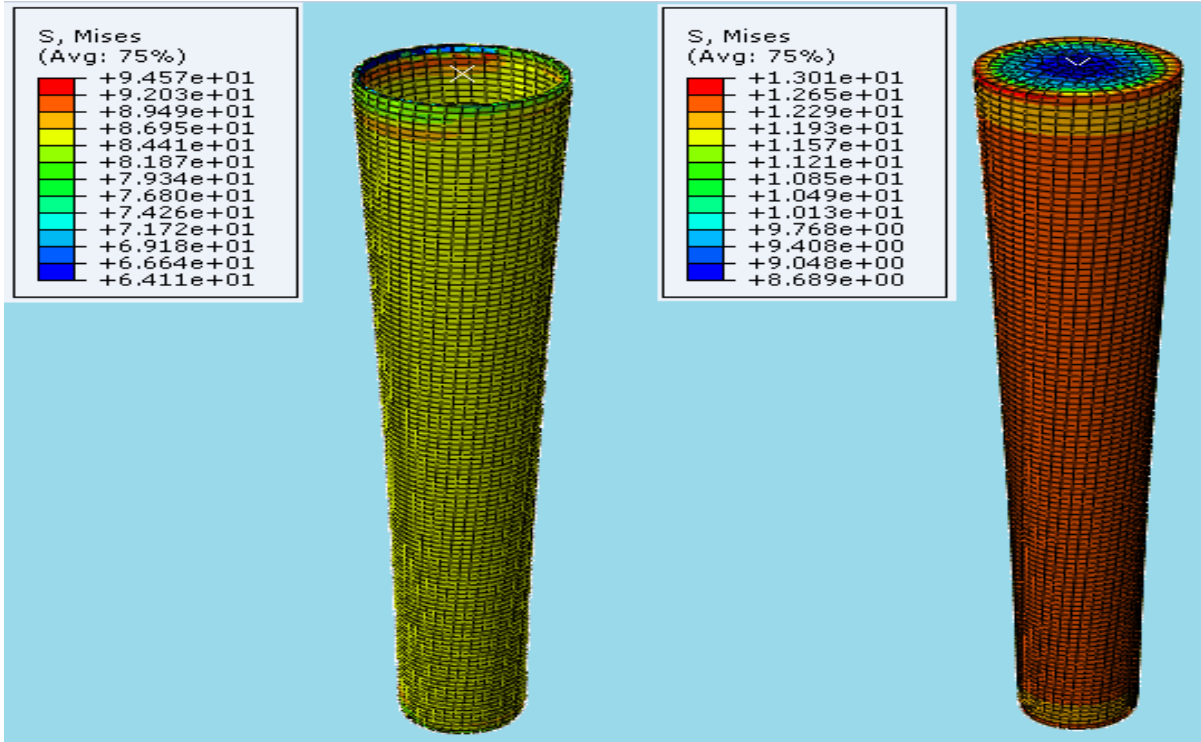


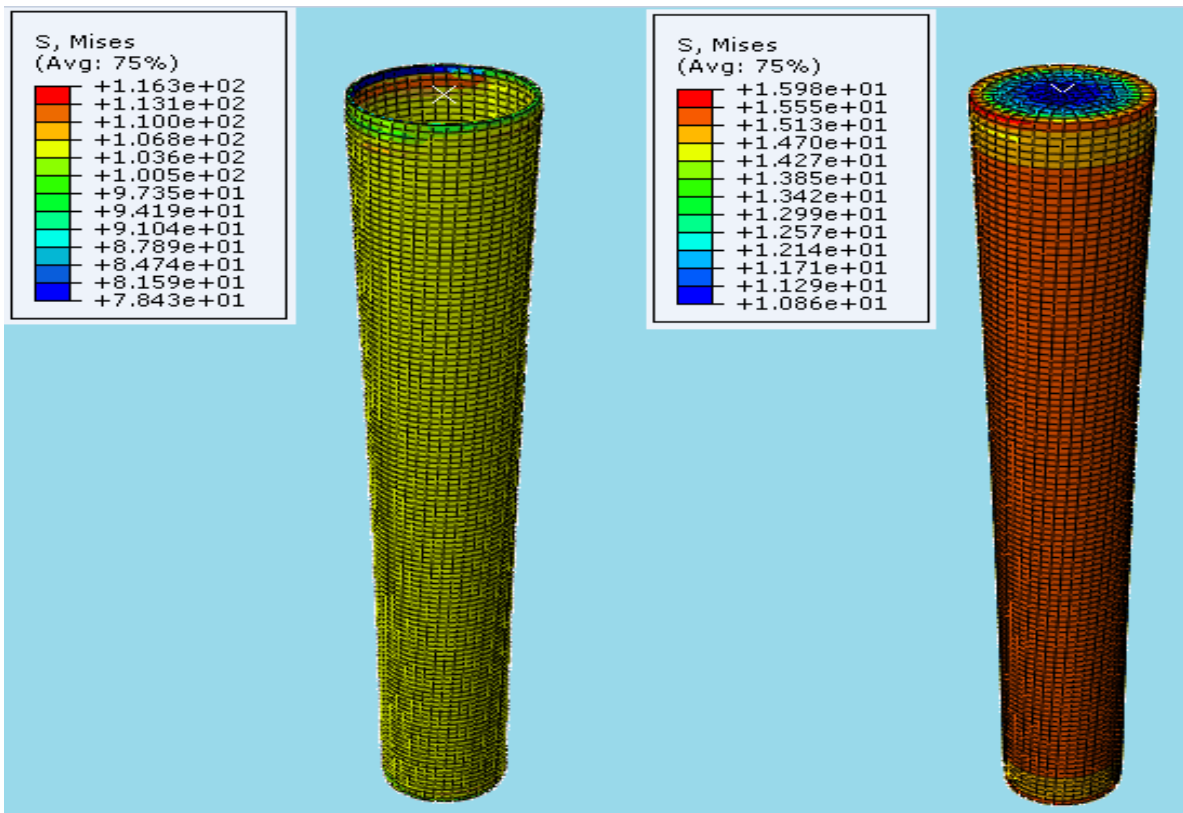
Fig.4.33 Stress of steel and concrete of SCC without longitudinal reinforcement @ 40%P (a & b), @50%P (c & d) and @ 60%P (e & f) respectively with constant Torsion.

In square composite column, without providing longitudinal reinforcement and keeping the concentrated load and torsion same as it is when longitudinal reinforcement provided and the stress analysis result is shown in the figure 4.33. The stress distribution of steel is about 87, 103 and 127 which is about 85, 105 and 125 in case of when providing longitudinal reinforcement while in concrete 12.5, 15.5 and 18 without longitudinal reinforcement while in case of providing longitudinal reinforcement, it is about 12, 15 and 18. This result shows that longitudinal reinforcement does not have much effect on stress distribution.



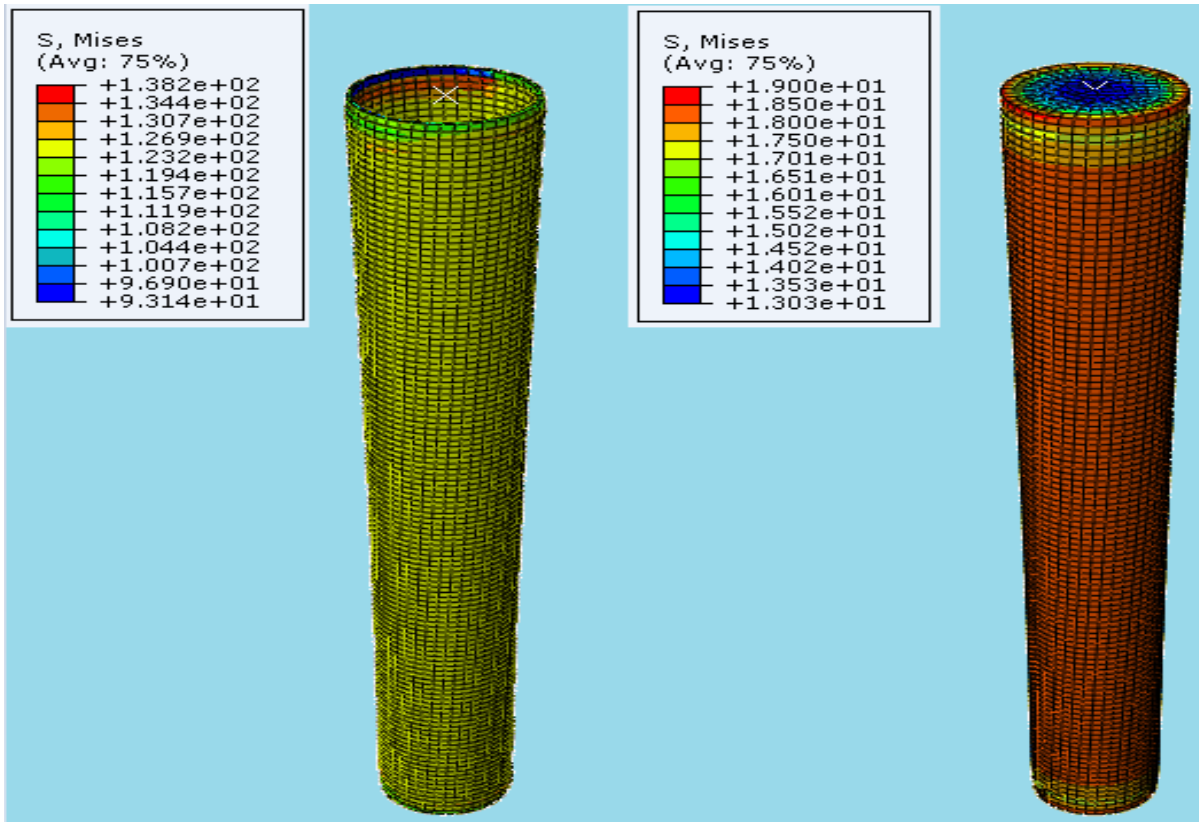
(a)

(b)



(c)

(d)



(e)

(f)

Fig.4.34 Stress of steel and concrete of CCC without longitudinal reinforcement @ 40%P (a & b), @50%P (c & d) and @ 60%P (e & f) respectively with constant Torsion.

Circular composite column without longitudinal reinforcement is analyzed using abaqus software. The result shows it is similar to that of rectangular composite column and square composite column which is discussed above.

CHAPTER 5

CONCLUSIONS AND RECCOMENDATION

5.1 Conclusion

The aim of this study was to investigate the behavior of different section of composite columns under combined compression and torsion by comparing the effects of different levels of axial loads on the torsion capacity of encased I-section and other different section of concrete filled composite columns.

The result shows that circular concrete filled composite column is better to be used for un-symmetric building in areas where earth quake may happen and when there is cantilever beam on column. A nonlinear 3-D finite element models were developed to model different composite column and Based on the Findings of this study, it was found out that.

- Under combined action of axial and Torsion load, CFST columns exhibits higher resistance than concrete Encased I-section.
- Concrete Encased I-section is highly affected in the case subjected to Torsion in terms of displacement/compression while CFST show approximately the same displacement/compression with or without Torsion.
- Circular concrete filled cross section is the most effective type of section and Encased I-section is the least.
- Provision of longitudinal reinforcement increases the resistance of composite column under compression and torsion.
- Twisting of column under constant Torsion decreases as the axial load increases.

5.2 Recommendation

This research focused on the assessment of behavior of composite column under axial and torsion load by Abaqus software, the recommendations of this thesis are as follows:

- The effect of thickness of steel section, material properties of concrete and steel and confinement effect of concrete on the behavior of composite column should be investigated.
- The behavior of composite column subjected to Axial Load, Bending Moment and Torsion at the same time should be studied.
- Finite element models should be developed to predict the behavior of composite column under various loading.
- This research is made based on theoretical basis, but it has to be checked by laboratory works before implementation.
- The influence of longitudinal reinforcement on compression and stress distribution on concrete filled composite column.

REFERENCES

1. Buick Davison, G. W. (2012). *Steel Designer's Manual*. Wiley- Blackwell.
2. Chen, C.-C., & Lin, N.-J. (2006). Analytical model for predicting axial capacity and behavior of concrete encased steel composite stub columns. *Journal of Constructional Steel Research*, 424–433.
3. Denavit, M. D., Hajjar, J. F., & Leon, R. T. (2011). *Seismic Behavior of Steel Reinforced Concrete Beam-Columns and Frames*. Structures Congress, 2852-2861.
4. Dundu, M. (2012). Compressive strength of circular concrete filled steel tube columns. Elsevier, *Thin-Walled Structures*, 62–70.
5. Ellobody, E., & Young, B. (2006). Nonlinear analysis of concrete-filled steel SHS and RHS columns. *Thin-Walled Structures*, 919–930.
6. Funakoshi M. and Okamoto T. (1981), “Effect of torsion on the ultimate strength of reinforced concrete members”, *Proceedings of CAJ*, 35, pp463-466.
7. Ellobody, E., Young, B., & Lam, D. (2011). Eccentrically loaded concrete encased steel composite columns. *Thin-Walled Structures*, 53-65.
8. El-Tawil, S., & Deierlein, G. G. (1999). Strength and Ductility of Concrete Encased Composite Columns. *Journal of Structural Engineering*, 1009–1019.
9. Eurocode, 4. (2004). BS EN 1994-1-1, Eurocode 4: Design of Composite Steel and Concrete Structure Part 1-1: General Rules and Rules for Buildings. London: British Standard Institution.
10. Eurocode, 8. (2004). BS EN 1998-1:2004 Design of structures for earthquake resistance Part1 General rules, seismic actions and rules for buildings. London: British Standard Institution.

11. Kim, D. K. (2005). A Database for Composite Columns. Georgia: Georgia Institute of Technology.
12. Li, Q., & Belarbi, A. (2011). Seismic Behavior of RC Columns with Interlocking Spirals under Combined Loadings Including Torsion. *Procedia Engineering*, 1281–1291.
13. Chen, Y.W. (2003). Research on torsion behavior of concrete filled steel tube. Taiwan: Central University.
14. Han, L.H. and Zhong,S.T. (1995). The studies of pure torsion problem for concrete filled steel tube. *Industrial Construction* 92:5, 562-573.
15. Lee, E.T., Yun, B.H., Shim, H.J., Chang, K.H. and Lee, G. C. (2009). Torsional behavior of concrete-filled circular steel tube columns. *Journal of Structural Engineering*. 135:10,1250- 1258
16. Beck, J. and Kiyomiya, O. (2003). Fundamental pure torsional properties of concrete filled circular steel tubes. *Journal of Material Construct Pavements* 739:60,85-96.
17. ABAQUS analysis user's manual version 6.13.

Appendix A: Design of Composite Columns

Composite column design sheet

Rectangular Composite Column

Section Geometry

Length (h1) = 300 mm

Width (h2) = 400 mm

Column length (L) = 3500 mm

Concrete cover to longitudinal reinforcement (from the inner face of steel tube to the outer face of the bar) (cr) = 35 mm

Characteristics of the Cross section

Steel Section

Steel Grade used S355

Yield Strength (f_y) = 355 Mpa

Elastic modulus of steel (E_a) = 210000 MPa

Thickness of steel tube (t) = 8 mm

Area of steel tube (A_a) = 10944 mm²

Moment of Inertia of steel tube (I_a)

$$I_{ax} = 2.6E+08 \text{ mm}^4$$

$$I_{ay} = 1.67E+08 \text{ mm}^4$$

Section modulus W_{pa}

$$W_{pa \ x} = 1.53E+06 \text{ mm}^3$$

$$W_{pa \ y} = 1.25E+06 \text{ mm}^3$$

Reinforcement bar

Reinforcement bar used	S400
Yield Strength of bars (f_{yr})	= 400 Mpa
Elastic modulus of reinforcing steel (E_s)	= 210000 Mpa
Area of Longitudinal Reinforced bar (A_b)	= 153.94 mm
No. of Longitudinal Reinforced bars n	= 4
Area of reinforcing steel (A_r)	= 615.75 mm ²
Moment of inertial of reinforcing steel I_r	

$$I_{rx} = 1.385E+07 \text{ mm}^4$$

$$I_{ry} = 6.157E+06 \text{ mm}^4$$

Section modulus of reinforcement bar

$$W_{pr\ x} = 9.236E+04 \text{ mm}^3$$

$$W_{pr\ y} = 6.16E+04 \text{ mm}^3$$

Concrete Core

Concrete grade C25/30

Cylinder strength $f_{ck} = 25$ Mpa

$E_{cm} = 31500$ Mpa

Area of concrete $A_c = 108,440.25$ mm²

Moment of inertial of concrete I_c

$$I_{cx} = 1.326E+09 \text{ mm}^4$$

$$I_{cy} = 7.268E+08 \text{ mm}^4$$

$$W_{pc\ x} = 1.04E+07 \text{ mm}^3$$

$$W_{pc\ y} = 7.68E+06 \text{ mm}^3$$

Design Procedure

1. Plastic resistance of the section :

$$N_{pl, Rd} = A_a f_{yd} + 0.85 A_c f_{cd} + A_s f_{sd} = 5553.4 \text{ KN}$$

2. Effective flexural and axial stiffnesses

$$EI_{eff} = E_a I_a + k_e E_{cm} I_c + E_s I_s$$

about the major axis

$$EI_{eff} = E_a I_a + k_e E_{cm} I_c + E_s I_s = 82,553.1 \text{ KNm}^2$$

about the minor axis

$$EI_{eff} = E_a I_a + k_e E_{cm} I_c + E_s I_s = 50,099.5 \text{ KNm}^2$$

3. Non dimensional slenderness

$$N_{crx} = \frac{\pi^2}{L_{eff}^2} EI_{effx} = 66,444.126 \text{ KN}$$

$$N_{cry} = \frac{\pi^2}{L_{eff}^2} EI_{effy} = 40,364.26 \text{ KN}$$

$$\lambda_x = \sqrt{\frac{N_{plR}}{N_{crx}}} = 0.32$$

$$\lambda_y = \sqrt{\frac{N_{plR}}{N_{cry}}} = 0.41$$

$$\delta = \frac{A_a f_{ad}}{N_{plRd}} = 0.63$$

$$\lambda_{vert} = \frac{0.8}{1 - \delta} = 2.198$$

Maximum bending design resistance of the cross section

$$M_{max, Rd} = w_{pa} f_{ad} + w_{ps} f_{sd} + \frac{w_{pc}}{2} f_{cd} = 612.38 \text{ KNm}$$

Square Composite Column**Section Geometry**

Length (h1) = 350 mm

Width (h2) = 350 mm

Column length (L) = 3500 mm

Concrete cover to longitudinal reinforcement (from the inner face of steel tube to the outer face of the bar) (cr) = 35 mm

Characteristics of the Cross section**Steel Section**

Steel Grade used S355

Yield Strength (f_y) = 355 Mpa

Elastic modulus of steel (E_a) = 210000 MPa

Thickness of steel tube (t) = 8 mm

Area of steel tube (A_a) = 10944 mm²

Moment of Inertia of steel tube (I_a) = 2.135E+08 mm⁴

Section modulus w_{pa} = 1.404E+06 mm³

Reinforcement bar

Reinforcement bar used S400

Yield Strength of bars (f_{yr}) = 400 Mpa

Elastic modulus of reinforcing steel (E_s) = 210000 Mpa

Area of Longitudinal Reinforced bar (A_b) = 153.94 mm

No. of Longitudinal Reinforced bars n = 4

Area of reinforcing steel (A_r) = 615.75 mm²

Moment of inertial of reinforcing steel I_r = 9.62E+06

$$\text{Section modulus of reinforcement bar } W_{pr} = 7.697E+04$$

Concrete Core

Concrete grade		C25/30
Cylinder strength f_{ck}	=	25 Mpa
E_{cm}	=	31500 Mpa
Area of concrete A_c	=	110,940.25 mm ²
Moment of inertial of concrete I_c	=	1.027E+09 mm ⁴
Section modulus of concrete section W_{pc}	=	9.24E+06 mm ³

Design Procedure

1. Plastic resistance of the section :

$$N_{pl, Rd} = A_a f_{yd} + A_c f_{cd} + A_s f_{sd} = 5595.17 \text{ KN}$$

2. Effective flexural and axial stiffnesses

$$EI_{eff} = E_a I_a + k_e E_{cm} I_c + E_s I_s = 66,257.1 \text{ KNm}^2$$

3. Non dimensional slenderness

$$N_{cr} = \frac{\pi^2}{L_{eff}^2} EI_{effx} = 53,328.04 \text{ KN}$$

$$\lambda = \sqrt{\frac{N_{plR}}{N_{crx}}} = 0.36$$

$$\delta = \frac{A_a f_{ad}}{N_{plRd}} = 0.63$$

$$\lambda_{vert} = \frac{0.8}{1 - \delta} = 2.16$$

Maximum bending design resistance of the cross section

$$M_{max, Rd} = w_{pa} f_{ad} + w_{ps} f_{sd} + \frac{w_{pc}}{2} f_{cd} = 556.81 \text{ KNm}$$

Circular Composite Column**Section Geometry**

Length (D) = 390 mm

Width (d) = 370 mm

Column length (L) = 3500 mm

Concrete cover to longitudinal reinforcement (from the inner face of steel tube to the outer face of the bar) (cr) = 40 mm

Characteristics of the Cross section**Steel Section**

Steel Grade used S355

Yield Strength (f_y) = 355 Mpa

Elastic modulus of steel (E_a) = 210000 MPa

Thickness of steel tube (t) = 10 mm

Area of steel tube (A_a) = 11932 mm²

Moment of Inertia of steel tube (I_a) = 2.155E+08 mm⁴

Section modulus w_{pa} = 1.444 E+06 mm³

Reinforcement bar

Reinforcement bar used S400

Yield Strength of bars (f_{yr}) = 400 Mpa

Elastic modulus of reinforcing steel (E_s) = 210000 Mpa

Area of Longitudinal Reinforced bar (A_b) = 153.94 mm

No. of Longitudinal Reinforced bars n = 6

Area of reinforcing steel (A_r) = 923.16 mm²

Moment of inertial of reinforcing steel I_r = 8.79E+06 mm⁴

$$\text{Section modulus of reinforcement bar } W_{pr} = 6.37\text{E}+04 \text{ mm}^3$$

Concrete Core

Concrete grade		C25/30
Cylinder strength f_{ck}	=	25 Mpa
E_{cm}	=	31500 Mpa
Area of concrete A_c	=	106,543.34 mm ²
Moment of inertial of concrete I_c	=	9.1E+09 mm ⁴
Section modulus of concrete section W_{pc}	=	8.378E+06 mm ³

Design Procedure

1. Plastic resistance of the section :

$$N_{pl, Rd} = A_a f_{yd} + A_c f_{cd} + A_s f_{sd} = 5948 \text{ KN}$$

2. Effective flexural and axial stiffnesses

$$EI_{eff} = E_a I_a + k_e E_{cm} I_c + E_s I_s = 64,299.9 \text{ KNm}^2$$

3. Non dimensional slenderness

$$N_{cr} = \frac{\pi^2}{L_{eff}^2} EI_{effx} = 51,752.76 \text{ KN}$$

$$\lambda = \sqrt{\frac{N_{plR}}{N_{crx}}} = 0.375$$

$$\delta = \frac{A_a f_{ad}}{N_{plRd}} = 0.64$$

$$\lambda_{vert} = \frac{0.8}{1 - \delta} = 2.22$$

Maximum bending design resistance of the cross section

$$M_{max, Rd} = w_{pa} f_{ad} + w_{ps} f_{sd} + \frac{w_{pc}}{2} f_{cd} = 558.1 \text{ KNm}$$

Encased I-section

Section geometry		
Hight (h1)	=	360 mm
Width (h2)	=	360 mm
Concrete cover (Cr)	=	35 mm
Column Length (L)	=	3500 mm

Steel Section

Section used		HE280A
Yield Strength of Shape Fyd	=	355 Mpa
Area of Steel Section Aa	=	9726 mm ²
Elastic modulus of steel shape	=	210,000 MPa

Section Geometric Properties:

h = 270 mm	bf = 280 mm
t _w = 8 mm	t _f = 13 mm
I _x = 1.367E+08 mm ⁴	W _{pl,x} = 1.112E+06 mm ³
I _y = 4.763E+07 mm ⁴	W _{pl,y} = 5.181E+05 mm ³

Reinforcement bar

Reinforcement bar used		S400
Yield Strength of bars (f _{yr})	=	400 Mpa
Elastic modulus of reinforcing steel (E _s)	=	210000 Mpa
Area of Longitudinal Reinforced bar (A _b)		= 153.94 mm
No. of Longitudinal Reinforced bars n		= 4
Area of reinforcing steel (A _r)	=	615.75 mm ²

Moment of inertial of reinforcing steel I_r

I _{rx}	=	1.1726E+07 mm ⁴
I _{ry}	=	1.1726E+07 mm ⁴

Section modulus of reinforcement bar

$$W_{pr\ x} = 8.497E+04 \text{ mm}^3$$

$$W_{pr\ y} = 8.497E+04 \text{ mm}^3$$

Concrete Core

Concrete grade C25/30

Cylinder strength f_{ck} = 25 Mpa

E_{cm} = 31500 Mpa

Area of concrete A_c = 108,440.25 mm²

Moment of inertial of concrete I_c

$$I_{cx} = 1.25E+09 \text{ mm}^4$$

$$I_{cy} = 1.34E+09 \text{ mm}^4$$

Section modulus of concrete core

$$W_{pc\ x} = 1.047E+07 \text{ mm}^3$$

$$W_{pc\ y} = 1.106E+07 \text{ mm}^3$$

Design Procedure

1. Plastic resistance of the section :

$$N_{pl, Rd} = A_a f_{yd} + 0.85 A_c f_{cd} + A_s f_{sd} = 5042.88 \text{ KN}$$

2. Effective flexural and axial stiffnesses

$$EI_{eff} = E_a I_a + k_e E_{cm} I_c + E_s I_s$$

about the major axis

$$EI_{eff} = E_a I_a + k_e E_{cm} I_c + E_s I_s = 54,794.46 \text{ KNm}^2$$

about the minor axis

$$EI_{eff} = E_a I_a + k_e E_{cm} I_c + E_s I_s = 37,790.76 \text{ KNm}^2$$

3. Non dimensional slenderness

$$N_{crx} = \frac{\pi^2}{L_{eff}^2} EI_{effx} = 44,146.91 \text{ KN}$$

$$N_{cry} = \frac{\pi^2}{L_{eff}^2} EI_{effy} = 30,447.33 \text{ KN}$$

$$\lambda_x = \sqrt{\frac{N_{pIR}}{N_{crx}}} = 0.376$$

$$\lambda_y = \sqrt{\frac{N_{pIR}}{N_{cry}}} = 0.45$$

$$\delta = \frac{A_a f_{ad}}{N_{pIRd}} = 0.622$$

$$\lambda_{vert} = \frac{0.8}{1 - \delta} = 2.116$$

Maximum bending design resistance of the cross section

$$M_{max,Rd} = w_{pa} f_{ad} + w_{ps} f_{sd} + \frac{w_{pc}}{2} f_{cd} = 475.67 \text{ KNm}$$